# Elucidating the recycling mechanism of ER resident proteins with ERD2

Jing An

Submitted in accordance with the requirements for the degree of
Doctor of Philosophy

The University of Leeds
Faculty of Biological Sciences

September, 2015

The candidate confirms that the work submitted is her own and that appropriate credit has been given where reference has been made to the work of others.

This copy has been supplied on the understanding that it is copyright material and that no quotation from the thesis may be published without proper acknowledgement.

*This isn't the end. This is a chapter.*

*Eric Betzig*

# Acknowledgements

# Abstract

One of the key steps for maintaining the endoplasmic reticulum (ER)-Golgi interface in the early secretory pathway is the receptor-mediated recycling of abundant soluble ER residents containing K/HDEL signals from the Golgi apparatus. The receptor was identified in yeast by screening for ER retention defective (ERD) mutants, and the ERD2 gene product was shown to mediate both the specificity and the capacity of ER retention in yeast. Since its discovery in 1990, ERD2 homologues have been identified from numerous eukaryotes including plants, and it is currently believed that it directly regulates the formation of retrograde transport vesicles from the Golgi. However, it is not understood how it recycles efficiently between the ER and the Golgi, and how it avoids leakage from the Golgi to later compartments. Although the recycling principle has been used as an argument to explain how few receptors could retain many ligands in the ER, it is unclear how receptors recycle to the Golgi faster than the unspecific anterograde bulk flow. Here I establish a quantitative receptor-ligand interaction study to determine the receptor to ligand ratio *in vivo*. Using the model cargo α-amylase-HDEL (Amy-HDEL) and co-expressed ERD2 I succeeded in up regulating the retention capacity of plant cells. This bioassay has been developed into a quantitative method using internal reference markers for normalising gene transfer, and tagging of receptors and ligands to permit simultaneous detection. Results are complemented by confocal laser scanning microscopy (CLSM) which demonstrates the ERD2 mediated ER retention. The activity assay was also used to identify critical amino acids in ERD2 function. Unexpectedly, the cytosolic C-terminus was found to be essential in maintaining the ability of ERD2 to retain HDEL proteins, in contrast to previous studies based on *in vitro* peptide binding assays. In addition to loss-of-function mutations, I also identified a new class of ERD2 mutant that causes induced secretion of HDEL proteins. These mutant classes are currently tested with respect to the sorting characteristics of the receptor, to distinguish between ligand-binding mutants and protein sorting mutants.

# Table of Contents

# Abbreviations

| | |
|---|---|
| **ADP** | Adenosine di-phosphate |
| **Amy** | $\alpha$-amylase |
| **ARF** | ADP ribosylation factor |
| **ATP** | Adenosine triphosphate |
| **BAP** | BiP-associated protein |
| **BFA** | Brefeldin-A |
| **BiP** | Binding Protein |
| **BP80** | Binding Protein 80 |
| **BSA** | Bovine serum albumin |
| **CCV** | Clathrin coated vesicles |
| **Chi** | C-terminal propeptide of chitinase |
| **CLSM** | Confocal Laser Scanning Microscopy |
| **COPI** | Coatomer protein I coated |
| **COPII** | Coatomer protein II coated |
| **CW** | Cell wall |
| **DV** | Dense vesicles |
| **EDTA** | Ethylenediaminetetraacetic acid |
| **EE** | Early endosome |
| **ER** | Endoplasmic reticulum |
| **ERAD** | ER associated degradation |
| **ERD2** | ER retention defective 2 |
| **ERES** | ER export sites |
| **ERP1** | ERD2 related protein |
| **ESCRT** | Endosomal sorting complex required for transport |
| **GAP** | GTPase activating protein |
| **GARP** | Golgi-associate retrograde protein |

| | |
|---|---|
| **GEF** | Guanine nucleotide exchange factor |
| **GFP** | Green fluorescent protein |
| **GPCR** | G protein couple receptor |
| **GTP** | Guanoside triphosphate |
| **IP** | Immunoprecipitation |
| **kDa** | Kilodaltons |
| **LV** | Lytic vacuoles |
| **M6P** | Mannose-6-phosphate |
| **MVB** | Multivesicular bodies |
| **PCR** | Polymerase chain reaction |
| **PM** | Plasma membrane |
| **SED** | Suppressor of export defect |
| **SV** | Protein storage vacuoles |
| **PVC** | Prevacuolar compartment |
| **LPVC** | Late prevacuolar compartment |
| **SDS-PAGE** | Sodium dodecyl sulphate polyacrylamine gel electrophoresis |
| **Spo** | N-terminal propeptide of sweet potato sporamin |
| **SR** | SRP receptor |
| **SRP** | Signal recognition particle |
| **TGN** | *Trans*-Golgi network |
| **VSR** | Vacuolar sorting receptor |
| **VSS** | Vacuolar-sorting-signal |

# Table of Figures

# 1 Introduction

## 1.1 General introduction

The secretory pathway transports not only proteins but also polysaccharides and lipids to various locations in eukaryotic cells. A better understanding of the underlying intracellular transport mechanism is not only relevant to fundamental research, but may also pave the way towards commercial applications such as the production of biofuel and pharmaceutical proteins. Moreover, due to the importance of this pathway in edible protein production and storage, as well as flowering and pathogen resistance, secretory pathway research also contributes to food security (Takaiwa *et al*., 2007; Yang *et al*., 2005).

Current understanding of the secretory pathway and intracellular traffic are originated after cell theory was established by using a combination of light microscopy from more than two hundred years ago. In addition to the morphological description of intracellular organelles by electron microscopy, protein transport by the secretory pathway was established to occur in a vectorial manner starting at the endoplasmic reticulum (ER) where proteins are synthesised, followed by traffic through the Golgi apparatus to later organelles such as lysosomes (Palade, 1975). The potential role of coated vesicles in mediating transport between organelles and the plasma membrane was recognised even earlier (Roth and Porter, 1964; Kanaseki and Kadota, 1969). The characterisation of clathrin coated vesicles (CCVs) and the dissection of the mannose-6-phosphate (M6P) mediated route to the lysosomes were important landmarks in our understanding of the secretory pathway (Pearse 1975; Kaplan *et al*. 1977; Pearse and Bretscher 1981). However, it was not until the eighties that basic principles of protein sorting and vesicle-mediated transport between organelles of the secretory pathway were established.

When proteins are translocated across the ER membrane, any further information on their destiny must reside within the mature portion remaining after cleavage of the signal peptide. At first it was thought that proteins have additional signals to mediate secretion, but the discovery of vacuolar sorting signals in yeast and the observed secretion of overproduced vacuolar proteins (Stevens *et al*., 1986) or mutants with defective vacuolar sorting signals (Valls *et al*., 1987) suggested that secretion may be the default pathway. This principle was confirmed by the discovery of the so-called ER retention signals (Munro and Pelham, 1987) and led to the concept that proteins require information to reach

intracellular organelles but that secretion occurs by non-selective bulk flow (Wieland et al., 1987). The bulk flow principle suggested that proteins do not require specific signals to reach the cell surface, in contrast to lysosomal proteins or ER residents.

The fact that deletion of the clathrin heavy chain in the yeast *Saccharomyces cerevisiae* had no influence on secretion across the plasma membrane (Payne and Schekman, 1985) suggested that besides CCVs, other vesicular carriers must be needed to mediate protein transport by the secretory pathway. Reconstitution of membrane traffic *in vitro* (Haselbeck and Schekman, 1986; Beckers *et al*., 1987) as well as genetic screens in the yeast *S. cerevisiae* (Novick and Schekman, 1979; Schekman, 1985) led to the identification of many machinery components required for vesicular transport. This included the discovery of non-clathrin coated vesicles (Orci *et al*., 1986), and the coatomer (Melançon *et al*., 1987; Malhotra *et al*., 1989; Orci *et al*., 1989) which was first proposed as a bulk flow carrier. Research into mechanisms of ER retention proved later that coatomer is involved in a selective retrograde transport route from the Golgi to the ER (Cosson and Letourneur 1994).

In addition, recent development in confocal laser scanning microscopy (CLSM) of fluorescent labelled fusion proteins has advanced our understanding of the intracellular localisation of specific protein as well its trafficking between organelles in the cell. In combination with in house biochemical assays, protein of interest of the secretory pathway can be dissected and studied without compromising other parts of the pathway or even to discover new organelles (Foresti *et al*., 2010). This thesis aims at introducing the key-findings leading to our further understanding of the ER-Golgi interface and the open questions remaining to formulate a complete transport cycle for the receptor that mediates accumulation of soluble proteins in the ER.

## 1.2 Overview of the plant secretory pathway

The plant secretory pathway has received much attention due to its importance as platform for the production of edible and pharmaceutical proteins and its putative role in development and stress resistance, all of which contribute to food security issues. There are three large membrane structures within the pathway: the endoplasmic reticulum (ER), the vacuole and the plasma membrane. These large membrane systems of the pathway are transiently connected by a set of intermediate compartments/organelles including the Golgi apparatus, the trans-Golgi network (TGN), the pre-vacuolar compartments (PVC) or endosomes, and the late pre-vacuolar compartment (LPVC)(Figure 1-1)(De Marcos Lousa *et al*., 2012; Foresti and Denecke, 2008; Foresti *et al*., 2010). The route from the ER towards the later part of the secretory pathway (PM or the vacuole) is called the biosynthetic transport or the anterograde transport pathway. Endocytosis or retrograde transport balances this biosynthetic pathway by constantly recycling proteins and receptors from the PM back to the internal organelles of the secretory pathway. A transport system via protein coated membrane carriers is responsible for the majority of the intracellular transport between the different organelles of the secretory pathway (Bonifacino and Glick, 2004; Hadlington and Denecke, 2000). In addition to vesicle transport, possible tubular membrane connections between the ER and the Golgi have also been reviewed and discussed but remain to be characterised (Robinson *et al*., 2015).

**Figure 1-1 Schematic overview of the plant secretory pathway**

Soluble cargo first enters the secretory pathway via the ER (endoplasmic reticulum) membrane and is then transported to the Golgi apparatus by COPII mediated vesicles. Further transport involves the *trans*-Golgi network (TGN), the pre-vacuolar compartment (PVC) and the late PVC (LPVC) to reach either the plasma membrane (PM) or the vacuolar. An alternate pathway to the vacuole is thought to occur via dense vesicles (DV) directly from the Golgi. Abbreviations: N, nucleus; CW, cell wall. Black "–" represents established routes and blue "–" represent proposed routes.

The early secretory pathway is normally considered to be the ER-Golgi interface, required for transport to the Golgi apparatus including the continuous recycling from the Golgi back to the ER to

maintain homeostasis between these two organelles in terms of membranes and machinery components. Continuous recycling is mediated by coat protein complex II (COPII) and coat protein complex I (COPI) which are responsible for anterograde and retrograde transport respectively.

Once residing in the ER lumen or embedded in the ER membrane, proteins can be transported to various destinations within the secretory pathway. Many of the basic molecular principles of protein sorting as well as the vesicular transport between organelles are described in detail (Bonifacino and Glick, 2004). Open questions remain regarding the early part of the plant secretory pathway and particularly the intensively researched ER-Golgi interface (De Marcos Lousa *et al*., 2012; Hawes *et al*., 2008; Klumperman, 2000; Vitale and Denecke, 1999).

### 1.2.1  Entry into the ER

Nuclear encoded proteins are synthesised by ribosomes either in the cytosol as free ribosomes or on the rough ER membrane by membrane-bound ribosomes (Blobel and Dobberstein, 1975a; Blobel and Dobberstein, 1975b). The latter is one of the major routes for entry into the secretory pathway, and it involves co-translational translocation of nascent proteins across the ER membrane (Dobberstein and Blobel, 1977). This could be achieved by either post-translational or co-translational mechanisms (Schwartz 2007). In the case of co-translational targeting, soluble cargo cannot be transported to the ER membrane without the signal-recognition particle (SRP) and specific SRP receptors (SR) which are embedded within the ER membranes to direct the signal sequence to the ER membrane (Egea *et al*. 2005). This route is typically used by soluble proteins that contain an N-terminal signal peptide (Blobel and Dobberstein, 1975a) which is recognised first by the signal-recognition particle (SRP) in the cytosol (Walter *et al*., 1981; Walter and Blobel, 1981b; Walter and Blobel, 1981a). Conformational changes are initiated after the binding of SRP to stop or slow down translation (Walter and Blobel, 1981a), and the mRNA-ribosome-nascent chain-SRP complex is then directed to the SRP receptor (SR) on the ER membrane, followed by release of SRP and resumption of protein synthesis. The nascent chain is then translocated across an aqueous channel in the translocation pore complex in the ER membrane whilst it is being synthesised (Kalies *et al*., 1994). If the protein contains a transmembrane domain in the rest of the coding sequence, it will act as a "stop-transfer" and leads to integration into the ER membrane by lateral diffusion out of

the pore complex (Walter and Blobel, 1981a). Some proteins translocate across, or integrate into the ER membrane via a post-translational mechanism, either in a SRP-dependent or independent manner. This is true for short secreted peptides, or tail-anchored proteins which are synthesised in the cytosol before ER targeting can be initiated. Although there are a variety of ER signal sequences, they still can be recognised by the same SRP due to the unique structure of a large hydrophobic pocket lined by methionines in the binding site of the SRP. This un-branched and flexible side chains structure of the SRP is sufficiently plastic to accommodate hydrophobic signal sequences of different sequences, sizes and shapes (Egea *et al*. 2005).

## 1.2.2 ER-Golgi network

Once the protein is translated and translocated, ER sorting takes place which directs the protein to other specific cellular compartments. Transport from the ER to the Golgi apparatus is vesicle-mediated and can occur via fluid phase bulk flow or specific ER export signals.  Soluble proteins are thought to be secreted via the default pathway (Denecke *et al*. 1990) but membrane proteins often require sorting signals to exit the ER (Hanton *et al*. 2006).

Due to the constant remodelling of the ER and the Golgi, the traffic between them has received much attention (Vitale and Denecke 1999;Klumperman 2000; Hawes *et al*. 2008). The sorting processes are restricted to defined points in the secretory pathway such as the Golgi or the ER export sites (ERES) which are thought to be localised on the smooth ER membrane (daSilva *et al*. 2004). However, recent review evaluates the morphology of the plant ER-Golgi interface in much more detail and indicates that the ERES may be localised to an area of highly curved ER membrane (Robinson *et al*., 2015). Many soluble proteins in this ER-Golgi interface are exported from the ERES to the *cis*-Golgi network via non-clathrin-type coat protein complex II (COP II) vesicles which are assembled by the initiation of GTPase Sar1 activation (as overview in Figure 1-2) (Barlowe *et al*. 1994; Lee *et al*. 2004). The cytosolic Sec23/Sec24 and Sec13/Sec31 protein complexes are responsible for the formation of the inner and outer layers of the COP II-coat respectively (Reiterer *et al*. 2008). Additionally, the Sec23 protein has GTPase activating properties for Sar1 and is thought to help the COP II vesicle to target the correct membrane for fusion (Phillipson *et al*. 2001; Cai *et al*. 2007).  In plants, anterograde transport from the ER to the Golgi apparatus may involve active

cargo selection as well as fluid phase bulk flow. Plants also contain an unusual anterograde transport carrier for vacuolar cysteine proteinases, large ER-derived vesicles which are expected to be non-COP II-coated (Toyooka *et al*. 2000).

On the other hand, retrograde transport balances this biosynthetic route via the transport from the Golgi back to the ER, which is mediated by COP I vesicles (Lee *et al*. 2004). This vesicle type is coated by a similar kind of coat protein complex known as the coatomer or COP I (Pimpl *et al*. 2000; Lee *et al*. 2004). The assembly of COP I is also controlled by three components 1) the GTPase ADP ribosylation factor (ARF1), 2) ARF1-specific GTPase-activating proteins and 3) ARF1-specific nucleotide exchange factors (GTP exchange factors, GEFs). In plants, the ARF-GEF family is less conserved and more complex than in animals (Foresti and Denecke 2008). The drug Brefeldin A (BFA) is used to study the sensitivity of ARF-GEFs and evidence has been obtained in plant cells suggesting some ARF-GEFs involved in the Golgi to ER recycling transport are sensitive to BFA (Ritzenthaler et al. 2002; Richter et al. 2007). However, BFA-resistant ARF-GEFs have also been observed in plants and specifically in *Arabidopsis* root cells (Richter et al. 2007). This may be an exception for the early secretory pathway in plants and ARF1 from the ARF-GEF family is thought to be
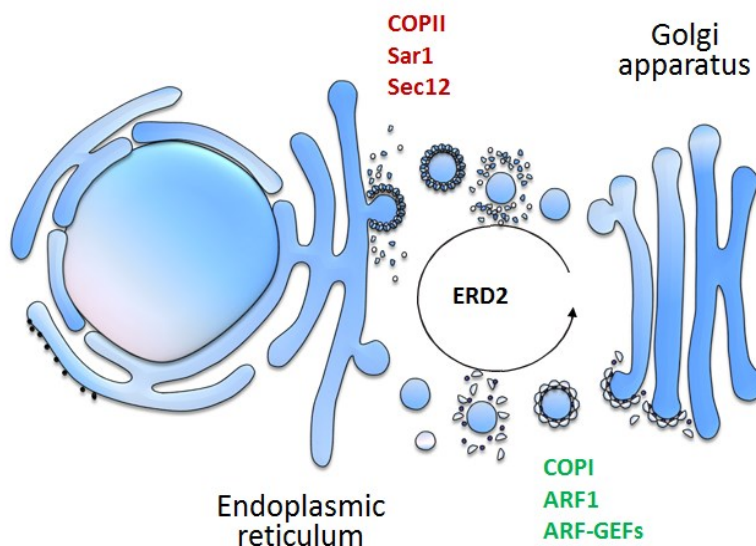


**Figure 1-2 ER-Golgi interface**
An overview of the ER-Golgi interface is illustrated. Key components which involved in anterograde transport from ER to the Golgi are in red letters whereas green letters represents major factors involved in retrograde transport. K/HDEL ligand receptor ERD2 is believed to shuffle between ER and Golgi constantly.

controlling the COP I mediated recycling transport from the Golgi to the ER as well as the maintenance of ERES integrity by indirectly affecting the COP II mediated transport. ARF and ARF-GEFs have also been implicated in post Golgi trafficking (Stefano *et al*. 2006; Richter *et al*. 2007; Langhans *et al*. 2008; Pimpl *et al*. 2003).

The well-known tetrapeptide HDEL motif is a typical ER retention signal which directs the sorting of soluble proteins in the Golgi apparatus to the retrograde COP I-mediated vesicle route. This motif is recognised by a receptor ERD2 (<u>ER</u> <u>R</u>etention <u>D</u>efective 2) in the Golgi apparatus which controls the recycling of ER resident proteins (Semenza *et al*. 1990). ERD2 is a seven transmembrane spanning protein and is thought to release its ligands in the ER and recycles continuously between the Golgi and the ER. The recycling principle has been proposed to explain how few receptor molecules can mediate the transport of many cargo molecules, but overexpression of stable HDEL proteins can gradually saturate the receptor as more *de novo* synthesised ligands join the group of recycled ligands that migrate to the Golgi apparatus (Phillipson *et al*., 2001). The same route is used to recycle ER chaperones when they leak out of the ER by bulk flow (Crofts *et al*. 1999). This topic of ER retention is discussed in detail later (1.3, p9)

### 1.2.3 Post-Golgi traffic

After the export from the ER and recycling of ER residents, the remaining soluble proteins in the Golgi are then either secreted or transported to the plasma membrane or vacuolar compartments. Interestingly, vacuolar sorting in plants is more complicated because it can either involve a Golgi-dependent route or a Golgi-independent route directly from the ER (Vitale and Raikhel, 1999; Chrispeels and Herman, 2000). Recent findings in pumpkin seeds have suggested a Golgi-independent route from the ER to the storage vacuole via KDEL-protease vesicles (Toyooka *et al*. 2000). However, the Golgi mediated biosynthetic route to the vacuole is much better understood and is controlled by the type I membrane spanning receptor BP80 (Paris and Neuhaus 2002; Hinz *et al*. 2007). This class of protein is also termed VSR (vacuolar sorting receptor) and is thought to cycle between the Golgi and the prevacuolar compartment (PVC) to mediate the targeting of soluble vacuolar proteins to the vacuoles. It was first purified from clathrin-coated vesicles and has a high concentration at the *trans*-cisternae of Golgi and an even higher steady-state level at the PVC, the final sorting compartment before the vacuoles (Kirsch *et al*. 1994; Hinz *et al*. 2007). Replacement of the luminal ligand-binding domain of BP80 by the green fluorescent protein (GFP-BP80) has provided an *in vivo* competition tool that saturates the recycling machinery of endogenous BP80 and induces the secretion of vacuolar proteins (daSilva *et al*. 2005). This provided first evidence for a role of BP80 in vacuolar sorting. The cytosolic tail of

BP80 is suggested to be important for not only the ER export and the Golgi to PVC traffic but also the recycling from the PVC (daSilva *et al*., 2006; Foresti *et al*., 2010).

More specifically, BP80 recognises soluble cargo via a sequence specific sorting signal such as the NPIRL motif found in pro-sporamin (Matsuoka and Nakamura, 1991) or pro-aleurain (Di Sansebastiano *et al*., 2001). It is through affinity binding *in vitro* that BP80 was originally purified from clathrin coated vesicles (Kirsch *et al*. 1994). A different class of vacuolar sorting signals are the so-called C-terminal vacuolar sorting signals, such as those of barley lectin or chitinase (Chi). These are less conserved, mostly hydrophobic, and often part of a C-terminally processed fragment or pro-peptide, such as the propeptide GLLVDTM from Chi (Neuhaus *et al*. 1991).

Sweet potato sporamin (Spo) is thought to be transported in a BP80-dependent manner to the lytic vacuoles (daSilva *et al*. 2005; daSilva *et al*. 2006) whereas chitinase is transported to the storage vacuole via a different route (Di Sansebastiano *et al*., 2001). Although this finding has supported the two-vacuole-hypothesis, evidence has suggested that the two type of sorting signals can lead to traffic to the same type of central vacuole (Hunter *et al*., 2007). The two conflicting data sets could be explained if two functionally different vacuoles merge together into the central vacuole over time. However, BP80 knock-down experiments suggested an indiscriminate effect on proteins carrying either type of vacuolar sorting signals (Craddock *et al*., 2008). In addition, new evidence from the host lab of using dominant negative mutants of GTPase Rab proteins has suggested the same (Bottanelli *et al*., 2012).

In conclusion, Golgi mediated recycling of ER residents is conserved between plants and other eukaryotes but sorting to the vacuoles may yet reveal plant-specific features, since it is still not clear how many routes to the vacuoles exist in plants. As vacuolar sorting is not the topic of this thesis it will not be discussed any further.

## 1.3  History and current state of research on ER retention

### 1.3.1  Discovery of ER retention signals

The topic of ER retention was first tackled by the group of Hugh Pelham whilst analysing ER resident chaperones. It was noticed that three abundant soluble ER residents share the same carboxyl terminal tetrapeptide (KDEL) sequence (Haas and Wabl, 1983; Munro and Pelham, 1986; Sorger and Pelham, 1987). Shortly afterwards it was discovered that deletion of the last six amino acids (SEKDEL) of the ER chaperone BiP led to secretion of the truncated molecule BiPΔKDEL (Munro and Pelham, 1987). This suggested that the C-terminus of BiP is necessary for ER retention. More importantly, fusion of the KDEL motif to chicken lysozyme resulted in efficient retention of the secreted enzyme in the ER of COS cells (Munro and Pelham, 1987). This suggested that the tetrapeptide is sufficient for ER retention and it was shown to be strictly present at the C-terminus of proteins. The KDEL motif as well as related sequences (RDEL, HDEL) became firmly established as ER retention signals for soluble proteins.

However, the term retention is misleading, because in order to function as a chaperone in the ER, proteins like BiP must diffuse freely in the lumen in order to interact with folding intermediates. This notion was reinforced by experiments in *Xenopus oocytes* suggesting that BiP can diffuse freely in the ER lumen regardless of the presence of the KDEL peptide and that retention could not be explained by interaction with a membrane spanning receptor in the ER (Ceriotti and Colman, 1988).  Also, ER residents are so abundant that it was difficult to envisage a true retention mechanism. The solution to the problem was provided by Hugh Pelham who proposed a recycling route from the Golgi apparatus (Pelham, 1988). This was based on an elegant study using the lysosomal enzyme cathepsin D as a cargo molecule. Carbohydrate side chains of cathepsin D undergo a Golgi-specific modification to generate the lysosomal targeting signal in the form of a M6P group, generally assumed to occur at the *cis*-Golgi (Waheed *et al.*, 1981; Pohlmann *et al.*, 1982; Deutscher and Creek, 1983; Goldberg and Kornfeld, 1983; Kornfeld and Kornfeld, 1985; von Figura and Hasilik, 1986). When a fusion protein of cathepsin D with the C-terminal KDEL motif (CDMK) was expressed in COS cells, it was found to be retained in the ER, but the fusion protein continued to receive Golgi-specific modifications (Pelham, 1988). Although it was not specifically shown that phosphorylated CDMK was present in the ER, the suggestion of selective retrieval

of KDEL proteins from the Golgi back to the ER was popular as it may explain how few receptor molecules could mediate the accumulation of many proteins in the ER. These experiments hence set the theme and foundation for the discovery of the postulated KDEL-receptor.

## 1.3.2 Isolation of ER retention defective mutants in yeast

By analogy to the success of the SEC mutants defective in constitutive secretion, the convenience of yeast mutant generation via active mutant selection was considered for the identification of ER retention machinery components thought to be non-redundant in yeast. Hence, the continued study of ER retention mechanisms was focused on the yeast system rather than on the mammalian model. To prove that yeast is a suitable model for all eukaryotic cells including mammals, the *S. cerevisiae* BiP homologue (Moran *et al.*, 1983) was first analysed in greater detail. In addition to high sequence homology to the rat BiP, the coding region included an N-terminal signal peptide for entry into the ER (not present in cytosolic hsp70 proteins) and a C-terminal HDEL sequence that strongly resembled the earlier described KDEL (Pelham *et al.*, 1988).

The functionality of the yeast motif HDEL was then tested in mammalian cells using the chicken lysozyme as cargo molecule. Likewise, the functionality of the KDEL signal was tested in yeast using the enzyme invertase as secretory cargo to which peptides were C-terminally fused. Results of these experiments have suggested that the retention motifs (KDEL and HDEL) are not interchangeable for their individual receptor binding systems. However, the high similarity between KDEL and HDEL was used as argument to postulate that the yeast *S. cerevisiae* must possess a very similar ER retention system based on a receptor molecule with high sequence homology, but exhibiting a slightly different ligand-binding specificity.

Invertase secretion/retention assays were carried out with chimeric genes under the transcriptional control of either strong or weak promoters and a noticeable secretion of the strong promoter-driven invertase-HDEL fusion indicated that the retention system in the yeast *S. cerevisiae* can be saturated. However, the invertase secretion assay was not based on measurement of the enzyme in the culture medium and cells, because much of the enzyme remains within the periplasmic space between the plasma membrane and the cell wall. Secretion assays were thus carried out on washed cells extracted in the presence or absence of detergent. The former was defined as "extracellular" whilst the latter was defined

as "total activity", whilst any invertase in the culture medium was ignored. The authors stated that absolute values for extracellular invertase may not be meaningful and that the measured "percentage secretion" values should be "regarded as approximate" (Pelham *et al*., 1988).

A much more polarised phenotype was observed after stable integration and associated low expression of the recombinant invertase fusions in the yeast genome within a SUC2 deletion mutant (Emr *et al*., 1983) lacking endogenous invertase. Whilst unmodified invertase and KDEL-tagged invertase contained sufficient enzymes in the periplasm to permit growth on sucrose, the HDEL-tagged enzyme was efficiently retained intracellularly so that growth on sucrose as sole carbon source was no longer possible. These pilot experiments set the stage for the isolation of the first ER Retention Defective (ERD) mutants selected on medium containing sucrose. Defective ER retention would induce leakage of invertase-HDEL to the periplasm and hydrolyse sucrose to fructose and glucose that can be transported into the cells and used as carbon source (Pelham *et al*., 1988).

## 1.3.3  Characterisation of potential receptors

After the complementation analysis in the yeast mutant screen, both ERD1 and ERD2 were isolated and further tested by immunoblotting of BiP secreted from a colony to a nitrocellulose filter in contact to test potential secretion of ER residents (Hardwick *et al*., 1990; Semenza *et al*., 1990). This secondary screen besides the invertase assay provided a firmer establishment of the ERD phenotype. In the case of *erd1* mutants, no change in the intracellular protein level of BiP was noticed when it was compared to wild type and negative control strain (which has replaced the HDEL with FGR (BiP-FGR)) (Hardwick *et al*., 1990). Although both *erd1* and BiP-FGR strains shown to have similar BiP secretion, the rate of BiP synthesis was increased in the BiP-FGR strain but not in the *erd1* strain (Hardwick *et al*., 1990). The BiP secretion of *erd1* was not a major re-distribution either and could be characterised as a weak mutant (Hardwick *et al*., 1990). In addition, *erd1* was shown to have a minor effect on the transport of vacuolar protease carboxypeptidase Y (CPY) as well its glycan modification in the *trans*-Golgi apparatus (Hardwick *et al*. 1990). Therefore, *erd1* was considered to induce inefficient retrieval of ER residents via a pleiotropic defect, possibly due to a function of ERD1p in the *trans*-Golgi for maintenance of structural integrity or the

environment of receptor-ligand binding of HDEL proteins rather than being the receptor itself (Hardwick *et al*. 1990).

In contrast to *erd1*, the second mutant *erd2* exhibited a higher level of BiP secretion which was compensated by increased BiP synthesis and did not show any influence on CPY transport and glycosylation modification (Semenza *et al*., 1990). ERD2p was shown to be an integral membrane protein of approximately 26 kDa and a C-terminally myc-tagged derivative of which continued to complement the *erd2* mutant. The tagged protein co-localised to the Golgi-associated GTPase YPT1 in punctate structures well distinguished from those obtained with anti-HDEL antibodies (Hardwick *et al*., 1990; Semenza *et al*., 1990). In addition, a small glycoprotein fusion pro-α-factor-HDEL (PAHDEL) that served to demonstrate a Golgi-mediated retrieval mechanism in yeast (Dean and Pelham, 1990) received less *trans*-Golgi modifications and was more efficiently retained in the ER when ERD2 was overproduced. Possibly, over-expression of ERD2 may increase the rate of HDEL protein retrieval from the *cis*-Golgi to the ER, thus avoiding exposure to late Golgi enzymes. Together the results demonstrated that ERD2 controls the capacity of ER retention in yeast (Semenza *et al*., 1990), but specific localisation of native ERD2 at the *cis*-Golgi remained to be demonstrated.

ERD2 over-expression also revealed a suppressive effect on other yeast mutants defective in secretion, notably *sec17, sec18, sec20, and sec22* which show partial secretion of HDEL proteins (Semenza *et al*. 1990) and accumulation of pre-Golgi transport vesicles (Kaiser and Schekman 1990). Secretion of HDEL-containing BiP from these four mutants could be suppressed by over-expressing ERD2, whilst secretion of BiP lacking the HDEL-motif was unaffected, demonstrating a specific effect on the HDEL-retrieval system only. ERD2 over-expression also suppressed BiP-secretion in *erd1* mutants (Semenza *et al*. 1990). Knowledge about possible interactions was also gained by screening for multi-copy suppressors of the lethal ERD2 deletion by 'plasmid-shuffle' technique (Hardwick *et al*., 1992; Hardwick and Pelham, 1992). The isolated suppressor genes (SED1, SED2, SED3, SED4 and SED5) however cannot compensate for the recycling retention of BiP and three of them: SED2, SED4 and SED3 were found to either be identical or exhibited high homology to known genes including SEC12, Sec12p and DPM1 respectively (Orlean *et al*., 1988; Hardwick *et al*., 1992). This ability to suppress was linked to overall slow transport from the ER and provided the first evidence of SEC12 titrating essential components involved in ER export (Hardwick

et al., 1992), well before the introduction of the coat protein complex II (COPII) as an ER export carrier (Barlowe et al., 1993; Barlowe and Schekman, 1993; Barlowe et al., 1994).

The specificity of the ERD2 ligand-binding was also investigated by ligand-binding comparisons of BiP homologues between *Kluyveromyces lactis* and *S. cerevisiae* (Lewis et al., 1990). BiP in *K. lactis* bears an ER retention signal DDEL instead of HDEL and the DDEL sequence is not efficiently recognised in *S. cerevisiae* (Lewis et al., 1990). However, upon exchange of the ERD2 gene from *K. lactis* to *S. cerevisiae*, both HDEL and DDEL retention signals were recognised and their fusion proteins were retained in the ER (Lewis et al., 1990). This strong line of evidence supported the notion that ERD2 encodes the true receptor for HDEL ligands, which was then widely accepted in the field. Isolation of ERD2 homologues from human (Lewis and Pelham, 1990), the plant *Arabidopsis thaliana* (Lee et al., 1993) and other organisms revealed a rather low degree of sequence similarity for such a crucial receptor candidate, but helped to establish the proposed seven trans-membrane domain structure (Figure 1-3) (Townsley et al., 1993).



Modified from Scheel A A , Pelham H R B J. Biol. Chem. 1998
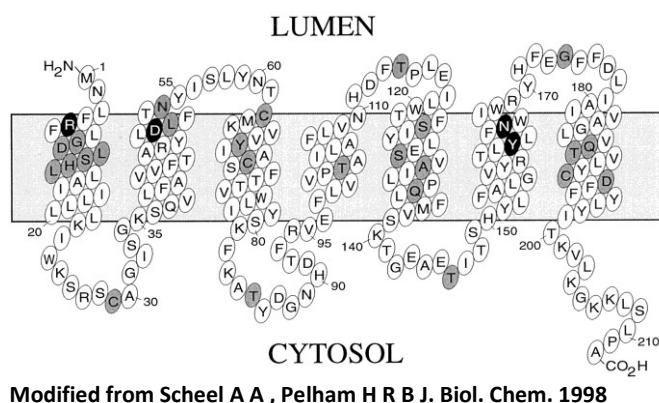
**Figure 1-3 Secondary structure model of the receptor ERD2**
The structure of human ERD2 was predicted as a seven transmembrane protein with a lumenal N-terminus and a cytosolic C-terminus. Mutations have been made as highlighted letters in order to study ligand-binding and receptor-transport mechanism.

## 1.3.4 Ligand binding *in vivo* and *in vitro*

Further experiments demonstrated that the subcellular location of mammalian ERD2 can be altered from a Golgi-like pattern to an ER pattern upon co-expression of ligands (Lewis and Pelham, 1992b). This ligand-induced re-distribution of the receptor was considered as a confirmation of its function in recycling, thus providing

an indirect ligand-binding assay *in vivo*. Moreover, *in vitro* binding studies using isolated total membranes from COS cells transfected with a plasmid mediating ERD2 overproduction showed a 5 to 7-fold higher binding of radiolabeled KDEL peptide binding compared to control membranes (Wilson *et al.*, 1993). The same study established that ligand binding affinity is high at low pH, and that ligand-release would be stimulated by the more neutral pH of the ER lumen. This reinforced the notion that retrieval of ER residents occurs by receptor binding in the Golgi apparatus, followed by retrograde transport and ligand release in the ER.

A combination of ligand-induced ERD2 redistribution *in vivo* as well as *in vitro* binding studies with total membranes loaded with recombinant ERD2 contributed to a functional analysis of critical amino acids required for ligand-binding and receptor trafficking (Townsley *et al.*, 1993). This was confirmed by sulfhydryl-specific labelling of mutagenised ERD2 (Scheel and Pelham, 1998). It remains to be shown if critical amino acids discovered in this study can serve as a model for the functional analysis of ERD2 homologues from other organisms. In addition, an attempt to map ligand-binding domains of ERD2 via cellulose-bound overlapping peptides has revealed different residues (Janson *et al.*, 1998). One of the main problems is the lack of experimental systems to study ERD2 in a native membrane bound configuration but yet purified from other membrane proteins.

Although ERD2 mutants are viable, deletion of ERD2 led to a recessive lethal phenotype (Semenza *et al.*, 1990). Replacement of ERD2 by a chimeric gene under control of a regulated promoter illustrated that depletion of the ERD2 gene product leads to growth arrest, defective protein transport through the Golgi and accumulation of abnormal membranes and lipid droplets in the cells, whilst CPY transport to the vacuole appeared to be less affected (Semenza *et al.*, 1990). This suggests that besides a function in retrieval of ER residents from the Golgi, ERD2 may have another essential function required for cell viability. More detailed work revealed however growth arrest was strictly correlated with defective retention of HDEL proteins, and viable mutants showing secretion of HDEL proteins exhibited weak but noticeable residual retrieval activity, explaining their survival (Townsley *et al.*, 1994).

### 1.3.5 Integration of ERD2 into the ER-Golgi interface

Despite the rapid advances after the discovery of ERD2, it remained unclear how few receptors can mediate the recycling of many soluble ER residents. In order

to function in the postulated manner (Pelham *et al.*, 1988), ERD2 would have to progress much faster to the Golgi than bulk flow of soluble proteins to retrieve the far more abundant ligands that continuously escape from the ER. A high ERD2 steady state level at the Golgi (Hardwick *et al.*, 1990; Semenza *et al.*, 1990) suggests that Golgi to ER recycling is rate-limiting whilst ER export to the Golgi is fast. However, the ligand-induced redistribution of ERD2 to the ER (Lewis and Pelham, 1992a) is difficult to reconcile with the need for rapid recycling back to the Golgi. There is currently no evidence regarding a particularly fast ERD2 ER export pathway that would explain how the receptor functions *in vivo*. More importantly, it was not clear why increased numbers of soluble ligands should lead to receptor accumulation in the ER as ligands are thought to dissociate with the receptor in this compartment (Wilson *et al.*, 1993).

The fact that ERD2 overexpression alone causes effects similar to those observed with the drug Brefeldin A (Hsu *et al.*, 1992) suggests that the receptor actively engages with the machinery that regulates the recycling of membranes from the Golgi. One of the most striking effects of the drug is the formation of uncoated membrane tubules emanating from the Golgi and causing mixing of ER and Golgi membranes in a super-compartment (Lippincott-Schwartz *et al.*, 1990). Soon after the discovery that coatomer- or COPI-coated vesicles carry retrograde cargo from the Golgi back to the ER (Cosson and Letourneur, 1994), this notion could be substantiated by the discovery that ERD2 may directly influence the COPI machinery (Aoe *et al.*, 1997). The authors show that ERD2 can be oligomerised, leading to the membrane recruitment of the GTPase activating factor (GAP) of ARF1, a key component in the recruitment of COPI to membranes to form COPI vesicles. When ARF1-GAP is recruited to membranes, it would inactivate ARF1, and prevent COPI formation. If ERD2 ligands disrupt the oligomerised state of ERD2, it may lead to GAP dissociation and the initiation of COPI vesicle formation, thus explaining the earlier observed ligand induced redistribution of ERD2 (Lewis and Pelham, 1992a), but this has yet to be demonstrated. It also remains to be elucidated how ERD2 reaches the Golgi faster than its ligands and how its progression to post-Golgi compartments is prevented by the transport machinery.

## 1.4  Remaining questions and aims of the project

Although the HDEL-receptor ERD2 has been widely accepted as the genuine receptor for recycling soluble ER residents from the Golgi, no direct evidence has

been shown to prove that the ERD2 is functioning as a receptor for HDEL-proteins in plants. Evidence that the HDEL or KDEL-mediated retrieval route can be saturated has been shown in transient expression experiments with protoplasts (Denecke *et al*., 1992; Crofts *et al*., 1999; Pimpl *et al*., 2006). Saturation is mainly observed with stable cargo molecules that continue to accumulate until *de novo* synthesized and recycling ligands combined are more abundant than the receptor. Ligand-induced ERD2 redistribution back to the ER, as well as functional studies on ligand-binding and release remain to be performed in plants. The crystal structure of ERD2 also remains to be generated and described.

Although the 7-transmembrane structure proposed by Pelham's group (Townsley *et al*., 1993) has been widely accepted by the field, an alternative 6-transmembrane structure was propose twice using different methods (Singh *et al*., 1993; Brach *et al*., 2009). In addition, other functions besides being the ER ligand receptor have also been proposed (Li *et al*., 2009; Xu *et al*., 2012), but it has yet to be shown if these are truly independent functions or merely indirect here are still some open questions remained to formulate a complete transport cycle for the receptor mediated accumulation in the ER. Finally, plants have shown to contain an ERD2-related protein (ERP) family which has the same structure as ERD2 except for an N-terminal extension of approximately 50 amino acids that may contain another transmembrane domain (Hadlington and Denecke, 2000). It is currently unknown why plants, algae and certain protists contain ERPs as well as ERD2, whilst fungi and animals only contain ERD2.

This PhD thesis project pursued the following aims:

1) Establishment of a robust bio-assay to monitor the biological activity of ERD2 in mediating ER retention of soluble proteins.

2) Evaluation of fluorescent fusion proteins of ERD2 with respect to biological activity and transport fidelity.

3) To test if few receptor molecules can indeed recycle many soluble ligands, or if the discrepancy between receptor numbers and ligand numbers is due to poor ER export of ER residents.

4) To use an ERD2 bio-assay to identify different classes of ERD2 mutants that has distinct functional disruptions, as well as experiments to shed light on the biological role of ERPs in plants.

## 2 Results

## 2.1 Chapter I ER retention and ERD2 functionality in plants

### 2.1.1 Introduction

The endoplasmic reticulum (ER) is responsible for the synthesis and further processing of the majority of edible proteins on Earth (Vitale and Denecke, 1999), and it has recently been harnessed for the production of high value proteins such as vaccines or antibodies in plant cells (Fischer *et al*., 2003). The discovery of ER retention signals (Munro and Pelham, 1987) was an important landmark in secretory pathway research because it strongly supported the newly introduced bulk flow hypothesis (Wieland *et al*., 1987). Rather than requiring signals to mediate effective secretion, soluble proteins require specific signals to avoid secretion and reach vacuoles or other organelles instead. When such signals are mutated or deleted, the resulting proteins are secreted (Valls *et al*., 1987; Munro and Pelham, 1987), which suggests that secretion is the default pathway.

The concept of secretory bulk flow was formulated based on experiments with short glycosylated peptides in animal cells (Wieland *et al*., 1987). In plants bulk flow to the cell surface was demonstrated with large cytosolic proteins forced into the ER lumen by fusion to signal peptides (Denecke *et al*., 1990). Whilst signals for vacuolar sorting are highly variable in plants and differ from those used in yeasts or mammals (Matsuoka and Neuhaus, 1999), ER retention signals are highly conserved amongst eukaryotic kingdoms and always constituted by strictly C-terminal tetrapeptides such as KDEL or HDEL. Whilst plant vacuolar sorting receptors (VSRs) are well characterised and signals for anterograde and retrograde receptor transport are clearly established (daSilva *et al*., 2006; Foresti *et al*., 2010), we know very little about the machinery that recognises ER retention signals.

The KDEL/HDEL receptor was identified via a genetic approach based on the selection of ER retention defective (ERD) mutants (Semenza *et al*., 1990; Hardwick *et al*., 1990), the second of which (ERD2) was shown to control the capacity and specificity of ER-retention (Lewis *et al*., 1990). Further functional analysis was restricted to ligand-interaction studies (Wilson *et al*., 1993; Townsley *et al*., 1993; Scheel and Pelham, 1998) and evidence for interaction with the COPI machinery for Golgi to ER retrograde transport (Lewis and Pelham, 1992a; Hsu *et al*., 1992;

Aoe *et al*., 1997). However, a complete transport cycle and signals for anterograde and retrograde transport were never established in any system (Pfeffer, 2007).

First experimental evidence for ER retention signals in plants arose from a study showing that C-terminal tagging of the vacuolar protein phytohaemagglutinin by a slightly extend KDEL sequence (LNKDEL) caused partial retention of the hybrid molecules in the ER and the nuclear envelope in seeds of transgenic tobacco, although the majority was still found in the storage vacuoles (Herman *et al*., 1990). In addition, the HDEL sequence was found at the C-terminus of a family of BiP homologues in tobacco (Denecke and Goldman, 1991) and in maize (Fontes *et al*., 1991). Further work revealed that soluble plant ER proteins can contain either KDEL or HDEL (Hesse et al., 1989; Inohara et al., 1989; Tillmann et al., 1989; Napier et al., 1992; Denecke et al., 1995). Specific experiments with neutral bulk flow cargo molecule phosphinothricin acetyl transferase (PAT) demonstrated that the plant ER retention machinery can recognise KDEL, HDEL and RDEL peptides, but not SDEL (Denecke *et al*., 1992). Further work demonstrated that the site of retrieval is probably the *cis*-Golgi in plants (Phillipson *et al*., 2001).

The plant equivalent of the receptor for retrieval of ER residents from the Golgi arose from random sequencing of *Arabidopsis thaliana* expressed sequence tags and revealed a cDNA clone (aERD2) capable of complementing the lethal *erd2* mutant of *S. cerevisiae* (Lee *et al*., 1993). C-terminally fluorescent tagged ERD2 labels the Golgi apparatus as well as the cortical ER network (Boevink *et al*., 1998), and Brefeldin A-mediated redistribution of Golgi and ER membranes was shown to occur rapidly and illustrates a retrograde transport route in plants (Boevink *et al*., 1998). Loss of function genetics suggested that one of the two *Arabidopsis thaliana* ERD2 forms (AtERD2b) may be a specific receptor for one calreticulin isoform (CRT3) but not for other HDEL-bearing proteins (Li *et al*., 2009), but further studies contradicted this hypothesis (Xu *et al*., 2012; Montesinos *et al*., 2014).

This first results chapter aims at exploring the existing state of the art in protein trafficking methods in plants in order to set the stage for a more in depth analysis of ERD2 function in plants.

## 2.1.2  Results

## 2.1.2.1 Secretion versus ER retention is difficult to quantify with fluorescence microscopy

The popularity of live fluorescent cell imaging in plants (Boevink *et al*., 1998) has prompted research groups to use secreted versions of fluorescent proteins to study ER retention (Xu *et al*., 2012; Batoko *et al*., 2000). One of the problems is that fluorescent imaging is biased by the volume of the cell compartment in which a protein is present. Whilst the volume of the ER and the Golgi is limited and allows accumulation of high protein concentrations, transport to vacuoles or the apoplast leads to an enormous dilution of the fluorescent marker. In addition, pH-mediated quenching of fluorescence and increased proteolytic activities systematically lead to under-representation of fluorescent signals (Batoko *et al*., 2000). Moreover, secreted GFP constructs, in particular when supplemented with the HDEL-signal for ER retention, were shown to weakly interact with the ER chaperone BiP (Brandizzi *et al*., 2003), suggesting that GFP folds very slowly. In the same study, secretion assays in protoplasts comparing secreted GFP (secGFP) and ER retained GFP (secGFP-HDEL) revealed that for both proteins the majority was found intracellularly whilst the effect of the HDEL was mainly appreciated in the extracellular fractions. secGFP appears to be very slowly secreted compared to other artificial cargo molecules (Denecke *et al*., 1990; Denecke *et al*., 1992). Figure 2-1 shows that secreted GFP (secGFP) and ER retained GFP (secGFP-HDEL) both strongly label the endoplasmic reticulum. It was not possible to see secreted GFP in the apoplast in either of the constructs. Furthermore, double blind experiments failed to predict which of the two constructs was harbouring an ER retention signal, due to high variance of overall expression levels in *Agrobacterium* mediated infiltrated leaf epidermis cells. This corresponds well with the earlier published secretion assays (Brandizzi *et al*., 2003). Similar results were obtained with GFP-fusion proteins harbouring the last 34 amino acids of the calreticulin carboxyl terminus. Figure 2-2 shows that the presence or absence of the HDEL tetrapeptide did not influence the fluorescent pattern reminiscent of a typical cortical ER network in infiltrated leaf epidermis cells.
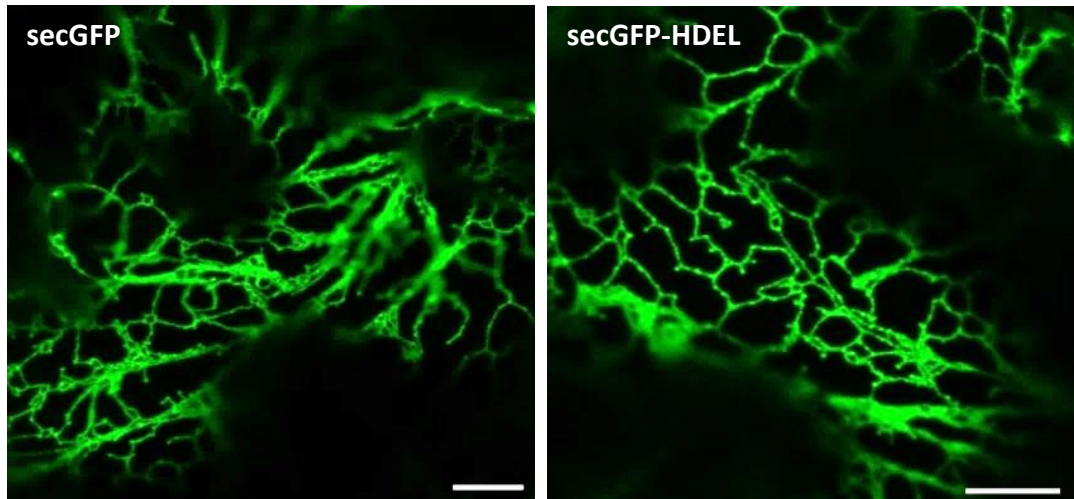
**Figure 2-1 Difference between secreted and ER retained GFP fusions is difficult to distinguish**

Recombinant fusions which containing a secreted GFP (secGFP, on the left) and a variant which bearing a HDEL motif at the C-terminus (secGFP-HDEL, on the right) were infiltrated in tobacco leaf epidermis cells via *Agrobacterium* mediated transformation (see Material and Methods). These fusions were constructed under the strong 35S promoter. Images were obtained after two and a half day of the infiltration. Scale bars are 10µm.
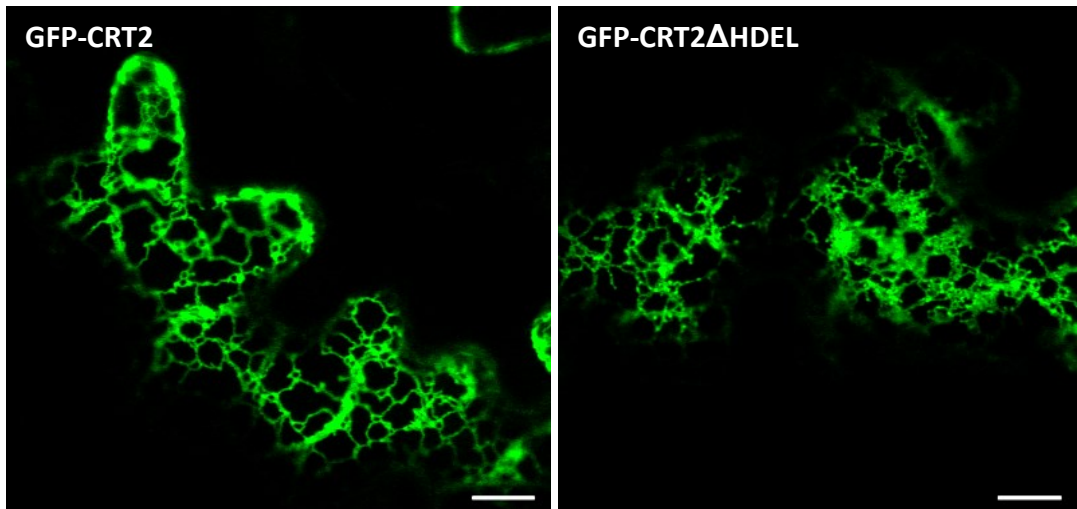


**Figure 2-2 HDEL dependent and independent calreticulin fusions**

GFP recombinant fusions which containing a ER retained calreticulin (GFP-CRT2, left) and a truncated version without HDEL motif (GFP-CRT2ΔHDEL, right) were infiltrated in tobacco leaf epidermis cells via *Agrobacterium* mediated transformation as before. 35S promoter was used for both fusions. Images were obtained after two and a half day of the infiltration. Scale bars are 10µm.

## 2.1.2.2 Evidence for signal dependent and signal-independent cell retention

In contrast to fluorescence microscopy, secreted enzymes such as barley α-amylase (Amy) have been successfully used as cargo molecules to quantify secretion versus cell retention in plant cells (Phillipson *et al*., 2001). Time-curves of secretion/retention assays revealed that the difference between secreted Amy and ER retained Amy-HDEL is dependent on the time after transfection, and thus the amount of cargo that has been synthesised by the cells. At early time points, cell retention of Amy-HDEL is absolute, whilst after reaching an intracellular steady state level, further accumulation of Amy-HDEL was only observed in the medium and occurred at the same rate as for secreted Amy. This suggests that once saturating levels of Amy-HDEL are reached, cells can no longer distinguish between Amy and Amy-HDEL. To expand these studies, different C-termini were compared to establish if differences in ER retention capacity can be revealed.

Figure 2-3 shows a comparison of secreted Amy with ER-retained Amy-HDEL, Amy-KDEL, Amy-EDDDHDEL and two Amy fusions harbouring the last 34 amino acids of the calreticulin C-terminus, either with (Amy-CRT2) or without the HDEL motif (Amy-CRT2ΔHDEL). All fusion proteins (boxed) are
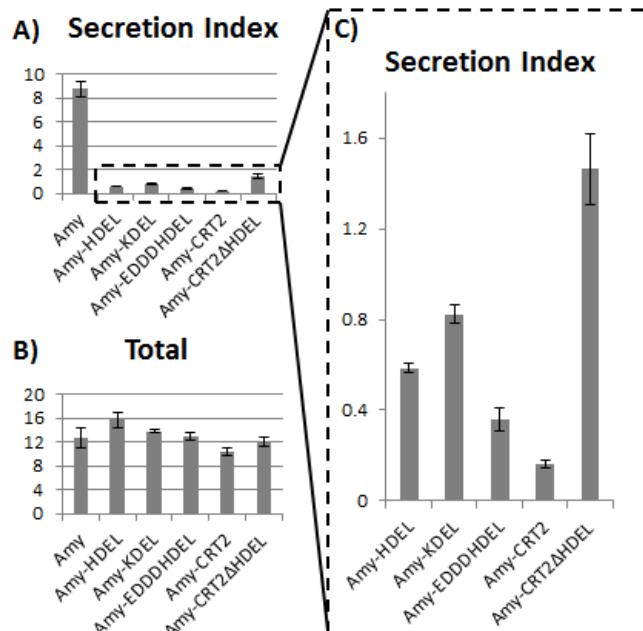


**Figure 2-3 HDEL dependent and independent ER retention**
Secreted α-amylase (Amy) and its recombinant fusions which bearing different ER retention signals (Amy-HDEL, Amy-KDEL, Amy-EDDDHDEL, Amy-CRT2 and Amy-CRT2ΔHDEL) were transiently expressed in tobacco protoplasts. Secretion index of each fusion was calculated by using the α-amylase activity from the medium divided by the activity from the cells and is represented in panel A. 10μg of DNA was used for each plasmid DNA preparations. Panel B illustrates the total α-amylase activity which obtained from each fusion. Secretion index of cell retained fusions is enlarged in panel C for close-up comparison. Error bars are standard deviations of three independent repeats. Units of α-amylase activity are ΔO.D./ml/min and secretion index units are considered as arbitrary.

strongly retained in the cells compared to secreted Amy (first lane, panel A) which is mainly found in the culture medium. Differences in the retention efficiency were unlikely due to differences in expression levels as all cargo was expressed at comparable levels (Figure 2-3B).

Upon close inspection of the secretion index of the fusion proteins (Figure 2-3C), it becomes obvious that the context of the retention signal can have a large influence of the effectiveness of the signal. Whilst HDEL and KDEL tetrapeptides showed small differences (with a p value of 0.0032 from their T-test) in the retention efficiency, the context of the HDEL signal appears to have a bigger effect on the secretion index. Addition of a short acidic stretch in front of the HDEL motif increased the retention efficiency by a factor two (with a p value of 0.0083 from their T-test). The long acidic C-terminus of calreticulin appears to favour ER retention even more, as seen by almost a 4-fold reduction in the secretion index of Amy-CRT2 compared to that of Amy-HDEL. However, the latter cannot be explained by a better display of the HDEL signal, because deletion of the HDEL motif did not reconstitute secretion to wild type Amy levels (compare first and last lane of panel A). In fact, Amy-CRT2ΔHDEL showed almost a 6-fold reduction in the secretion index, which suggests the presence of an HDEL-independent retention mechanism. It is possible that the acidic C-terminus of calreticulin mediates interactions with other ER residents harbouring acidic C-termini, possibly via calcium bridges (Koch, 1987; Macer and Koch, 1988), and thus mediating an indirect ER retention mechanism. In addition to signal-mediated ER retention, other mechanisms may thus contribute to ER retention (Rose and Doms, 1988).

## 2.1.2.3 Up-regulation of cell retention by AtERD2a/b

A model system to study functionality of the HDEL receptor should involve a cargo that is totally dependent on the HDEL system for ER retention and is not influenced by interactions with stationary components in the ER which could interfere with export to the Golgi and secretion. The use of an artificial cargo designed to pass through the plant secretory pathway rapidly and by bulk flow is therefore a better candidate for studying the functionality of the receptor, since endogenous ER residents such as BiP or calreticulin may have too many interactions with stationary components of the ER, such as translocation pores or other ER export incompetent structures.

Since it was shown that partial Amy-HDEL secretion is not due to poor ligand-binding but gradual saturation of the HDEL receptor as Amy-HDEL accumulates in the cells after plasmid transfection (Phillipson *et al*., 2001), it was timely to test if Amy-HDEL secretion can be suppressed by ectopically expressed ERD2 molecules. After complete genome sequencing, two ERD2 isoforms were found in *Arabidopsis thaliana*, AtERD2a and AtERD2b. In order to investigate the role of these genes in ER retention of HDEL ligands, these two genes were cloned into a double expression vector with the Golgi marker ST-CFP which acts as an internal reference to normalise plasmid transfection efficiency. Figure 2-4 illustrates the plasmid borne genes of three plasmids, encoding either secreted α-amylase (Amy), its ER retained derivative (Amy-HDEL) or the double construct harbouring overexpression gene fusions for AtERD2a or AtERD2b (DV ST-CFP-ERD2a/b).

| Amy | 35S | Amylase | | |
|---|---|---|---|---|
| Amy-HDEL | 35S | Amylase | HDEL | |
| DV ST-CFP-ERD2a/b | TR2 | ST-CFP | 35S | ERD2a/b |
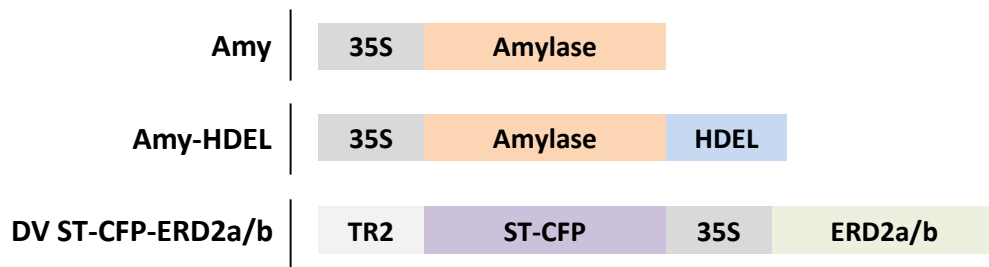
**Figure 2-4 Schematic view of transient expression constructs**
Names of the expression constructs are on the left and their corresponding schematic views are on the right. The secreted α-amylase (Amy), the ER retained α-amylase (Amy-HDEL) and AtERD2a/b (ERD2a/a) were driven by a strong expression 35S promoter. ST-CFP is driven by a weak promoter TR2 and is used as an internal marker for the double expression vector (DV ST-CFP-ERD2a/b) with either AtERD2a or AtERD2b.

To test if overexpression of ERD2 can increase the capacity of ER retention in a dose-dependent manner and thus suppress partial secretion of Amy-HDEL, plasmids harbouring either Amy or Amy-HDEL encoding genes were co-transfected with either of the two ERD2 overexpression plasmids. Figure 2-5 shows that both ERD2 isoforms strongly inhibited Amy-HDEL secretion in a strictly dose-dependent manner whilst no reduction in Amy-secretion was observed (panel A). Figure 2-5B shows that total expression levels of the cargo molecules were comparable and not influenced by overexpression of ERD2 proteins. Moreover, detection of the Golgi marker ST-CFP in both Amy and Amy-HDEL samples shows that the double expression vectors were co-transfected at comparable levels. This indicates the exclusive influence of receptor ERD2 on HDEL mediated retrieval without affecting constitutive secretion.

The results provide the first quantitative functional assay for ERD2 function in plants that is sufficiently robust to permit evaluation of ERD2 variants and ERD2 mutants with partial loss-of function phenotypes.
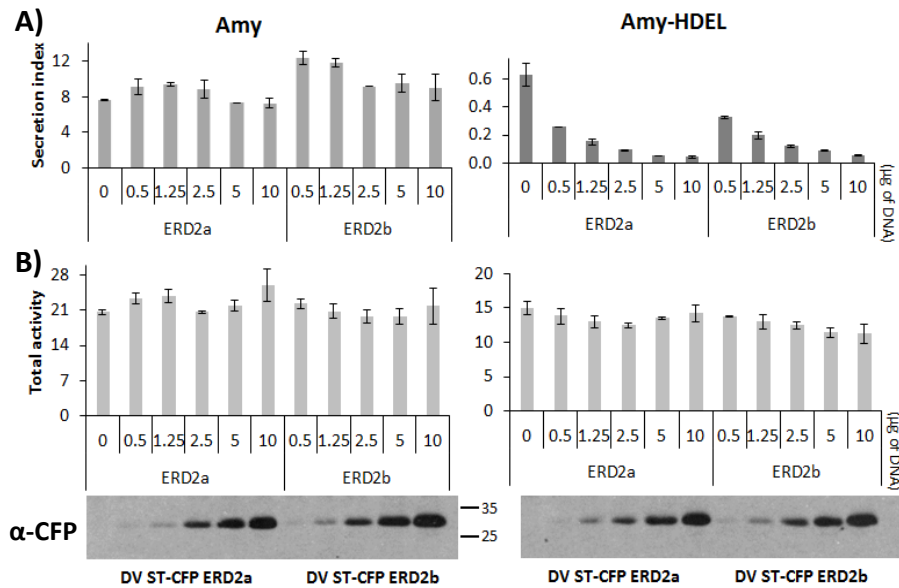


**Figure 2-5 Co-expression of α-amylase fusions with ERD2 in tobacco protoplasts**
Co-expression of DV ST-CFP-ERD2a/b with the secreted α-amylase (Amy, top left) is compare with co-expression with the ER retained α-amylase derivative (Amy-HDEL, top right). Secretion index of both co-expressions were calculated as before (results are shown in panel A). Constant amount of 10μg DNA from either Amy or Amy-HDEL was used across all relevant samples. The amount of DV ST-CFP-ERD2a and DV ST-CFP-ERD2b is indicated below each lane. The negative controls contain only cargo DNA (either Amy or Amy-HDEL). Panel B shows the total activity of medium plus cell samples followed by bottom panel (α-CFP) which illustrates the corresponding immunoblot against CFP (32kDa) to confirm the relative transfection efficiency of the ERD2-bearing plasmids. Error bars are standard deviation of three independent repeats. Units of α-amylase activity are ΔO.D./ml/min and secretion index units are considered as arbitrary.

## 2.1.2.4 Establishment of a fluorescent membrane cargo to study ER retention *in situ*

Experiments shown in Figure 2-5 are highly quantitative, but do not demonstrate that ERD2 mediates retention in the ER. To test if cell retention is due to accumulation in the ER, it was necessary to establish a model that permits detection of GFP fluorescence in the ER and in a post-ER compartment without losing fluorescence. In addition, ERD2 has only shown to recycle soluble cargo molecules, HDEL containing membrane protein may also be recognised by the receptor. To test this, I used the Golgi marker ST-YFP as it represents a type II

membrane protein with a short cytosolic N-terminus and YFP exposed in the lumen of the secretory pathway. The marker accumulates to very high steady state levels in the Golgi, and fluorescence is readily observed for this type of molecule (Boevink et al., 1998). To test if this molecule can serve as cargo for ERD2, the tetrapeptide HDEL was fused to the C-terminus of ST-YFP (Figure 2-6). The subcellular location of ST-YFP and ST-YFP-HDEL was subsequently compared after *Agrobacterium*-mediated transient expression in infiltrated tobacco leaf epidermis cells.
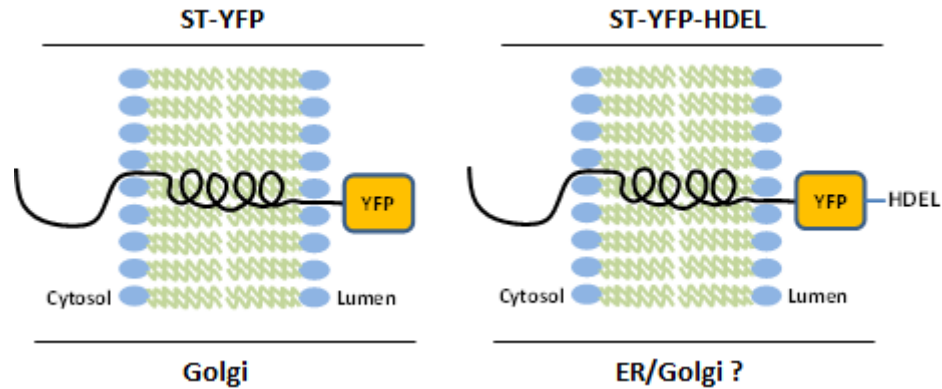


**Figure 2-6 Schematic view of the Golgi marker and its modified variant**
The name of each cargo tools is on the top and their corresponding schematic views are in the middle. Known/predicted localisation is indicated at the bottom of each schematic view. Golgi marker sialyltransferase (ST) is a type II transmembrane protein with its N-terminus in the cytosol and C-terminus in the lumen which fused with YFP (ST-YFP, as shown in the left panel). Addition of HDEL motif to the C-terminus of YFP (ST-YFP-HDEL) could be localised to either the ER or the Golgi.

Figure 2-7 shows a comparison of ST-YFP (panel A) with ST-YFP-HDEL (panel B) when expressed from the weak TR2 promoter shown to yield 10-fold lower signals compared to the CaMV35S promoter in tobacco leaf epidermis cells (Bottanelli *et al*., 2012). The image illustrates that the fusion protein totally redistributes to the ER when the HDEL-tetrapeptide is present at the YFP-C-terminus. The dramatic difference between the fluorescence pattern of ST-YFP and ST-YFP-HDEL is much more convincing than any potential differences in expression levels between secGFP and secGFP-HDEL (Figure 2-1) and therefore ideally suited to study ERD2 saturation and suppression of saturation via overexpressed ERD2.

### 2.1.2.5 Demonstration of receptor saturation *in situ*

To test if ERD2 saturation can be mediated by overexpressed Amy-HDEL in leaf epidermis cells, dual expression vectors were generated in *Agrobacterium* T-

DNA to co-express TR2-ST-YFP-HDEL either with Amy or Amy-HDEL which driven by the strong CaMV35S promoter. Since the two genes are present on the same T-DNA, co-expression is guaranteed as demonstrated before (Bottanelli *et al*., 2012) and although Amy or Amy-HDEL are invisible in fluorescence microscopy, their presence is confirmed if ST-YFP-HDEL fluorescence is observed.
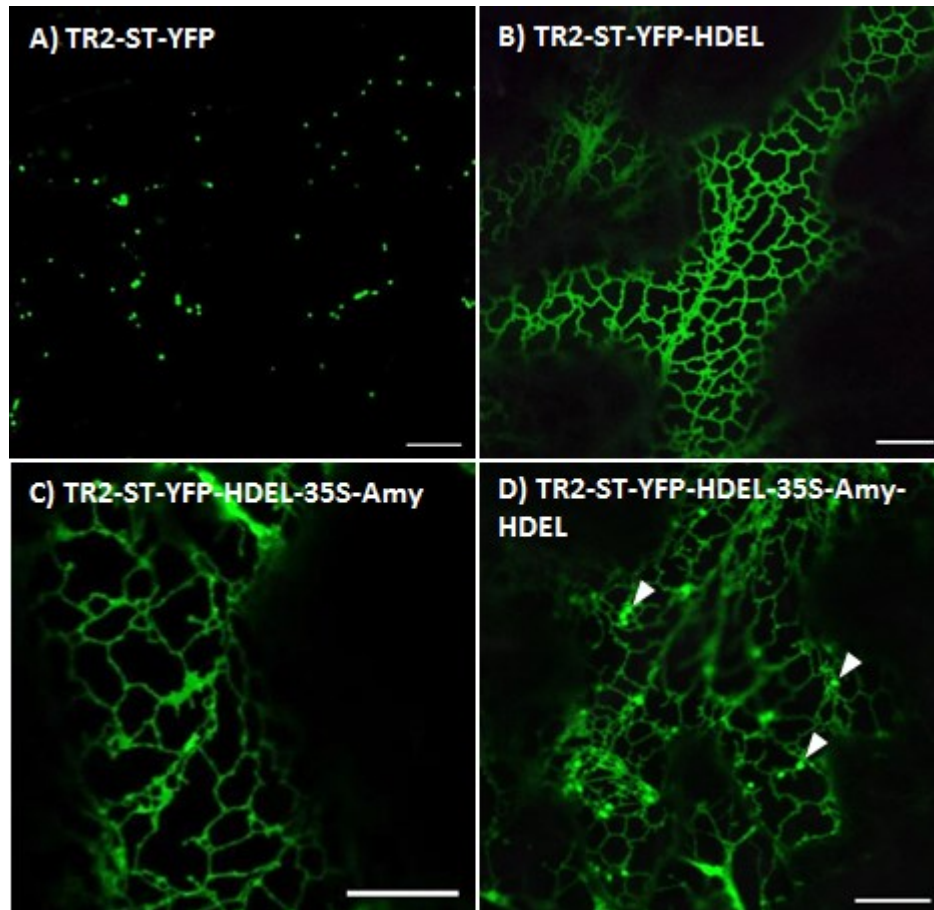


**Figure 2-7 Tools for ERD2 mediated ER retention *in situ***
TR2-ST-YFP and its variants (TR2-ST-YFP-HDEL, TR2-ST-YFP-HDEL-35S-Amy/Amy-HDEL) were infiltrated in tobacco leaf epidermis cells via *Agrobacterium* mediated transformation (see Material and Methods). Examples of HDEL saturation induced punctate structures are indicated by white arrowheads (bottom right panel). Images were obtained after two and a half day of the infiltration. Scale bars are 10µm.

Figure 2-7C shows that the overexpressed non-ligand Amy has no effect on the subcellular localisation of ST-YFP-HDEL. All images obtained continued to show the typical ER pattern, regardless of expression levels. In sharp contrast, overexpressed Amy-HDEL caused significant leakage of ST-YFP-HDEL out of the ER in the vast majority of the images, except those with extremely low expression of ST-YFP-HDEL. ST-YFP-HDEL was seen in punctate structures that show strong

resemblance to Golgi bodies based on the even size distribution of the structures and their association with the ER network (white arrowheads).

### 2.1.2.6 Evidence for ERD2 mediated ER retention *in situ*

In order to test if saturation-mediated leakage of ST-YFP-HDEL indeed leads to the Golgi apparatus and to test if this can be suppressed by increasing levels of ERD2, dual expression T-DNA vectors were generated harbouring the Golgi marker ST-RFP (Foresti et al., 2010) and an overexpression construct of mock effector PAT or effector AtERD2b. Figure 2-8 shows that PAT has no influence on the leakage of ST-YFP-HDEL to punctate structures, which co-localise with the Golgi marker ST-RFP. In sharp contrast, ERD2 overexpression resulted in a complete re-distribution of ST-YFP-HDEL back to the ER, as illustrated by a lack of green fluorescence in the ST-RFP labelled Golgi bodies (as shown in enlarged close-up picture, top panel, Figure 2-9).

Leakage to the Golgi was quantified by correlation analysis from at least 400 punctate structures of many different cells for either the mock effector PAT or the ERD2 overexpression constructs using the PSC co-localisation plug-in for ImageJ (French *et al*., 2008). This provided a typical red-green scatter plot (bottom panel, Figure 2-9). The scatterplot generated from images of cells overexpressing the mock effector PAT revealed a population of yellow pixels (containing red and green) which represents the Golgi bodies and a close population of predominantly green pixels, which represent ER close to imaged Golgi bodies that was impossible to avoid. Notice that upon ERD2 co-expression, punctate structures were significantly red-shifted compared to the data obtained with the mock effector PAT and there was a distinct red-only population, in addition to a green only population that again represents ER that was difficult to avoid whilst selecting areas covering Golgi bodies. The results illustrate that ST-YFP-HDEL leaks to ST-RFP labelled Golgi bodies, and that this leakage is suppressed by ERD2 overexpression. Importantly, ectopic expression of ERD2 results in re-distribution of ST-YFP-HDEL back to the ER, but no other organelle. Therefore, ERD2 mediated cell retention is due to accumulation in the ER.
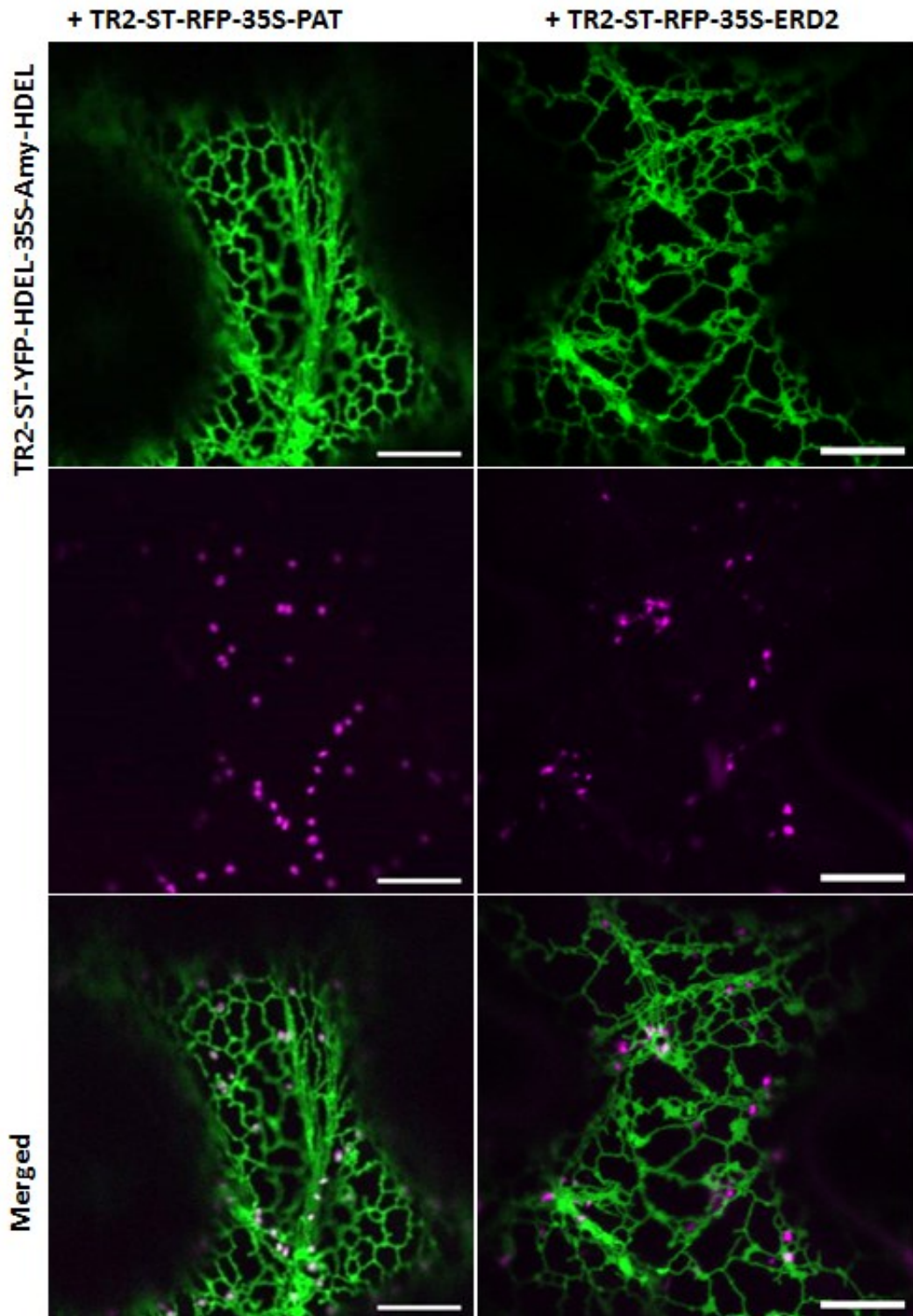
**Figure 2-8 ERD2 mediated ER retention *in situ***
Double expression vector containing ST-YFP-HDEL with additional HDEL ligand (TR2-ST-YFP-HDEL-35S-Amy-HDEL) is co-expressed with another double expression vector of ST-RFP either containing AtERD2b (TR2-ST-RFP-35S-ERD2) or PAT (TR2-ST-RFP-35S-PAT) as a neutral control. These fusions were co-infiltrated in tobacco leaf epidermis cells via *Agrobacterium* mediated transformation (see Material and Methods). TR2-ST-YFP-HDEL-35S-Amy-HDEL is shown on the top panel and the effectors containing ERD2 as well as control PAT is shown in the middle panel. Merged images are presented at the bottom panel. Images were obtained after two and a half day of the infiltration. All scale bars are 10µm.
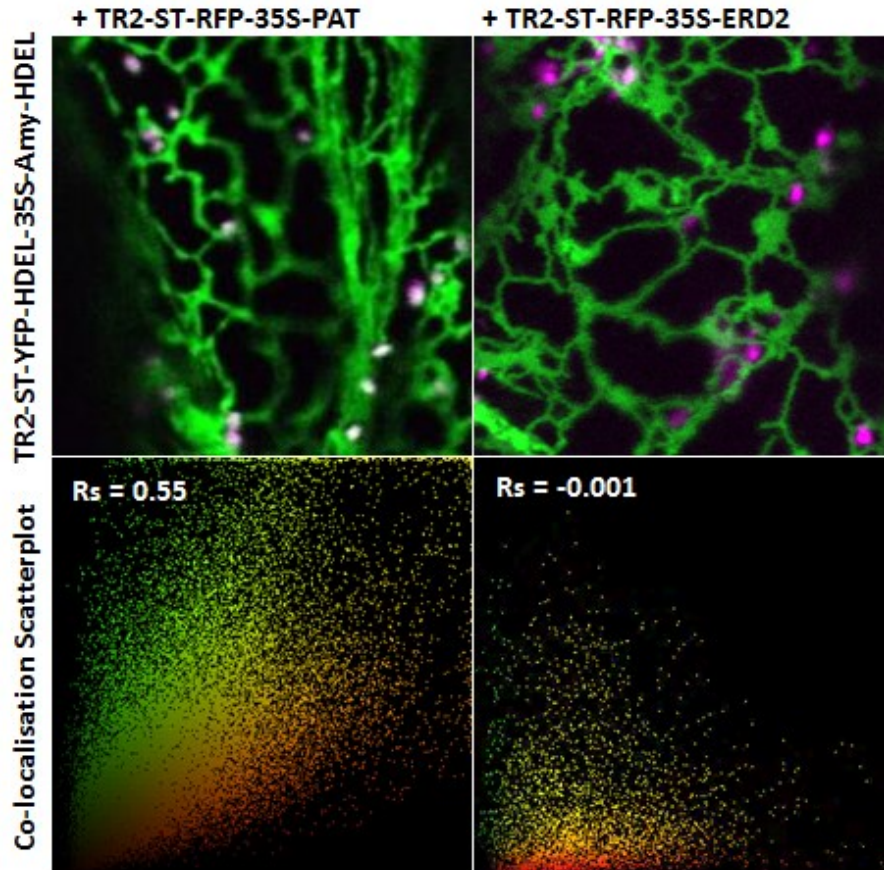
**Figure 2-9 Co-localisation analysis of saturated ST-YFP-HDEL**
Close-up merged image of TR2-ST-YFP-HDEL-35S-Amy-HDEL with either TR2-ST-RFP-35S-ERD2 (top left) or TR2-ST-RFP-35S-PAT (top right) is shown at the top panel. Their resulting Sperman's correlation coefficient scatter plot is shown at the bottom panel accordingly. Results of correlation are indicated as Rs values whereas -1 is not correlated and 1 is highly correlated. Over 25 images were sampled for the coefficient analysis. Confocal images were obtained after infiltration in tobacco leaf epidermis cells via *Agrobacterium* mediated transformation (see Material and Methods).

## 2.1.2.7 Establishment of a quantitative internal marker for amylase secretion assays

In order to compare different cargo molecules, it is important to normalise expression levels. A double expression vector, as illustrated in Figure 2-4, yields only semi quantitative data from the western blot and is not ideal as quantitative reference for plasmid transfection rates. Moreover, the reference marker should ideally not influence the secretory pathway. The cytosolic reporter GUS has been successfully used as an internal marker to distinguish ER stress from general cell mortality (Leborgne-Castel *et al*., 1999) and was recently used to simplify effector dose-response assays in vacuolar protein sorting research (Gershlick *et al*., 2014). Here this double expression plasmid was re-constructed to harbour either the

control cargo Amy or the ER-retained derivatives Amy-HDEL and Amy-KDEL (as illustrated in Figure 2-10A)

The internal marker GUS expression can be readily measured enzymatically upon transfection and the result is applied for equalisation of different DNA preparations. Figure 2-10B shows a pilot assay to compare three newly prepared plasmid preps in transient expression assays. Measuring GUS activity for a typical
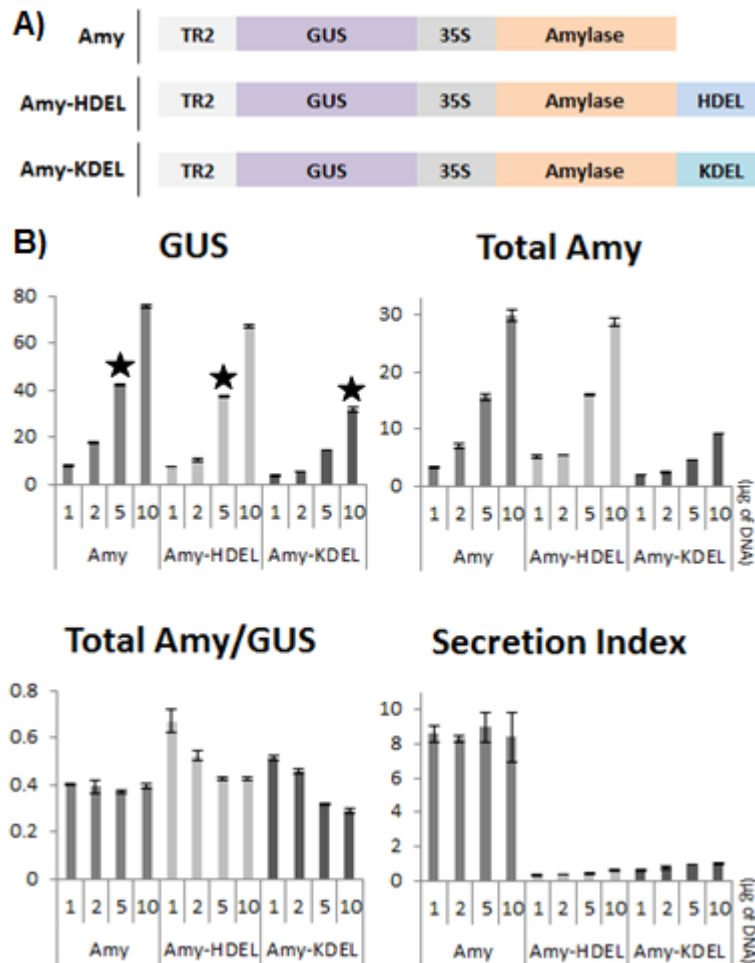


**Figure 2-10 Comparison of Amy fusions in tobacco protoplasts via transient expression**
Secreted α-amylase (Amy) and its ER retained variants containing either HDEL (Amy-HDEL) or KDEL motif (Amy-KDEL) were sub-cloned into GUS double vector (as shown in panel A). The amount of DNA used is indicated below each lane (panel B). Suitable dosage of DNA for all future analysis is indicated (black stars, panel B, top left) without compromising total DNA expression (as represented by total Amy activity, panel B, top right). Total α-amylase activity against GUS expression (Total Amy/GUS) was used for comparison of transfection efficiency (bottom left, panel B). Secretion Index of all fusions is illustrated (bottom right, panel B). Since it's difficult to compare the secretion index value for Amy-HDEL and Amy-KDEL their values are listed as following: 1)0.35, 2)0.34, 5)0.42 and 10)0.6; 1)0.63, 2)0.76, 5)0.95 and10)1.02 respectively. Error bars are standard deviation of three independent repeats. Units of α-amylase activity are ΔO.D./ml/min and secretion index units are considered as arbitrary.

dilution series of plasmids revealed that the Amy-KDEL encoding plasmid was transfecting at much lower efficiency. This is reflected by the total Amy activity. However, analysis of the Total Amy/GUS ratio reveals that data can be normalised via a common reference, yet it is also illustrated that it is worthwhile to adjust the DNA concentrations to equalise expression levels as much as possible. The Total Amy/GUS ratio also reveals that constructs harbouring an ER retention signal show a systematic reduction of expression against the internal marker with higher plasmid concentrations. As such reduction was not observed for the control marker Amy; it is possible that it is caused by the retention signal.

A plausible hypothesis for the obtained reduction in expression is that progressive saturation of the ER retention machinery causes not only increased secretion of the artificial cargo molecules to the medium, but may also lead to leakage of endogenous ER residents, such as the chaperone BiP, to the culture medium. Since these ER residents may be needed for protein translocation and folding in the ER lumen, saturation of the retention machinery may lead to inhibition of protein synthesis on the rough ER, but not in the cytosol (as measured by the marker GUS). A reduction in the Total Amy/GUS ratio was successfully used to document ER stress (Leborgne-Castel *et al*., 1999). Here the ratio reports on a more specific difference between the presence and absence of ER retention signals.

Calculation of the secretion index reveals that with higher plasmid concentrations the leakage of cargo harbouring retention signals increases steadily. A factor two increases in the secretion index can be seen between the lowest and highest plasmid concentration, which is much larger than the standard deviation in those measurements (see numbers in figure legend). In contrast, the control cargo Amy showed no significant change in the secretion index with increased plasmid concentrations and certainly no upwards trend. This result further illustrates the need to normalise expression as much as possible for subsequent transport experiments. This is accomplished by choosing plasmid concentrations yielding comparable GUS expression levels (concentrations chosen for comparative studies are indicated by a black star above the lanes of the GUS panel).

## 2.1.2.8 Ligand specificity of AtERD2a/b

Results in Figure 2-3 and Figure 2-10 indicate that Amy-KDEL has a slightly higher secretion index than that of Amy-HDEL. Even though both AtERD2 isoforms

were shown to recognise Amy-HDEL, it could not be ruled out that the two isoforms have different ligand binding specificities and show small preferences to one of the two signals, HDEL or KDEL. For this reason, appropriate plasmid concentrations for comparable GUS expression levels were chosen to specifically compare the effect of ERD2a and ERD2b on both Amy-HDEL and Amy-KDEL as cargo. Figure 2-10 shows a dose-response analysis and confirms that Amy-KDEL is marginally faster secreted than that of Amy-HDEL, but that ERD2a and ERD2b reveal no cargo preference.

Both receptors can clearly recognise either the KDEL or the HDEL motif and there is no indication from the dose response that could be used to distinguish the two receptor isoforms, which should therefore be regarded as fully interchangeable. Any differential effects observed from single gene knockouts (Li *et al.*, 2009) are therefore likely due to endogenous ERD2 expression levels which are probably higher for ERD2b. The results in Figure 2-11 completely refute the earlier hypothesis that ERD2b is specifically responsible for the ER retention of CRT3 but
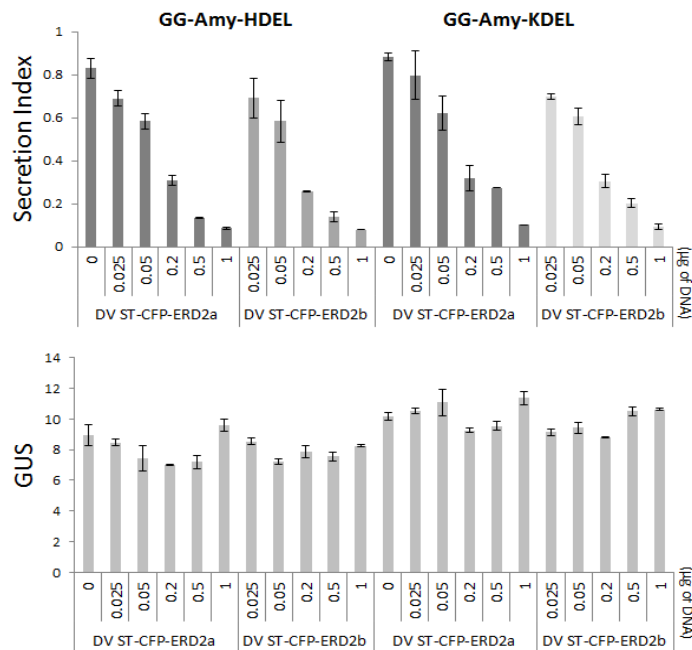


**Figure 2-11 Co-expression of ER retained fusions with ERD2 in tobacco protoplasts**
Co-expression of DV ST-CFP-ERD2a/b with the ER retained α-amylase derivative (GG-Amy-HDEL and GG-Amy-KDEL) is performed in tobacco protoplasts. Secretion index of both co-expressions is shown in panel A. Constant amount of DNA from either GG-Amy-HDEL or GG-Amy-KDEL was used across all designated samples. The amount of DV ST-CFP-ERD2a and DV ST-CFP-ERD2b is indicated below each lane. The negative controls contain only cargo (either Amy-HDEL or Amy-KDEL) DNA. Panel B shows the GUS activity for both HDEL and KDEL plasmids. Error bars are standard deviation of three independent repeats. Units of α-amylase activity are ΔO.D./ml/min and secretion index units are considered as arbitrary.

not for other HDEL proteins (Li *et al.*, 2009).

### 2.1.3  Discussion

### 2.1.3.1 Study of ER retention mechanisms has to be above endogenous levels

Endogenous ER residents are highly abundant and represent the vast majority of proteins in this compartment, even in cell types that secrete large amounts of proteins. This has led to the idea that they may be slowly exported from the ER and that recycling from the Golgi plays only a minor role in ER retention (Pagny et al., 2000).  Many ER residents could also be present in large complexes (Tatu and Helenius, 1997), which would show slow diffusion rates and poor ER export properties. However, the fact that ER residents have quite variable properties is illustrated by the fact that deletion of HDEL from the ER chaperone BiP leads to almost undetectable secretion of the truncated molecule, whilst the same deletion in calreticulin led to much faster secretion (Crofts *et al.*, 1999). One explanation was that truncated BiPΔHDEL could be retained by association with HDEL containing wild type calreticulin, as the two molecules interact quite strongly with each other *in vivo* (Crofts *et al.*, 1998).

Results in Figure 2-1, Figure 2-2 and Figure 2-3 illustrate that even artificial cargo molecules may show highly different secretion rates. Secreted GFP is slowly folded (Brandizzi *et al.*, 2003) and mostly accumulates in the ER (Figure 2-1), and is therefore ill-suited for the analysis of ER retention signals and machinery. Barley α-amylase is a naturally secreted protein in barley aleurone layer, and when introduced to the secretory pathway of tobacco cells, it continues to secrete well, but is quite strongly retained upon fusion to the tetrapeptide HDEL (Phillipson *et al.*, 2001). Introduction of three different cytosolic proteins to the ER of tobacco cells resulted in three different secretion rates (Denecke *et al.*, 1990), suggesting that many parameters contribute to the rate of exocytic protein flow through the secretory pathway.

Figure 2-3 illustrates that signal-independent ER retention mechanisms can significantly contribute to ER retention. The C-terminus of calreticulin 2 (CRT2) is mainly composed of negatively charged acidic amino acids preceding the HDEL tetrapeptide. Two α-amylase fusions bearing this C-terminus were created to show if context-dependence influences the efficiency of the HDEL signal. The results

suggest that the effect of HDEL and the acidic C-terminus are independent and additive. The α-amylase fusion was quite effectively retained in the cells even in the absence of the HDEL signal, whilst in its presence the retention was several times more effective than in the fusion bearing only the HDEL signal.

It is possible that negatively charged residues can bind to $Ca^{2+}$ ions in the ER and form bridges between proteins in addition to their role in $Ca^{2+}$ storage (Nash *et al.*, 1994). In addition, the α-amylase fusion containing the calreticulin C-terminus may thus form complexes with other ER residents and only a fraction would then be escaped from the ER by bulk flow.

*In vivo* protein transport assays are hampered by the fact that the biochemical conditions of ligand-binding and receptor transport are unknown, but perfectly optimised for biological function. *In vitro* assays have the advantage that they are carried out with purified components and under controlled biochemical conditions. In this case, the conditions will be known, but may not be optimised for biological function. In order to establish a receptor-ligand binding assay *in vivo* that has a minimal number of variables but yet benefits from ideal biochemical conditions for biological function, it is necessary to establish a model system that permits the analysis of a single type of cargo with a single type of receptor. This was achieved by saturating the ER retention machinery with the artificial cargo Amy-HDEL, which is completely dependent on the HDEL motif for ER retention.

## 2.1.3.2 ER retention can be up-regulated in a dose-dependent manner by overexpression of ERD2

Earlier results obtained with transport assays describing the behaviour of Amy-HDEL (Phillipson *et al.*, 2001) strongly suggested that secretion was not caused by poor binding to the receptor ERD2, but by gradual saturation of the retention machinery since the cargo is very stable and continues to accumulate in the ER-Golgi system until a steady state is reached. The central working hypothesis in this project was that under saturating conditions, ERD2 levels are the limiting factor in the system and represent a partial loss-of-function phenotype for ERD2. Figure 2-5 shows strong experimental support for this hypothesis. Increasing concentrations of co-transfected plasmids encoding ERD2 had no effect on constitutive secretion of the control cargo Amy, but strongly influenced the ligand Amy-HDEL to restore effective cell retention. This result was reproduced *in situ* by creating a unique membrane spanning HDEL protein (ST-YFP-HDEL, Figure 2-6)

that accumulates in the Golgi when ER retention is saturated by a second overexpressed HDEL protein (Figure 2-7). ERD2 overexpression could effectively prevent leakage of this marker to the Golgi (Figure 2-8), and since no other organelle was labelled besides the ER, the results show that ERD2-mediated cell retention is in the ER. The dramatic difference between the strict Golgi pattern of ST-YFP expressed from the weak TR2 promoter and the typical ER pattern from ST-YFP-HDEL expressed from the same promoter provides a new model system to study HDEL-mediated transport processes *in situ*.

In order to render the protoplast model system more quantitative for proper dose-response analysis, the dual expression vector system using the cytosolic enzyme GUS for normalising plasmid transfection efficiency (Gershlick *et al*., 2014) was adapted to carefully control ligand expression. Using this system it was possible to show that ERD2-saturation with HDEL ligands may cause ER stress. Using normalised cargo expression, it was also possible to demonstrate that both isoforms of ERD2 in *Arabidopsis* show the same ligand-specificity for Amy-HDEL or Amy-KDEL. Although the two cargos were transported with slightly different ER retention efficiencies, there was no evidence that permitted a functional differentiation of ERD2a and ERD2b. Since there was no noticeable functional difference between the two isoforms, only isoform AtERD2b (ERD2b) was used in the remainder of this thesis project and considered representative of *Arabidopsis* ERD2 gene family. The combined data in Figures 2-5, 2-8 and 2-11 also justify the use of Amy-HDEL as an ideal ERD2-ligand representative of typical ERD2-cargo, and Amy as a control (non-ligand).

Importantly, the resulting experimental system permits the analysis of the sorting of one specifically defined ligand in function of an equally defined receptor molecule, well above the endogenous levels of receptors and ligands with variable abundance and binding specificities. Although the model system is a true *in vivo* bio-assay, it yet deals with defined variables and permits analysis of receptor variants for quantitative functional analysis.

## 2.2 Chapter II Localisation and topology of ERD2 in plants

### 2.2.1 Introduction

Although ERD2 was identified and characterised more than two decades ago, important questions regarding the function of this important receptor molecule remain unanswered. Extensive mutagenesis studies were conducted (Townsley *et al*., 1993; Scheel and Pelham, 1998) but it is still unclear how a low abundant protein such as ERD2 can mediate the retention of the far more abundant reticuloplasmins. Does it recycle faster than bulk flow, or does it bind and transport several ligands simultaneously? It is still unknown which conditions cause ligand binding and ligand release *in vivo*. It is even less clear what prevents ERD2 from reaching post-Golgi compartments (Pfeffer, 2007). More importantly, signals for Golgi to ER retrograde transport and ER to Golgi anterograde transport are yet to be identified and clearly differentiated from ligand-binding domains.

Since ligand-binding studies were not conducted with purified components but instead with microsome preparations from cells overexpressing ERD2, it cannot even be certain if HDEL or KDEL cargo directly binds to ERD2, or if there are other proteins involved in this process. Finally, not even the topology has been established, as recent studies questioned the seven transmembrane domain structure originally proposed (Townsley *et al*., 1993; Scheel and Pelham, 1998). Experiments with a fused N-glycosylation reporter suggested a six transmembrane domain structure (Singh *et al*., 1993). Redox-based topology analysis using redox-sensitive GFP fusions also supported this alternative six transmembrane domain model for ERD2 with both N-terminus and C-terminus exposed to the cytosol (Brach *et al*., 2009). However, GFP fusion could have induced a positive charged amino acid at the beginning of the ERD2 N-terminus which might have flipped the molecule thus changing the native luminal topology of the N-terminus to cytosolic.

This results chapter aims at establishing further insight into the nature of ERD2 molecules via subcellular localisation of fluorescent proteins and experiments that may shed light on the topology of these two classes of proteins.

## 2.2.2  Results

### 2.2.2.1 N-terminal and C-terminal fluorescent tagging of ERD2 results in different subcellular localisation

Although earlier studies have been conducted with N-terminal and C-terminal fluorescent fusions of ERD2 (Brach *et al.*, 2009), these studies did not include details about any differences in the subcellular localisation of ERD2, dependent on the position of fluorescent tagging. For this reason, N-terminally fused YFP-ERD2 and C-terminally fused ERD2-YFP were created in this study and their subcellular localisation was tested in tobacco leaf epidermis cells after *Agrobacterium*-mediated transformation.
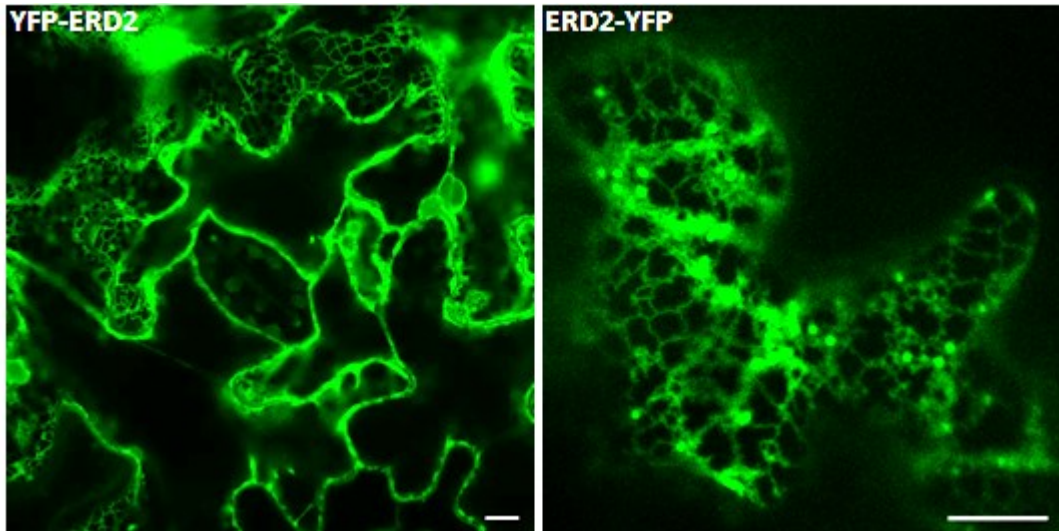


**Figure 2-12 N-terminal and C-terminal fusions of ERD2 *in vivo***
YFP was fused to ERD2 either at the N-terminus or the C-terminus for localisation studies and both fusions are driven under the strong 35S promoter. N-terminal fusion (YFP-ERD2) is always poorly expressed and difficult to find suitable regions. On the other hand, C-terminal fusion (ERD2-YFP) is relative easy to find. Confocal images were obtained after infiltration in tobacco leaf epidermis cells via *Agrobacterium* mediated transformation (see Material and Methods). Images were obtained after two and a half day of the infiltration.  All scale bars are 10μm.

Figure 2-12 shows that the position of fluorescent tagging crucially influences the subcellular localisation. N-terminally YFP-tagged ERD2 was difficult to detect due to low expression levels and required high detector gains and laser power for high quality imaging. YFP-ERD2 was seen in the ER, but also in the cytosol as indicated by occasional negative stains. Since cytosolic stains are pseudo-reticular by nature and can easily be confused with the ER, sharp well defined negative stains representing organelles excluding cytosol are typically used as indications for

cytosolic localisations, but the crisp tubular pattern in some areas of the cells also show clear evidence for ER labelling. There was no evidence for labelling of typical punctate and mobile structures representing Golgi bodies (Figure 2-13), as there was no co-localisation with the Golgi marker ST-RFP. Furthermore, overlap with the ER marker RFP-HDEL was also not absolute, and the fluorescence pattern of RFP-HDEL was a-typical, suggesting that YFP-ERD2 overexpression may have a detrimental effect on cell viability (Figure 2-14).
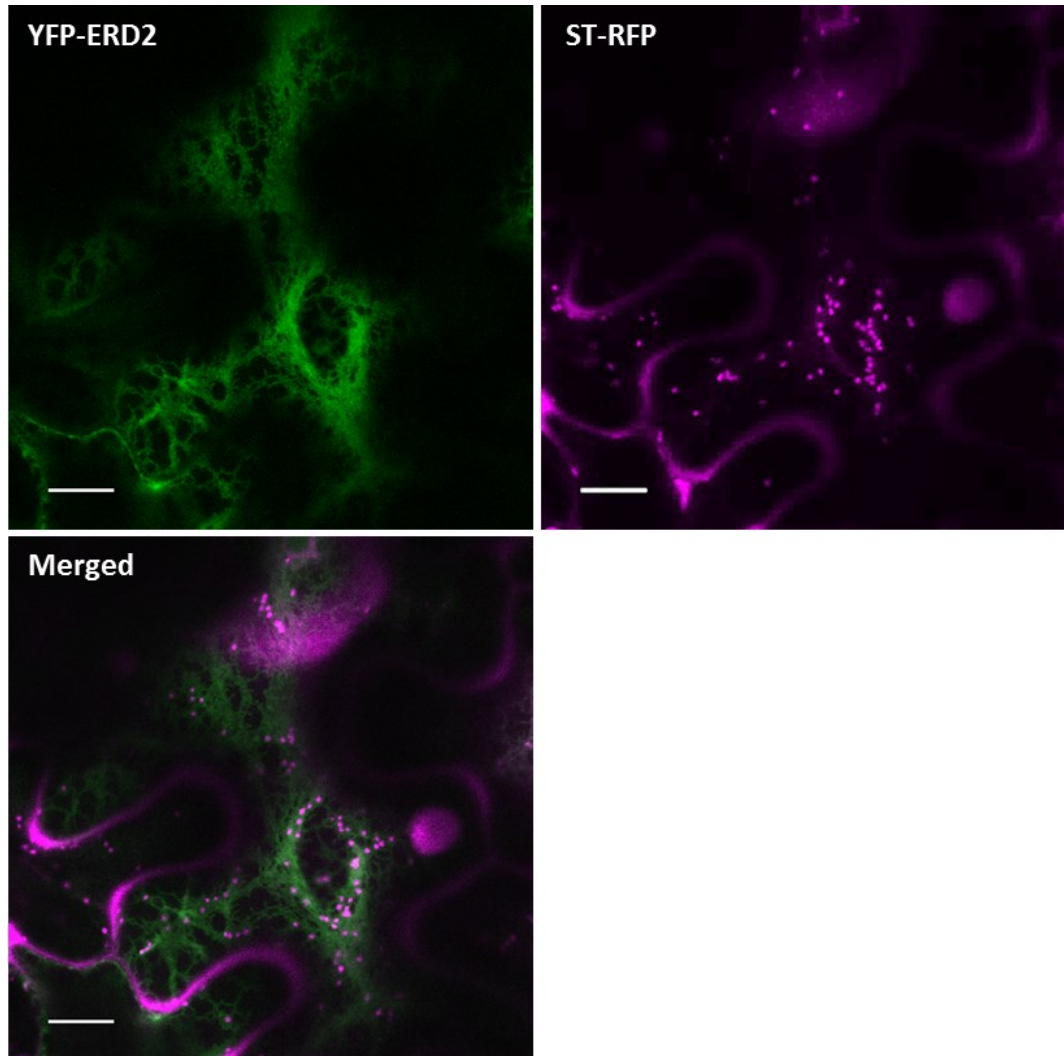


**Figure 2-13 N-terminal tagged ERD2 co-localisation with Golgi marker *in vivo***
YFP-ERD2 (top left) was co-expressed with Golgi marker ST-RFP (top right). Images were difficult to obtain due to poor expression. When expressed, YFP-ERD2 does not co-localise with ST-RFP (as shown in the merged image, bottom left). All fusions are driven by 35S promoter. Confocal images were obtained after two and a half day of the infiltration in tobacco leaf epidermis cells via *Agrobacterium* mediated transformation (see Material and Methods). All scale bars are 10μm.

In sharp contrast, C-terminally YFP-tagged ERD2 was predominantly found in the Golgi bodies, giving rise to typical uniformly sized bright punctate structures that move on the ER network. ERD2-YFP was also detected in transit via the ER, as published earlier (Boevink *et al.*, 1998). The dramatic difference in subcellular localisation between the two types of fusion proteins justified a closer investigation, as the result has significant implications for earlier studies based on the study of N-terminal fusions (Brach *et al.*, 2009).
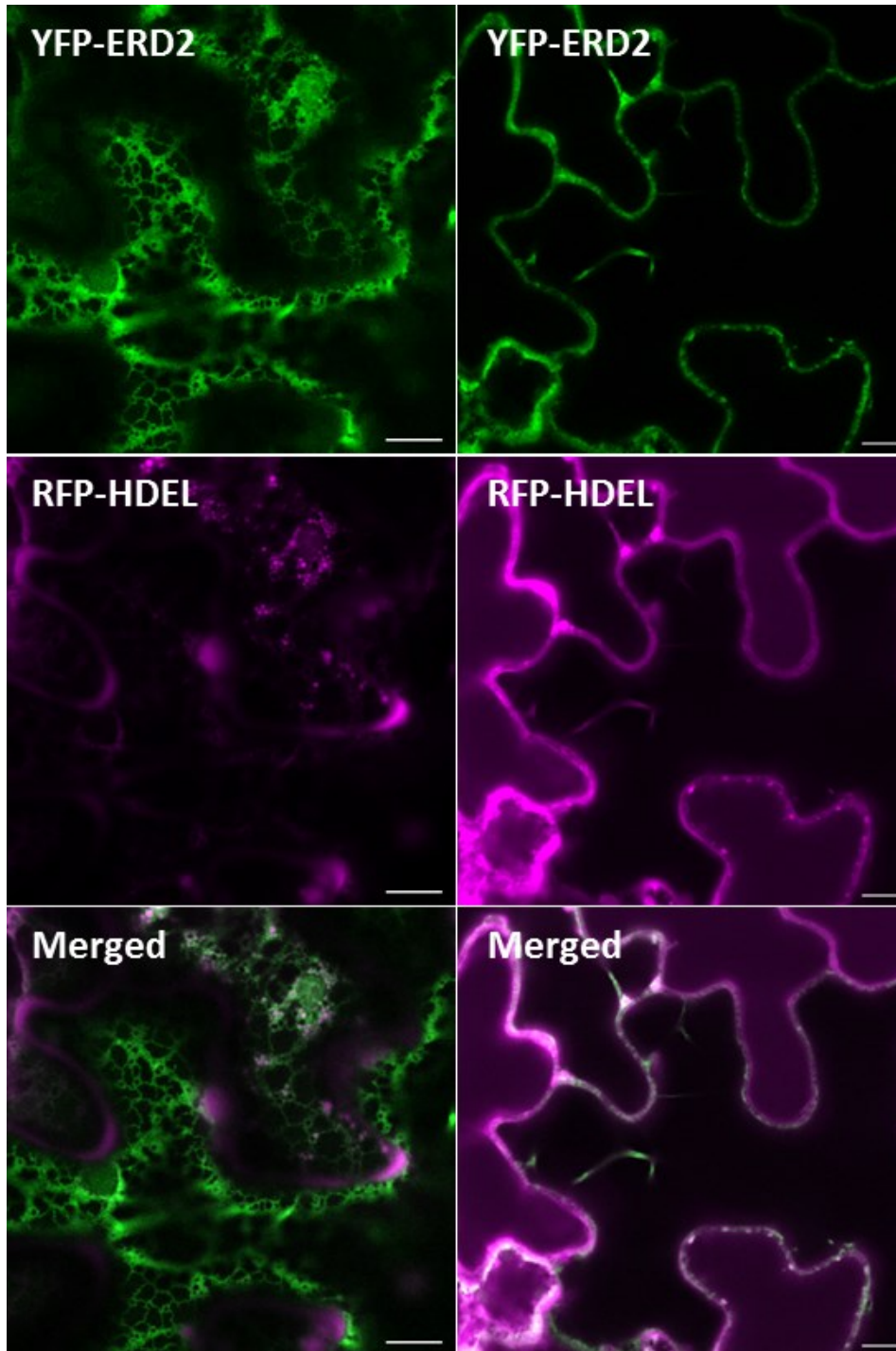
**Figure 2-14 N-terminal tagged ERD2 co-localisation with ER marker *in vivo***
YFP-ERD2 (top panels) was co-expressed with ER marker RFP-HDEL (middle panels). Images were difficult to obtain due to poor expression. When expressed, YFP-ERD2 localised partially to RFP-HDEL (bottom merged panel). The expression of RFP-HDEL upon co-expression with YFP-ERD2 however is disturbed and distribute to either punctate structures or the vacuole. All fusions are driven by 35S promoter. Confocal images were obtained after two and a half day of the infiltration in tobacco leaf epidermis cells via *Agrobacterium* mediated transformation (see Material and Methods). All scale bars are 10µm.

## 2.2.2.2 The nature of the fluorescent tag does not influence localisation

In order to create more tools for the analysis of ERD2 transport in conjunction with other fluorescent probes of known localisation, the YFP portion in the C-terminally tagged ERD2 was replaced by RFP. Figure 2-15 shows that ERD2-RFP and ERD2-YFP strongly co-localise to the same punctate structures, suggesting that the nature of the fluorophore does not influence the subcellular location of ERD2. However, when two fusions were co-expressed with each other under the weak promoter TR2, ERD2-RFP is mostly found in punctate structures whereas ERD2-YFP is not only found in punctate structures but also in reticulum networks (Figure 2-16). Close-up merged image of their co-localisation is shown have a slightly polarised effect of the punctate structures and indicated by white arrowheads. Although the two ERD2 C-terminal fusions have a non-perfect co-localisation when ERD2-RFP was co-expressed with both the Golgi marker ST-YFP and the ER marker GFP-HDEL, ERD2-RFP was strongly co-localised with ST-YFP but not GFP-HDEL which is undetectable in Golgi bodies (Figure 2-17).
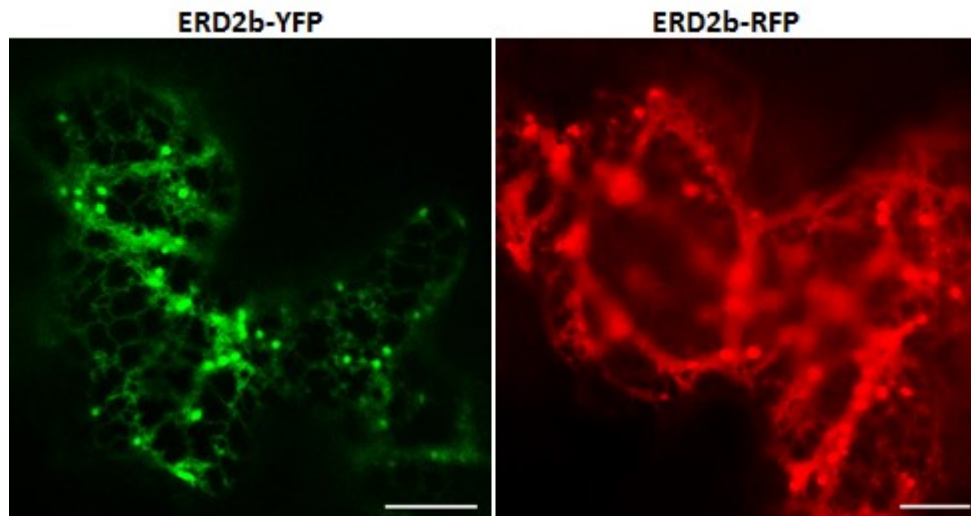


**Figure 2-15 C-terminus fusions of ERD2 morphology *in vivo***
ERD2 was fused with either YFP (ERD2-YFP, left panel) or RFP (ERD2-RFP, right panel) at its C-terminus and *in vivo* images show little differences between these two constructs. Both fusions are constructed under 35S promoter. Confocal images were obtained after infiltration in tobacco leaf epidermis cells via *Agrobacterium* mediated transformation (see Material and Methods). Images were obtained after two and a half day of the infiltration. All scale bars are 10µm.
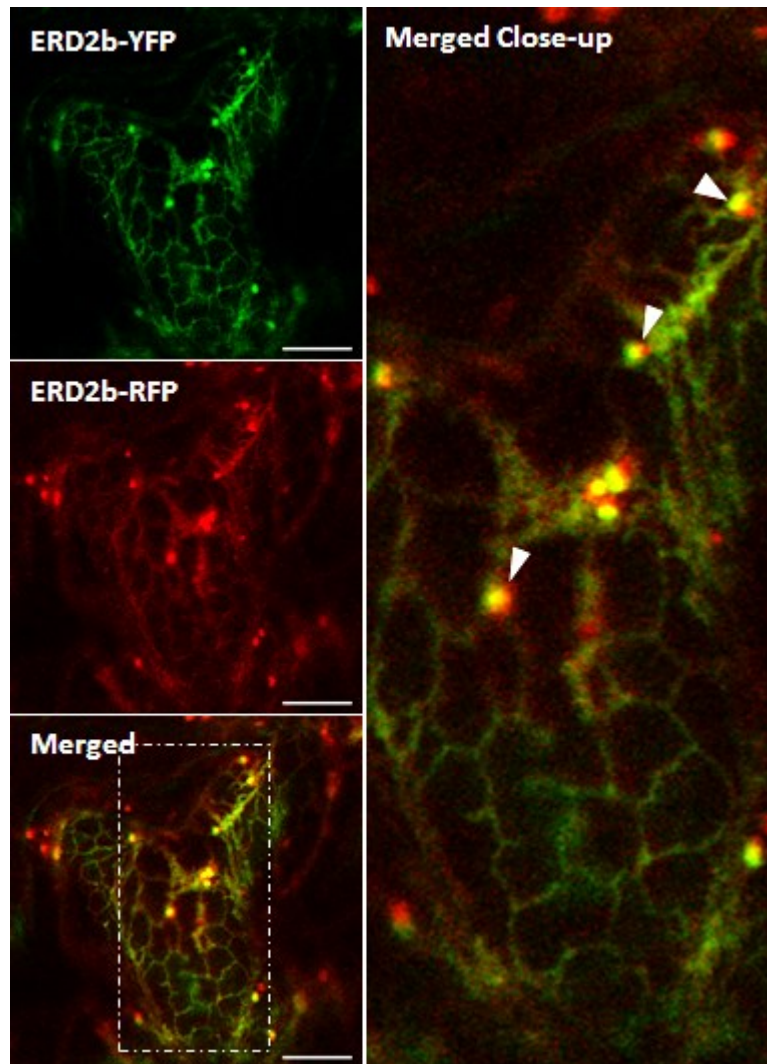
**Figure 2-16 C-terminus fusions of ERD2 localisation comparison**
ERD2 was fused to either YFP (ERD2-YFP, top left panel) or RFP (ERD2-RFP, middle left panel) at its C-terminus. Both C-terminal fusions label punctate structures as well as some reticulum network. Merged close-up image (right panel) is enlarged from the highlighted dashed rectangle area (left bottom). Examples of fluorescence polarisation are indicated by white arrows. To obtain high quality *in vivo* images, weak promoter TR2 was used. Confocal images were obtained after infiltration in tobacco leaf epidermis cells via *Agrobacterium* mediated transformation (see Material and Methods). Images were obtained after two and a half day of the infiltration. All scale bars are 10µm.

Since ERD2-RFP yields essentially the same results as ERD2-YFP, it was possible to test if N-terminal fusion of YFP would influence the fate of the C-terminal RFP fusion. For this reason, a double tagged ERD2 fusion was created bearing YFP at the N-terminus and RFP at the C-terminus. Fluorescent imaging revealed that the resulting fusion (YFP-ERD2-RFP) was now very difficult to detect due to low expression levels and labelled the ER in both fluorescent channels (Figure

2-18). This shows that N-terminally fused YFP dominantly changes the fate of the ERD2 protein.
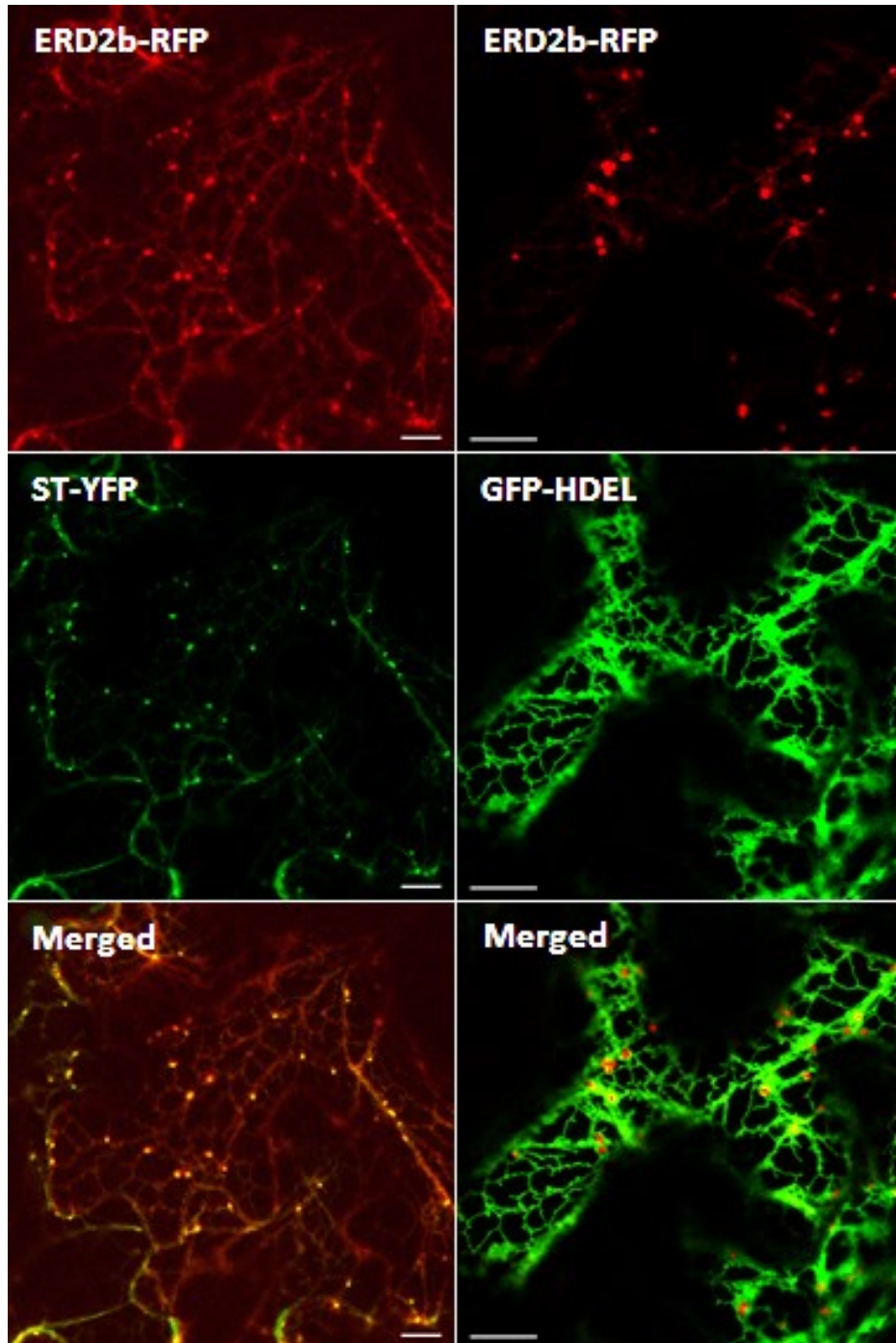


**Figure 2-17 C-terminal RFP fusion of ERD2 localisation *in vivo***
RFP was fused to the C-terminus of ERD2 (ERD2-RFP, top left panel) and co-expressed with either Golgi marker ST-YFP (middle left panel) or ER retained marker GFP-HDEL (middle right panel). All fusion proteins are driven by 35S promoter. Confocal images were obtained after infiltration in tobacco leaf epidermis cells via *Agrobacterium* mediated transformation (see Material and Methods). Images were obtained after two and a half day of the infiltration. All scale bars are 10μm.
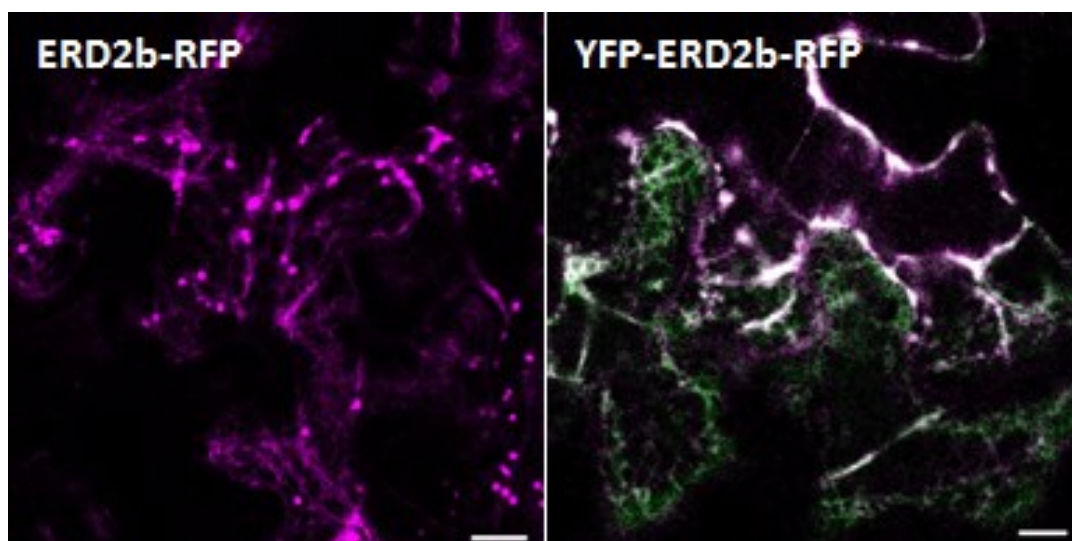
**Figure 2-18 N-terminal fusion of ERD2 is poorly expressed**
ERD2-RFP (left panel) illustrates typical punctate structures whereas on the right-hand panel the double fusion protein (YFP-ERD2-RFP) is localised to reticulum network pattern. N- and C- termini of ERD2 were fused with YFP and RFP respectively. Higher detector gain was used. All fusion proteins are constructed under the 35S promoter. Confocal images were obtained after infiltration in tobacco leaf epidermis cells via *Agrobacterium* mediated transformation (see Material and Methods). All scale bars are 10μm.

## 2.2.2.3 N-terminal tagging leads to ER retention and poor expression

Since expression levels are notoriously variable and difficult to quantify in single cell imaging, large areas of infiltrated tobacco leaves were extracted with the aim to detect specific degradation products of the fusion proteins that may shed light on the effect of the N-terminal YFP fusion. For this purpose, ERD2-RFP was compared with YFP-ERD2-RFP and YFP-ERD2, together with a mock-infiltrated sample as negative control. Detection of recombinant proteins by anti-RFP antibodies revealed very strong expression of the ERD2-RFP fusion, as well as two degradation products that must contain the RFP portion but only a portion of the ERD2 protein (Figure 2-19). In sharp contrast, the YFP-ERD2-RFP protein was very hard to detect and did not permit any specific hypothesis regarding its fate, although the weak band that was observed has the same mobility as one of the two degradation products in the ERD2-RFP lane. YFP-ERD2 and mock infiltrated sample yielded no detection with anti-RFP antibodies, as expected. The results confirm the fluorescence microscopy results suggesting that N-terminal tagging with YFP results in very low expression.
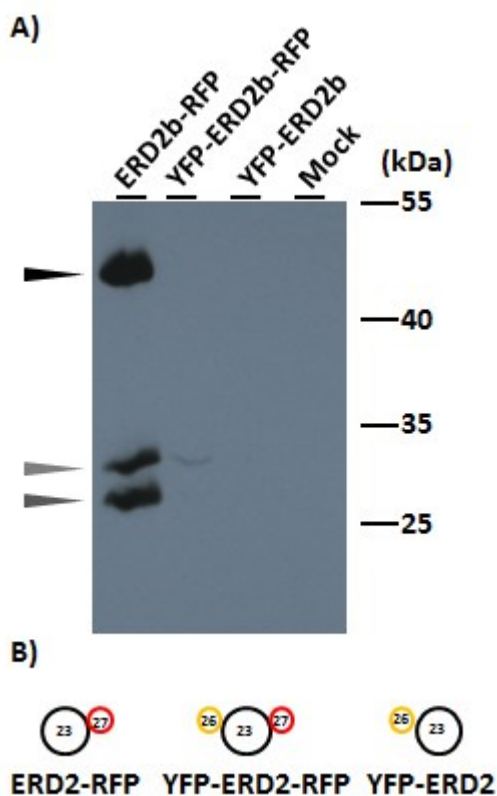
**Figure 2-19 ERD2 C- and N-terminal fusion topology in transient expression**
ERD2-RFP (ERD2b-RFP), YFP-ERD2-RFP (YFP-ERD2b-RFP) and YFP-ERD2 (YFP-ERD2b) were expressed in tobacco leaves via *Agrobacterium* mediated infiltration and harvested after two days (see Material and Methods). 35S promoter was used for all fusions. Protein concentrations of each sample were equalised and equal amount of each was loaded. Black arrowhead indicates the correct size for ERD2-RFP whereas the light and dark grey arrowheads indicate the degradation product perhaps. Immunoblot using RFP antibody is illustrated in panel A and the size marker is indicated on the right. Simple diagram of their predicted structure and size is presented in panel B.

## 2.2.2.4 N-terminal fluorescent tagging of ERD2 may result in membrane flipping of the resulting fusion protein.

Although the experiments carried out with redox-sensitive GFP fusions suggested that both the N-terminus and the C-terminus of ERD2 are exposed to the cytosol as explained by the six transmembrane domain model for ERD2 (Brach *et al.*, 2009), the differential localisation of N-terminally versus C-terminally fused ERD2 fusions to YFP leaves room for significant concerns. ER retention and poor expression of the N-terminal fusion (YFP-ERD2) could also be reminiscent of protein mis-folding, ER retention by ER quality control and subsequent degradation by the ERAD pathway (Brandizzi *et al.*, 2003), explaining the low expression levels of YFP-ERD2-RFP (Figure 2-19). In this respect it should be noted that the YFP C-

terminus contains a lysine residue, and the charge distribution on either side of the first transmembrane domain generally determines the membrane orientation of multi-membrane spanning proteins (Hartmann *et al.*, 1989). If N-terminally fused YFP promotes a cytosolic location of YFP, caused by the positive charge of the lysine residue preceding the first transmembrane domain in the fusion protein, then the earlier redox-sensitive GFP fusion results could also be explained if ERD2 has a seven transmembrane domain structure. It simply means the fusion protein has been flipped to the opposite membrane orientation, and it is easily conceived that this may lead to severe problems with protein sorting and function.

To test if membrane orientation may be erroneous in the YFP-ERD2 fusion, YFP was replaced by an N-terminal signal peptide fusion of YFP (secYFP), earlier used in the host laboratory (daSilva *et al.*, 2006) (Figure 2-20A). N-terminal signal peptides dominantly mediate translocation of the N-terminus of the nascent polypeptide across the ER membrane and would thus result in an YFP-ERD2 fusion with the YFP portion localised to the lumen of the ER. After cleavage of the signal peptide, the resulting protein would have an identical primary sequence as the YFP-ERD2 fusion without a signal peptide (Figure 2-20B). Any differences in localisation would thus be due to the manner in which ERD2 is inserted into the membrane during translocation.
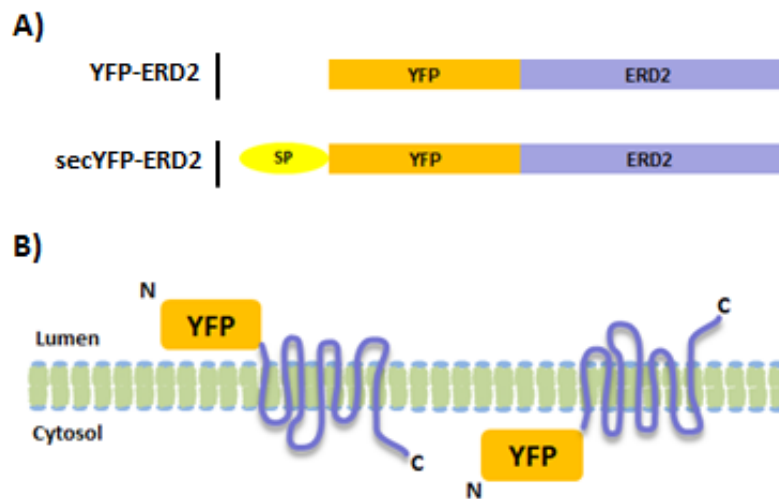


**Figure 2-20 ERD2 topology scenario**
Panel A illustrates the difference between YFP-ERD2 and secYFP-ERD2 (containing a signal peptide at the N-terminus of YFP). Possible topology is predicted and illustrated in panel B as the left one indicates the widely accepted model and the right one represents a flipped version due to the lack of signal peptide.

Figure 2-21 shows that replacement of YFP by secYFP resulted in a dramatic change in subcellular localisation and expression. The fluorescent fusion was strongly expressed and clearly labelled the Golgi bodies in tobacco leaf epidermis cells. In addition, tubular extensions of Golgi bodies (white arrowheads, Figure 2-22) could also be observed, that were not seen with the C-terminal fusions. Figure 2-22 shows an almost perfect co-localisation of secYFP-ERD2 with the Golgi marker ST-RFP, except for the tubular extensions which appear to be enriched in the new ERD2 fusion. Compared to the C-terminally tagged ERD2 fusions secYFP-ERD2 is particularly crisp and has well defined Golgi bodies with very little fusion protein in transit through the ER (Figure 2-23). In addition, merged image of secYFP-ERD2 with the Golgi marker ST-CFP has indicated a polarised sub-organelle localisation and a slightly shifted fluorescence of one or another when Golgi bodies are on sideways (Figure 2-23).
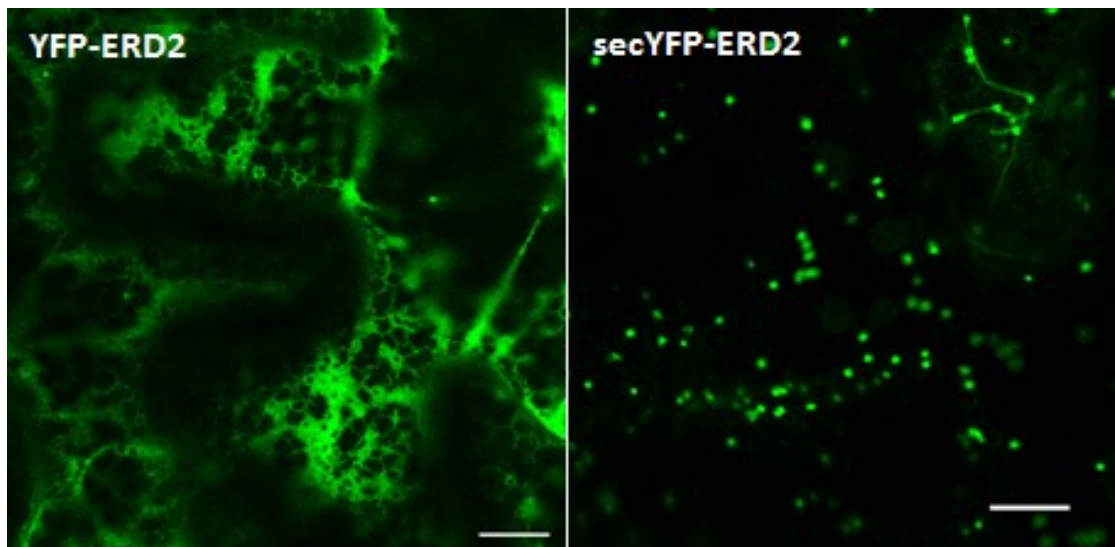


**Figure 2-21 Comparison of ERD2 N-terminal fusions**
YFP-ERD2 (on the left panel) illustrates cytosolic and a little reticulum network pattern whereas on the right panel signal peptide containing secYFP-ERD2 is localised mostly to punctate structures with some tubular structures. Both fusion proteins were constructed under the 35S promoter. Confocal images were obtained after infiltration in tobacco leaf epidermis cells via *Agrobacterium* mediated transformation (see Material and Methods). Images were obtained after two and a half day of the infiltration. All scale bars are 10μm.
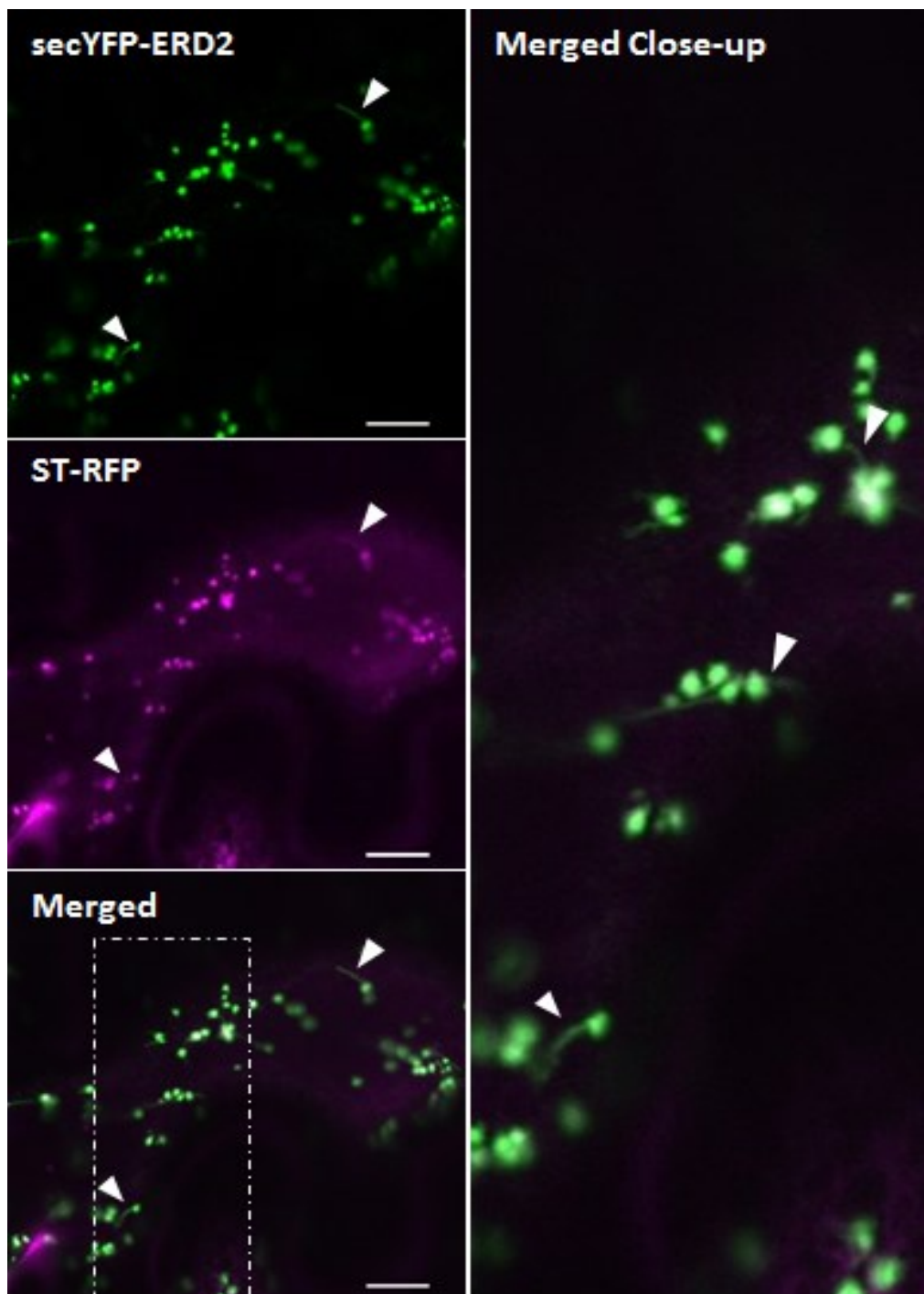
**Figure 2-22 Tubular structure by secYFP-ERD2 *in vivo***
Tubular structures (indicated by white arrows) are labelled by secYFP-ERD2 (top left) but not Golgi marker ST-RFP (middle left). Close-up of the enlarged dashed rectangle area is illustrated on the right. Both fusion proteins are constructed under the 35S promoter. Confocal images were obtained after infiltration in tobacco leaf epidermis cells via *Agrobacterium* mediated transformation (see Material and Methods). Images were obtained after two and a half day of the infiltration. All scale bars are 10μm.
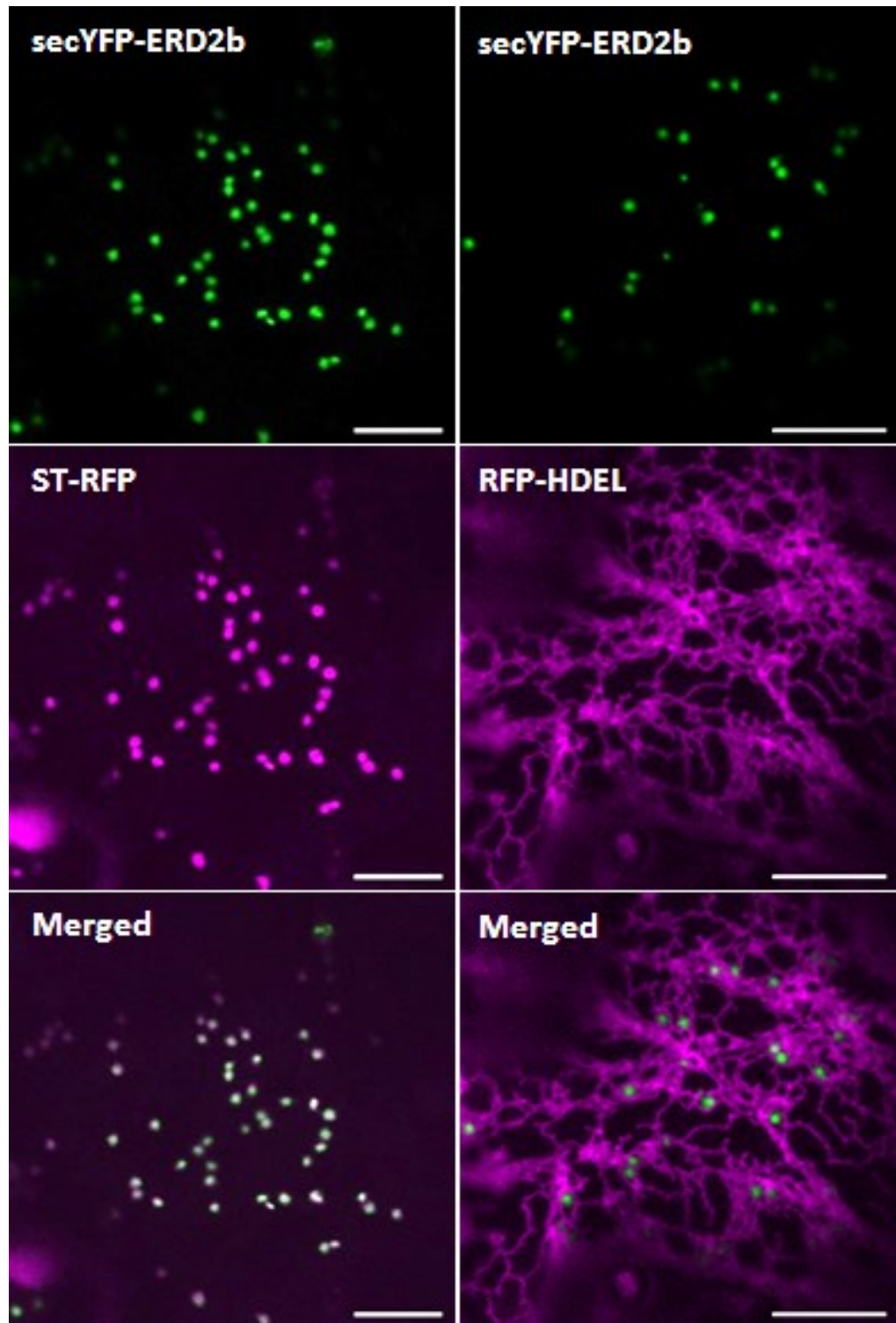
**Figure 2-23 Co-localisation of secYFP-ERD2** *in vivo*
SecYFP-ERD2 (top left) is co-expressed with Golgi marker ST-RFP (middle left) and ER marker RFP-HDEL (middle right). Merged images are illustrated at the bottom panel. All fusion proteins are constructed under the 35S promoter. Confocal images were obtained after infiltration in tobacco leaf epidermis cells via *Agrobacterium* mediated transformation (see Material and Methods). Images were obtained after two and a half day of the infiltration. All scale bars are 10μm.

To re-confirm that YFP without a signal peptide causes a dramatic change in the ERD2 behaviour, the signal peptide was introduced in front of the double labelled construct YFP-ERD2-RFP. Figure 2-24 shows that secYFP-ERD2-RFP is now also better expressed and reaches the Golgi apparatus, although some fusion protein is detectable in the ER too. Perhaps folding and ER export of such a large molecule takes more time but it confirms that addition of the signal peptide causes a fundamental change in the behaviour of the fusion protein. Since after cleavage of
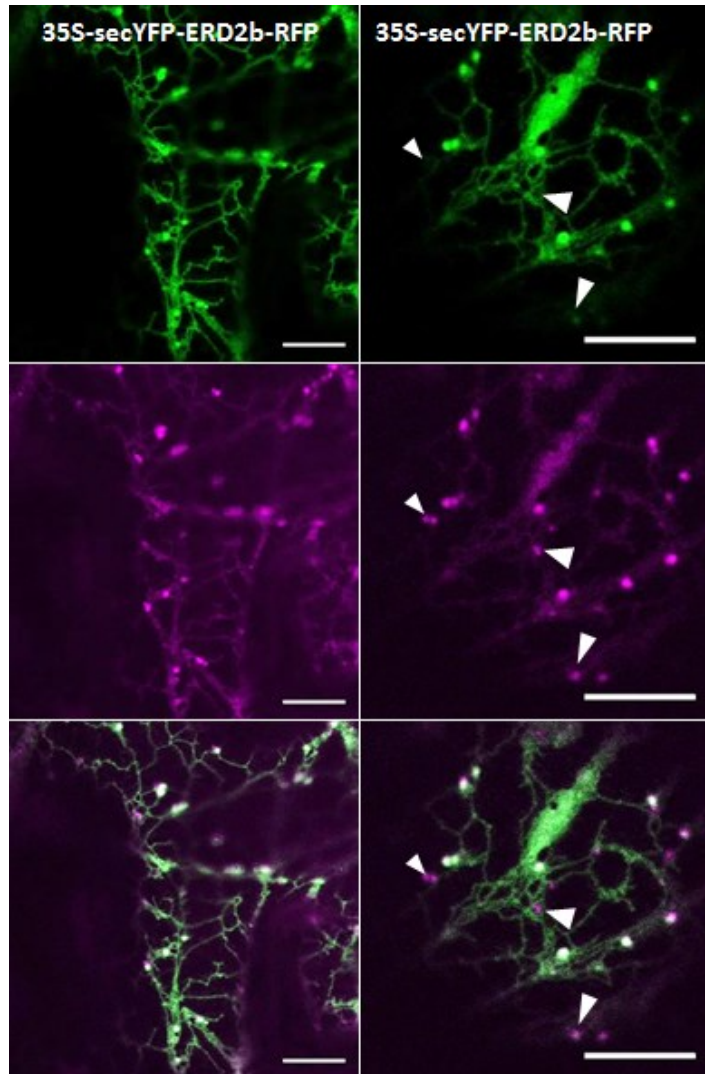


**Figure 2-24 Signal peptide containing N-terminal ERD2 fusion resumes its localisation**
A signal peptide added version of YFP-ERD2-RFP was expressed *in vivo* (secYFP-ERD2-RFP). It's localised to both punctate and reticulum structures. Top panel illustrates the YFP channel and middle panel represents the RFP channel. Merged channel images are shown at the bottom panel. Examples of only-RFP-labelled punctate structures are indicated by the white arrows. This fusion is constructed under the 35S promoter. Confocal images were obtained after infiltration in tobacco leaf epidermis cells via *Agrobacterium* mediated transformation (see Material and Methods). Images were obtained after two and a half day of the infiltration. All scale bars are 10µm.

the signal peptide the resulting protein will have the same primary sequence as YFP-ERD2-RFP, only a reverse membrane orientation can explain such a dramatic change in the fluorescence pattern.

## 2.2.2.5 Fluorescent ERD2 tagging abolishes or reduces biological activity in the ER retention of HDEL proteins

To implement a quantitative bio-assay for ERD2 function, the dual expression carrying the cytosolic marker GUS (Figure 2-10A) was re-constructed to replace the Amy construct by a CaMV35S promoter driven wild type ERD2 coding region or the various fluorescent fusions. Plasmid preps were first normalised for GUS activity and then co-electroporated together with a constant amount of plasmid encoding Amy-HDEL alone as pilot experiment. Figure 2-25A shows that compared to the
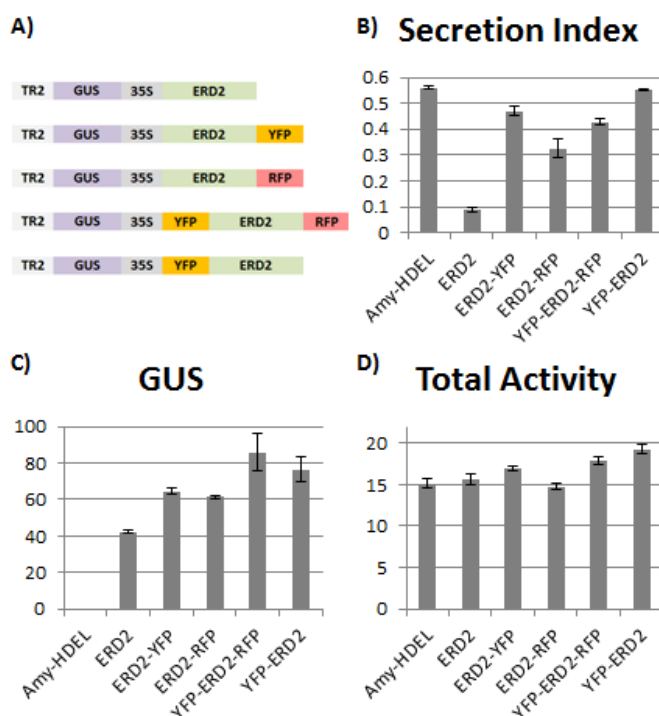


**Figure 2-25 Co-expression of HDEL ligand with ERD2 and its various fluorescent fusions in tobacco protoplasts**
Co-expression of the ER retained α-amylase derivative (Amy-HDEL) with ERD2 and its different fluorescent fusions (ERD2-YFP, ERD2-RFP, YFP-ERD2-RFP and YFP-ERD2) is tested in tobacco protoplasts and their schematic view is presented in panel A. Secretion index of ligand alone (Amy-HDEL) and with addition of the receptor fusions are indicated in panel B. Panel C shows the GUS activity for all plasmids and panel D illustrates the total amylase activity in all cases. 10µg of DNA preparation from each fusion is used. Error bars are standard deviation of three independent repeats. Units of α-amylase activity are ΔO.D./ml/min and secretion index units are considered as arbitrary.

wild type ERD2, most fusion proteins exhibited extremely weak or no biological activity, despite being transfected at higher efficiency compared to the untagged ERD2 construct as they showed higher GUS expression levels (Figure 2-25C). The ERD2-RFP fusion was the only construct that mediated a recognisable reduction of the Amy-HDEL secretion index by about half.
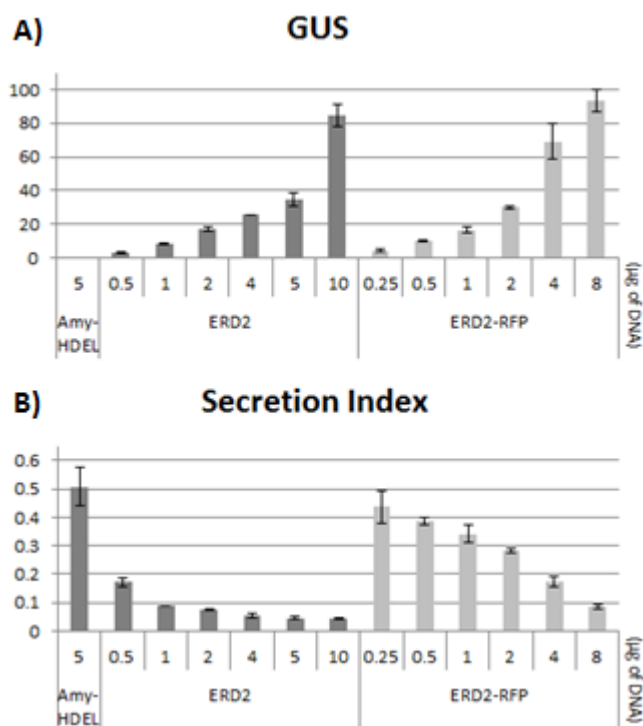


**Figure 2-26 Functionality comparison of ERD2 and its C-terminal fusion**
The ER retained α-amylase derivative (Amy-HDEL) was co-expressed with either ERD2 or its C-terminal fusion (ERD2-RFP) with constant amount of Amy-HDEL ligand and increasing amount of ERD2 fusions (indicated at the bottom of each lane). Both ERD2 and ERD2-RFP were constructed in GUS double expression vector and their GUS activity is shown in panel A. Secretion index of ligand alone (Amy-HDEL) and with addition of the receptor fusions are indicated in panel B. Error bars are standard deviation of three independent repeats. Units of α-amylase activity are ΔO.D./ml/min and secretion index units are considered as arbitrary.

More detailed dose-response assays revealed that only ERD2-RFP maintained a biological activity that was measurable in a typical dose-responsive manner (Figure 2-26), but which was merely 10% of the activity of the untagged ERD2 construct. The two signal peptide containing N-terminal fusions (secYFP-ERD2 and secRFP-ERD2) were constructed at a later stage in the project and were analysed separately. Neither of the constructs shows biological activity in a dose-responsive manner (shown for secRFP-ERD2 in Figure 2-27). The results indicate that

experiments with fluorescently tagged ERD2 may not yield biologically meaningful localisation data as the receptor is no longer functional in the bio-assay.
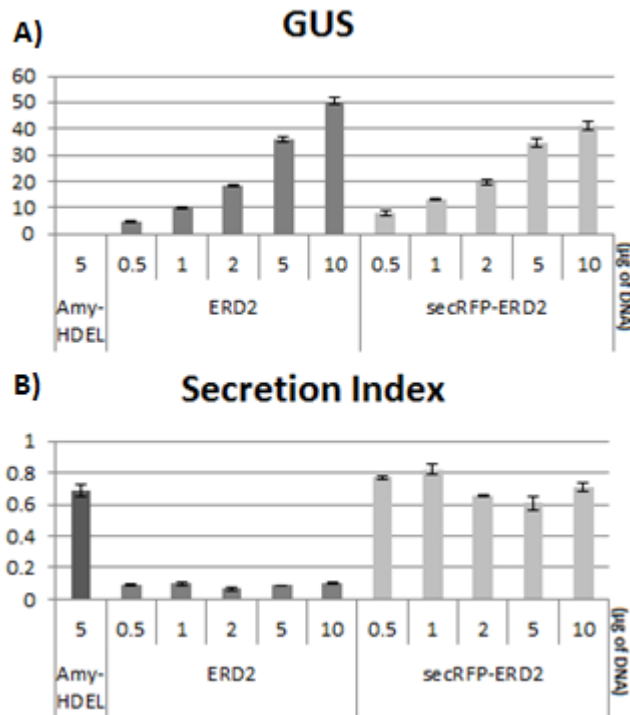


**Figure 2-27 Functionality of signal peptide containing N-terminal ERD2 fluorescent fusion**

ER retained α-amylase derivative (Amy-HDEL) was co-expressed with either ERD2 or its signal peptide contained RFP fusion (secRFP-ERD2) in tobacco protoplasts. Both ERD2 and secRFP-ERD2 were sub-cloned into the GUS vector and their GUS activity is illustrated in panel A. Secretion index of both co-expressions was calculated and is shown in panel B. Constant amount of Amy-HDEL was used and the amount of ERD2 and secRFP-ERD2 is indicated below each lane. The negative controls contain only cargo (Amy-HDEL) DNA. Error bars represent standard deviation of three independent repeats. Units of α-amylase activity are ΔO.D./ml/min and secretion index units are considered as arbitrary.

## 2.2.3 Discussion

### 2.2.3.1 On the transmembrane topology of ERD2

The production of fusion proteins for *in vivo* fluorescent imaging has revolutionised plant cell biology, but it has also become apparent that not every fluorescent fusion functions as well as the untagged native protein. Keeping this in mind, it was decided at an early stage of the project to compare N-terminal and C-terminal fluorescent fusions of ERD2. Results in this chapter show that this was a worthwhile endeavour as the subcellular localisation of the N-terminal fusion yielded

extremely low expression and remained trapped in the ER. Since ERD2 is predicted to bind ligands in the Golgi stack (Pelham, 1988), the Golgi localisation of the C-terminal fusion ERD2-RFP was therefore deemed more representative of the native ERD2 localisation. A C-terminal fusion to GFP, which has a very similar primary structure as YFP, was originally introduced as typical marker for both ER and Golgi bodies and instantly accepted by the field (Boevink *et al.*, 1998). In mammalian cells, the subcellular localisation of the human ERD2 gene product was the Golgi complex (Lewis and Pelham, 1990). However, it should be noticed that the human protein was C-terminally tagged with the peptide TMEQKLISEEDLN (myc epitope tag) and overexpressed before detection was feasible. Overexpression could change the ratio between ligands and receptors, and thus influence receptor-distribution between the ER and the Golgi stacks.

Experiments in which N-terminally tagged YFP-ERD2 was compared with a derivative supplemented with a N-terminal signal peptide for protein translocation across the ER membrane (secYFP-ERD2) strongly suggested that YFP-ERD2 may be misfolded or disoriented in the membrane. In the presence of the signal peptide expression was much stronger and yielded particularly crisp Golgi signals. The same effect was observed when a signal peptide was introduced to the N-terminus of the double labelled ERD2 fusion YFP-ERD2-RFP. After cleavage of the signal peptide, the primary structure of the two types of proteins in each comparison is identical, but the protein yield is higher and the subcellular localisation has shifted from the ER to the Golgi apparatus. However, caution is still advised regarding the biological function, because a bulky fluorescent protein on the lumenal side of ERD2 may interfere with ligand binding and thus retrograde trafficking (see next subheading).

Experiments in this chapter can only serve as indications that a seven-transmembrane topology can be supported by the data in spite of the earlier reports showing that N-terminal and C-terminal fusions of redox-sensitive GFP to ERD2 yielded a cytosolic location for the fused fluorescent tag (Brach *et al.*, 2009) and that ERD2 may have only six transmembrane domains. To firmly establish the membrane topology, specific antibodies recognising different parts of ERD2 could be generated followed by protease protection experiments on microsomal preparations. Similar protease protection experiments could be carried out after fusion with epitope tags. Finally, the tools generated in this chapter could be instrumental, for instance a comparison of ERD2-RFP, YFP-ERD2-RFP and

secYFP-ERD2-RFP could shed light on the location of the RFP tag and establish if YFP tagging flips the orientation whilst addition of a signal peptide reverses this change.

## 2.2.3.2 What is the subcellular distribution of endogenous ERD2?

An important finding of this chapter is the fact that the bio-assay mercilessly reveals that hardly any of the constructed ERD2 fusions retain biological activity in the process of mediating ER retention (Figure 2-25, Figure 2-26 Figure 2-27). Only the C-terminal fusion protein ERD2-RFP retained measurable biological activity, but this was estimated to be merely 10% of the original performance. The fact that ERD2-YFP was completely inactive suggests that it may not merely be a problem of steric hindrance by a bulky fluorescent protein but that the actual protein sequence flanking the ERD2 C-terminus in the fusion protein may influence how the C-terminus functions *in vivo*.

A serious consequence of the observation is that earlier imaging results obtained with fluorescently tagged ERD2 suggesting a predominant Golgi localisation (Boevink et al., 1998; daSilva et al., 2004) may be erroneous. If the fusion protein no longer interacts with ligands due to a problem of overall protein folding, it may not initiate retrograde transport and thus remain trapped in the Golgi apparatus. On the other hand, ligand-binding may not be affected at all, but it is possible that ERD2 no longer integrates into COPI-coated vesicles or interfaces with other machineries such as ARF-GAP (Lewis and Pelham, 1992b; Hsu *et al.*, 1992; Aoe *et al*., 1997). The structure of typical G protein coupled receptors (GPCRs) has longer N-terminal and C-terminal polypeptides compared to ERD2, and the length of the transmembrane domains is generally more suited for the thickness of the plasma membrane. It is not clear if GPCRs are the ideal model for ERD2 structure and it will be hard to ask more specific questions about its localisation and function without further research on the exact membrane topology of ERD2.

## 2.3  Chapter III Receptor-ligand stoichiometry

### 2.3.1  Introduction

To establish an *in vivo* transport assay for plant ERD2 gene products, the standard approach of genetic complementation in plants is not appropriate because complete ERD2 knockout is lethal and partial knockout is difficult to select for as it is difficult to quantify ER retention efficiency in cells of whole plants *in situ* (p20,Figure 2-1). In the yeast *Saccharomyces cerevisiae* complete knockout of ERD2 is lethal whilst only mutants with partial ER retention capacity are viable (Townsley *et al*., 1994). This indicates that ER retention itself is crucial for cell viability (Pimpl and Denecke, 2000), rather than merely a rescue pathway for a minority of ER residents that have escaped to the Golgi apparatus (Pagny *et al*., 2000). Studying the functionality of the receptor is therefore not a trivial task.

The finding that HDEL-mediated retention in plants can be saturated when the stable barley α-amylase enzyme (Amy) is used as cargo molecule harbouring the HDEL-tetrapeptide (Phillipson *et al*., 2001) can be exploited to study ERD2 function in plants. I could show that progressive overproduction of Amy-HDEL is accompanied by a reduction in secretory protein synthesis relative to cytosolic protein synthesis (Chapter I, Figure 2-10). This reduction was not observed with the control cargo Amy, suggesting that it is not caused by competition for protein translocation, but instead by HDEL-mediated saturation of the receptor ERD2. Earlier studies in the host laboratory revealed that in transgenic plants, HDEL-saturation also leads to auxin-related developmental defects such as loss of apical dominance and increased tendency for gene silencing. These effects could be partially due to ERD2 saturation and loss of soluble ER chaperones such as BiP due to inefficient recycling and followed by depletion. Insufficient BiP in the ER would not only compromise protein folding but the ability of the ER to translocate proteins across its delimiting membrane. Auxin-related developmental effects could be due to mis-targeting of the auxin-binding protein (ABP1), as it has been shown that arrival of ABP1 at the apoplast causes auxin-related phenotypes (Robert *et al*., 2010). These data suggest that harnessing the secretory pathway and the ER as production and storage compartment for recombinant proteins will be limited by the capacity of ERD2-mediated ER retention if reduction in protein translocation and normal development of the plants are at stake.

In Chapter I, I have demonstrated in protoplasts and in tobacco leaf epidermis cells that progressive overexpression of ERD2 leads to strictly dose-dependent suppression of the partial secretion that is caused by receptor saturation (Chapter I, Figure 2-5). This suggests that the limiting factor in ER retention is the number of ERD2 molecules. ERD2-mediated inhibition of Amy-HDEL secretion is not caused by a general reduction of exocytic transport, because ERD2 overexpression does not influence constitutive Amy-secretion. Two ERD2 isoforms identified by genome sequencing (ERD2a and ERD2b) show no differences in their dose-responses and do not differentiate between HDEL and KDEL-ligands, and it was possible to select one of these isoforms as representative for further analysis.

Receptor saturation can be regarded as a partial loss-of function phenotype for endogenous ERD2, and a genetic approach to introduce additional ERD2 proteins is a gain-of-function, or modified-function assay, as it can suppress HDEL-saturation and restore efficient ER retention. The quantitative nature of the assay permits me to carry out dose-response assays well above endogenous receptor-ligand interactions due to the semi-dominant effect of ERD2 overexpression. In this chapter I aim to establish firm experimental evidence for the hypothesis that few ERD2 molecules can mediate the ER accumulation of many ligands.

## 2.3.2 Results

### 2.3.2.1 Normalising transfection efficiency of receptor- and ligand- encoding plasmids

Efficient receptor recycling between the ER and the Golgi apparatus (Pelham, 1988) could explain how few receptors may mediate the accumulation of many proteins in the ER. In order to function in the postulated manner, ERD2 would either have to progress much faster to the Golgi than bulk flow of abundant soluble ER proteins (Crofts *et al*., 1998), or bind to many ER-residents simultaneously whilst initiating retrograde traffic. A combination of the two sorting principles cannot be ruled out either. In this respect it is noteworthy that dose response studies in chapter I revealed that ERD2 encoding plasmids could be diluted quite strongly and still yield a measurable effect on the retention of Amy-HDEL. Given the fact that co-transfection of protoplasts with two plasmid types is never 100%, the assays systematically underestimate the ability of co-expressed ERD2 to mediate ER retention. The true retention efficiency of ERD2 could therefore be very high.

To test if ERD2 is capable of mediating the retention of extra-stoichiometric numbers of ligands, it was first necessary to normalise the transfection-rate of the model ligand Amy-HDEL encoding plasmid with the ERD2 encoding plasmid. Both the model ligand (Amy-HDEL) and the receptor construct (ERD2) were expressed from a dual expression plasmid harbouring the quantitative cytosolic marker GUS (Gershlick *et al.*, 2014), as illustrated in Figure 2-28A. The resulting plasmids were first pre-tested using the GUS assay only, to establish conditions yielding equal GUS activities. Then appropriate quantities of Amy-HDEL and ERD2-encoding plasmids to yield identical GUS activities were mixed and co-transfected.
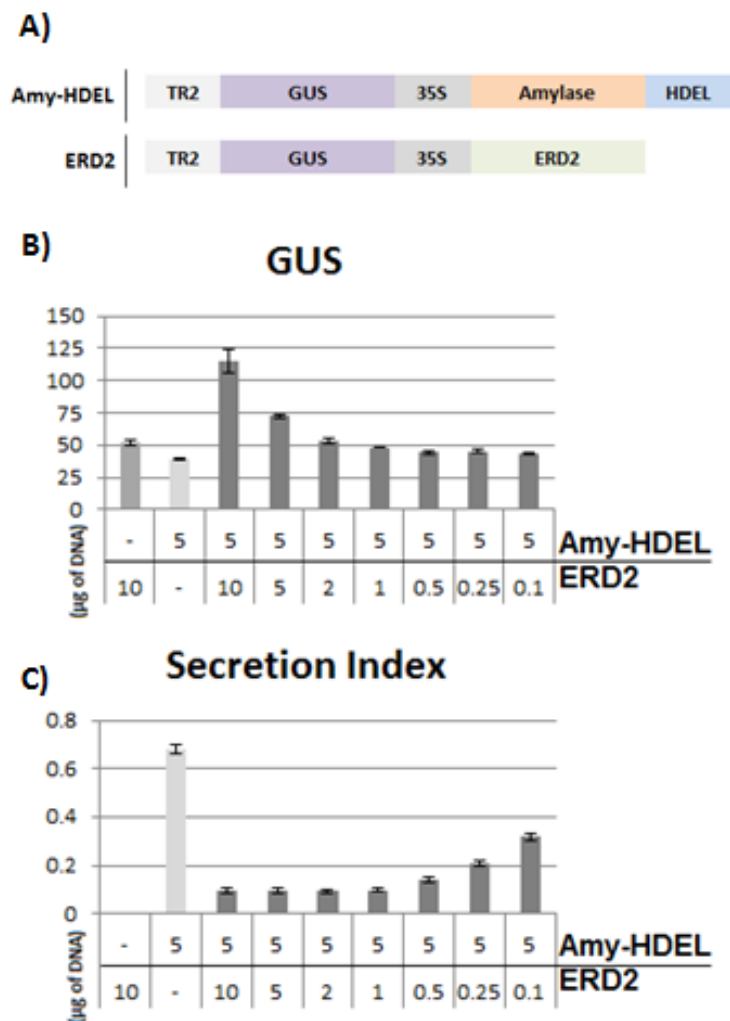


**Figure 2-28 Co-expression of HDEL ligand with dilution series of ERD2**
HDEL ligand (Amy-HDEL) and ERD2 were sub-cloned into GUS vector (panel A) and co-expressed in tobacco protoplasts. The amount of DNA used is indicated below each lane. GUS activity is illustrated in panel B. Secretion index was calculated and shown in panel C. Error bars represent standard deviation of five independent repeats. Units of α-amylase activity are ΔO.D./ml/min and secretion index units are considered as arbitrary.

Figure 2-28 confirms that transfection of Amy-HDEL-encoding plasmid yielded comparable levels as ERD2-encoding plasmids (first two lanes, panel B), and that the sum of the two yielded approximately the sum of the individual GUS activities. This shows that plasmid concentrations well below saturation of transfection were used for the co-expression experiments. Amy activity measured in the medium and the cells of these samples confirmed that Amy-HDEL secretion was all but abolished when ERD2-encoding plasmid was co-transfected at a similar rate.

In the same transfection, further mixtures of Amy-HDEL and ERD2 encoding plasmids were co-transfected, and whilst keeping the cargo plasmid at a constant concentration, the ERD2-encoding plasmid was progressively diluted up to 100-fold. From the 20-fold dilution of ERD2 plasmid onwards, total GUS activities were within the margins of the standard deviation of the Amy-HDEL plasmid alone (Figure 2-28B, last three lanes). Figure 2-28C shows that Amy-HDEL exhibits no change in the secretion index up to 10-fold dilutions of the receptor encoding plasmid. A slight reduction in the retention was observed after 20-fold dilution of the ERD2 plasmid. This reduction progressively becomes more noticeable after 50-fold dilution, but even when diluted 100-fold compared to the ligand plasmid, the Amy-HDEL secretion index was still less than half of the value obtained without co-electroporated ERD2 plasmid (Figure 2-28C, compare second and last lane).

The data indicate that with 100-fold diluted ERD2 plasmid, more than 50% of the retention capacity of undiluted ERD2 plasmid remained. Given the fact that the co-transfection rate is less than 100% to start with and progressively decreases further as one of the two plasmids is diluted, the data certainly underestimate the true retention capacity of the additionally introduced ERD2 molecules. Overall, this result strongly suggests that very few ERD2 molecules can mediate ER retention of many ligands.

## 2.3.2.2 Epitope tagging of the ERD2 C-terminus reveals its importance in mediating ER retention.

Results in Figure 2-28 are highly suggestive but equal transfection rates do not guarantee equal numbers of ligands and receptors. Both proteins are synthesized on the rough ER, but Amy-HDEL is encoded by a much longer coding region. On the other hand, Amy-HDEL contains only an N-terminal signal peptide which is cleaved after translocation, whilst ERD2 contains seven hydrophobic domains that are slowly integrated into the ER membrane during translocation and

folding. Given these differences it is difficult to predict if the two proteins are synthesised at the same rate or not, and if not, which of the two proteins is synthesised faster. In order to verify the synthesis rate and establish the total protein levels after transient expression, it is necessary to detect the proteins directly and using a strategy that permits detection at equal sensitivity, in spite of the different nature of the two proteins.

Immunodetection using a common denominator such as an epitope tag is thought to be one way forward to detect proteins with different affinities (Brizzard, 2008). However, to establish the true ratio between ectopically expressed ligands and receptors needed to restore retention, epitope tagging must not alter the properties of either molecule. In addition, the antibody-affinity to the epitope must be truly context-independent and permit detection of Amy-HDEL and ERD2 with the same affinity per number of molecules. To test this approach, Amy-HDEL and ERD2 were tagged with the HA tag (Field *et al*., 1988). Earlier studies suggested that the ERD2 C-terminus did not contain critical amino acids for ligand-binding or subcellular localisation of ERD2 (Townsley *et al*., 1993). Given the observed mis-targeting of N-terminally tagged ERD2 (Chapter II), a dual strategy was adopted to maximise the chances for success.

One strategy was a replacement of the last 9 amino acids by the HA tag, in order to prevent lengthening the C-terminus (ERD2-HAa). If the C-terminal tail is unimportant, increasing its length may yet influence the function of the rest of ERD2 and the replacement strategy avoids this. In the second strategy the HA tag was fused between the last amino acid of ERD2 coding region and its stop codon, thus extending the C-terminus without deleting any amino acid residue (ERD2-HAb). This was essentially a backup in case the C-terminal tail contained important information after all, and in the hope that an extension by 9 amino acids would be much less than extending it by an entire RFP polypeptide.

Figure 2-29A illustrates the two types of constructs that were to be compared with untagged ERD2 on the same kind of GUS reference vector as used before. The three plasmids were first characterised by a GUS pilot assay to adjust the concentrations to obtain comparable GUS activities. Western blotting analysis of extracts from the three transfections allowed the detection of the HA-tagged proteins by western blotting and illustrating a slight increase in the molecular weight of ERD2-HAb, as expected (Figure 2-29). Appropriately adjusted plasmid preparations were then transfected in three dilutions. Figure 2-29B confirms that

GUS activities were comparable in the three cases and that the HA-tagged plasmid yielded certainly no lower GUS levels than the plasmid encoding untagged ERD2 (last three lanes).
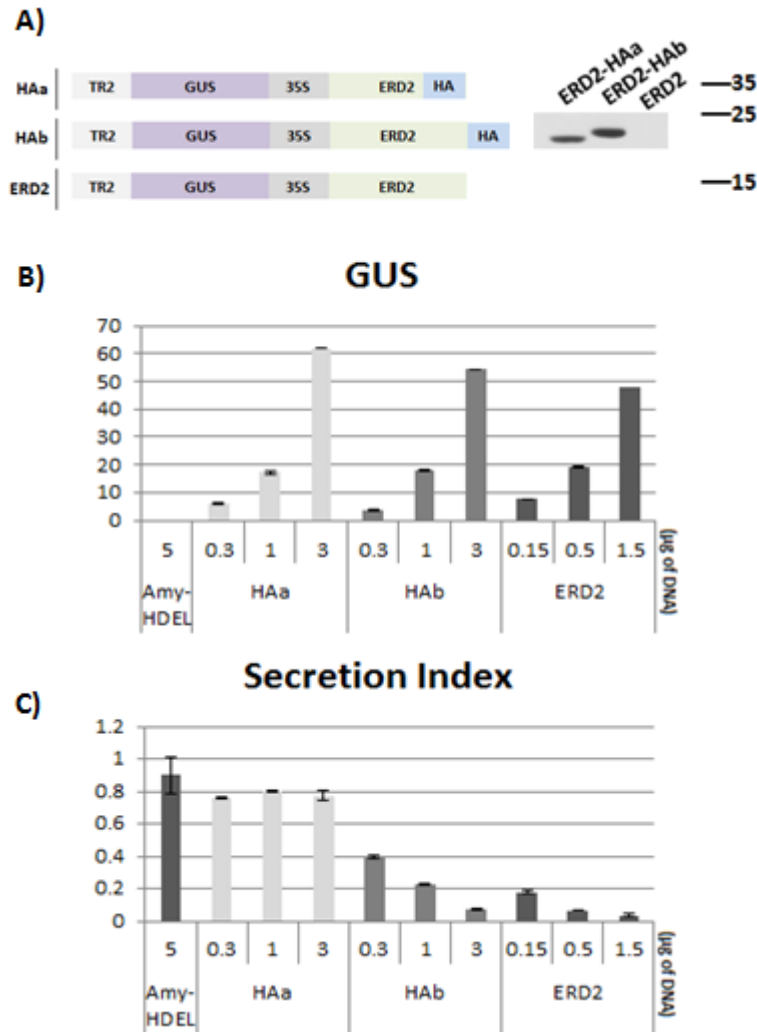


**Figure 2-29 Epitope tagged ERD2 functionality in tobacco protoplasts**
Epitope HA was fused with ERD2 at its C-terminus either by replacement (HAa) or addiction (HAb) in the GUS vector and co-expressed with HDEL ligand (Amy-HDEL). Panel A illustrates the schematic view of ERD2 and its HA tagged fusions as well as a HA immunoblot (top right) indicating the different sizes between HAa (21kDa) and HAb (23kDa) (with molecular marker on the right). GUS activity is illustrated in panel B and secretion index was calculated and shown in panel C. The amount of DNA used is indicated below each lane. Constant amount of Amy-HDEL was used in all samples. Error bars represent standard deviation of three independent repeats. Units of α-amylase activity are ΔO.D./ml/min and secretion index units are considered as arbitrary.

Figure 2-29C shows that replacement of the short C-terminus of ERD2 by the number of amino acids of the HA tag completely abolishes biological activity of ERD2 (HAa lanes), whilst addition to the C-terminus reduces the activity by

approximately 50%, as at each plasmid concentration the GUS levels were comparable to those of the untagged ERD2 plasmid, but the secretion indexes were approximately 2-fold higher each time. The results suggested that despite a 2 fold reduction in the biological activity, ERD2-HAb could be used for functional studies. In a second more elaborate dose-response analysis (Figure 2-30), the 2-fold reduction in the biological activity of ERD2-HAb was confirmed for the lower concentration range, whilst at higher concentrations the difference became undetectable. This illustrates the limits of the resolution of the harvesting technique to separate cells from medium. Secretion indexes are usually no lower than 0.05 as this value is also seen for vacuolar proteins or even cytoplasm markers, and can be explained by the small portion of cell-mortality and unspecific leakage of cellular contents to the medium during the pipetting of the cell suspensions and subsequent centrifugation steps.

Interestingly, the 2-fold lower biological activity of ERD2-HAb (Figure 2-30),
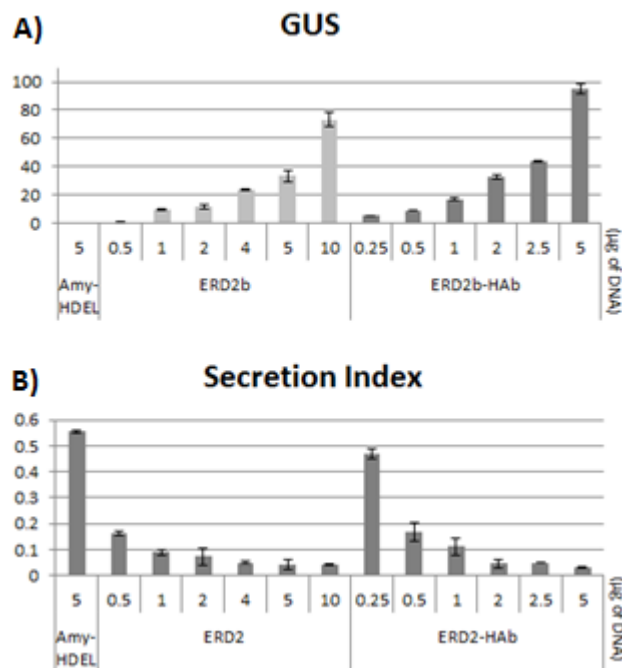
**Figure 2-30 Functional epitope tagged ERD2 in tobacco protoplasts**
GUS vector containing either ERD2 or its C-terminal fusion of HA epitope by addition (HAb) was co-expressed with HDEL ligand (Amy-HDEL). The amount of DNA used is indicated below each lane. Constant amount of HDEL cargo was used for all samples. GUS activity is illustrated in panel A. Secretion index was calculated and shown in panel B. Error bars represent standard deviation of five independent repeats. Units of α-amylase activity are ΔO.D./ml/min and secretion index units are considered as arbitrary.

the completely inactive properties of ERD2-HAa (Figure 2-29), and the 10-fold lower biological activity of ERD2-RFP (Figure 2-26) show that the C-terminus of ERD2 carries important information for its biological function and that simple masking by a short peptide or a larger fluorescent protein can quite significantly reduce its activity in mediating ER retention.

### 2.3.2.3 HA-tag is context dependent

In spite of the two-fold reduction in biological activity, the properties of ERD2-HAb were deemed adequate enough to carry out a receptor-ligand stoichiometry analysis, as a correction factor of 2 could easily be applied in the calculations. For this purpose, Amy and Amy-HDEL were reconstructed to display an HA epitope at the C-terminus. Whilst for Amy, the HA tag was fused directly to the C-terminus of its coding sequence (Amy-HA), Amy-HDEL was reconstructed to contain the HA epitope between the C-terminus of the Amy coding region and the HDEL tetrapeptide (Amy-HA-HDEL). This was necessary because the tetrapeptide was shown to be functional only when present at the C-terminus (Munro and Pelham, 1987).

Figure 2-31 shows a pilot assay in which secreted and cellular Amy-HA was compared to Amy-HA-HDEL either by western blotting or by enzymatic activity. The results indicate that Amy-HA-HDEL was detected with much lower affinity than Amy-HA. The leakage of Amy-HA-HDEL as measured by activity (panel B) does not correspond to the almost undetectable signals in the western blot (panel A). Activities in the cells show the opposite distribution, but despite a similar difference between Amy-HA and Amy-HA-HDEL in the measured activities, the signals in the western blot are almost equal this time. The data indicate that addition of HDEL at the C-terminus of the HA tag causes a 5-fold reduction in the immunological detection of the epitope tag. If such differences in activity are observed, it cannot be ruled out that display of the HA tag in ERD2 is also influenced by the peptide sequence preceding the HA tag. Therefore, the strategy to carry out stoichiometry measurements between ERD2 and Amy-HDEL by western blotting was dismissed due to the obvious context dependence of the HA tag.
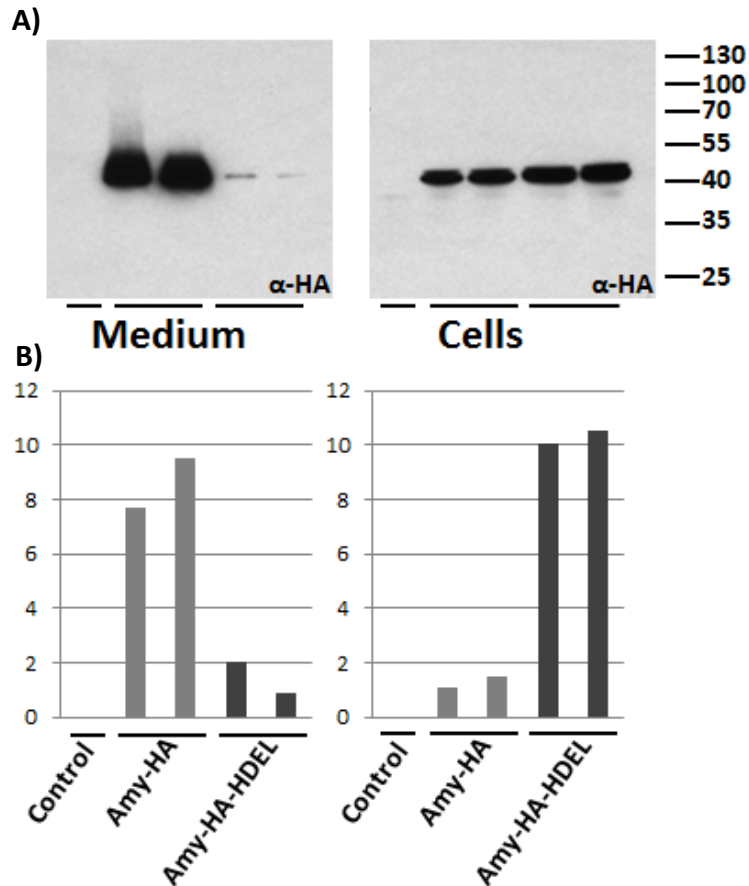
**Figure 2-31 Epitope tagged ligand complication**
Epitope HA was fused to secreted α-amylase (Amy-HA) and its ER retained derivative (Amy-HA-HDEL) and both were expressed in tobacco protoplasts. Immunoblot with HA antibody of medium (left) and cells (right) samples is shown at panel A with the molecular size marker on the right. Size of around 45kDa is expected and observed. Corresponding α-amylase activity in the medium and cells is shown in panel B. Sample repeats are illustrated and due to the natural of this experiment further repeats were not necessary. Units of α-amylase activity are ΔO.D./ml/min.

## 2.3.2.4 Generation of anti ERD2 antibodies

To overcome the difficulty with epitope tagging, we generated antibodies to peptides corresponding to the first cytosolic loop of ERD2 or the C-terminus of ERD2. Figure 2-32 shows that antisera from two rabbits directed against the first cytosolic loop were able to detect recombinant secYFP-ERD2 at the expected molecular weight of the fusion protein. In contrast, antisera directed against the ERD2 C-terminus did not yield a useful reagent. Antibodies from the second rabbit directed against the first cytosolic loop (termed "anti-loop" hereafter) were selected for immunoprecipitation of native ERD2.
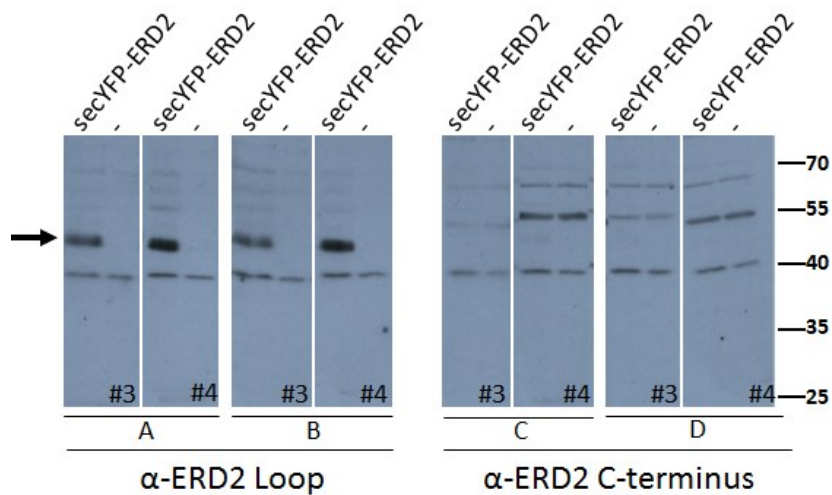
**Figure 2-32 ERD2 antibody generation**
Two different ERD2 antibodies were designed for either against the first cytosolic loop of ERD2 (ERD2 loop) or the C-terminus of ERD2 (ERD2 C-terminus). Two rabbits were used each antibody (A and B for loop, C and D for C-terminus). Bleed number 3 (#3) and number 4 (#4) were used as example here. Size marker is illustrated on the right and the correct fusion size is indicated by the black arrow on the left (49kDa). Transient expressed secYFP-ERD2 and mock samples were obtained after infiltration in tobacco leaf epidermal cells. Protein concentrations was equalised and the same amount of secYFP-ERD2 and mock was loaded.

## 2.3.2.5 Establishment of an immunoprecipitation strategy for ERD2

To test if either the anti-HA antibodies or the newly generated anti-loop antibodies were suitable for immunoprecipitation of native ERD2, tobacco leaf protoplasts we transfected with ERD2-HAb encoding plasmid and compared with mock transfected protoplasts. Extracts were immunoprecipitated either with anti-HA or anti-loop antibodies using protein-A sepharose, followed by western blotting of the boiled proteinA-sepharose pellet in SDS-PAGE sample buffer. Figure 2-33 shows that immunoprecipitation by anti-HA antibodies, followed by detection with anti-HA antibodies was the only successful combination (first two lanes). All other combinations failed to yield a differential banding pattern between mock-transfected cells and those transfected with ERD2-HAb.
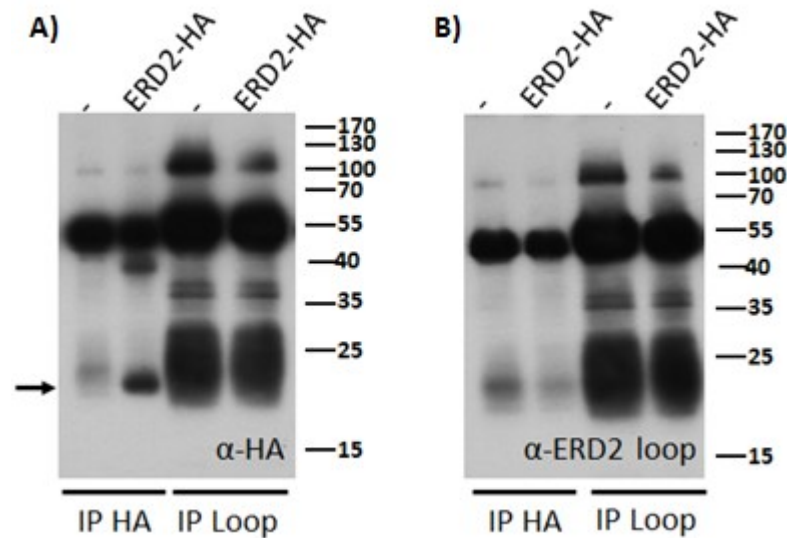
**Figure 2-33 Co-immunoprecipitation with either HA or ERD2 antibody**
Epitope tagged ERD2 (ERD2-HA) in GUS vector was expressed in tobacco protoplasts
and the expression is confirmed by GUS expression (data no shown). Samples were
IP with either HA antibody (IP HA) or ERD2 antibody (IP Loop) and immunoblot was
obtained by either HA antibody (α-HA, panel A) or ERD2 antibody (α-ERD2 loop,
panel B). Size marker is illustrated on the right and the correct fusion size is
indicated by the black arrow on the left (23kDa). Negative control is indicated as "-".

## 2.3.2.6 Measuring receptor-ligand stoichiometry by metabolic labelling and quantitative immunoprecipitation

A fundamental difference between western blotting and immunoprecipitation
of *in vivo* labelled proteins is that the former yields unpredictable signals, whilst the
latter can be quantified by radiation, corrected for the number of methionine and
cysteine residues in either receptor or ligand. Western blotting is only quantitative if
careful calibration curves have been produced with pure proteins of known
concentrations. Since pure proteins of ERD2 or Amy-HDEL were not available,
quantitative immunoprecipitation of metabolically labelled cell extracts was chosen
as the method of choice. If antibodies are used in excess of antigen during the
binding step, and protein A-sepharose is used in excess of antibodies during the
immunoprecipitation step, the method will lead to the recovery of all recombinant
proteins added to the system regardless of the affinity of the antibodies. Strict
volumetric dosage of the starting material related to a defined percentage of the
original protoplast suspension will therefore permit to quantify the number of
introduced ligands and receptors and in particular how many ligands were re-
distributed from the medium to the cells as a consequence of the added receptors.

Since only the anti-HA antibodies were functional in immunoprecipitation, ERD2-HAb was used as the model receptor, even though it exhibited only 50% of the wild type receptor activity. Amy-HDEL was used as ligand since high quality antibodies to Amy were available (Phillipson *et al*., 2001). Both receptor and ligand were expressed from the dual expression vector harbouring the common cytosolic marker GUS for normalisation of transfection. Cell suspensions were continuously labelled with a mixture of $^{35}$S methionine and cysteine during the entire expression period in order to quantify the total number of introduced molecules and their distribution between cells and medium. Pilot assays were carried out to demonstrate that anti-Amy antibodies or anti-ERD2 antibodies were used in excess of their respective antigens. This was essentially done by re-immunoprecipitation of the first supernatant from each immunoprecipitation to see a lack of signal, indicating that all antigens had been removed. Figure 2-34 illustrates the number of methionine and cysteine residues in Amy-HDEL and ERD2-HAb respectively,

A)
>ERD2b 4M2C
MNIFRLAGDMTHLASVLVLLLKIHTIKSCAGVSLKTQELYAIVFA
TRYLDIFTSFVSLYNTSMKLVFLGSSFSIVWYMKYHKAVHRTYDR
EQDTFRHWFLVLPCFLLALLIHEKFTFLEVLWTSSLYLEAVAILP
QLVLLQRTRNIDNLTGQYIFLLGGYRGLYIILNWIYRYFTEPHFVH
WITWIAGFVQTLLYADFFYYYFLSWKNNKKLQLPA

B)
>Amy-HDEL 6M3C
MANKHLSLSLFLVLLGLSASLASGQVLFQGFNWESWKHNGGWYNF
LMGKVDDIAAAGITHVWLPPASQSVAEQGYMPGRLYDLDASKYGN
KAQLKSLIGALHGKGVKAIADIVINHRTAEHKDGRGIYCIFEGGT
PDARLDWGPHMICRDDRPYADGTGNPDTGADFGAAPDIDHLNLRV
QKELVEWLNWLKADIGFDGWRFDFAKGYSADVAKIYIDRSEPSFA
VAEIWTSLAYGGDGKPNLNQDQHRQELVNWVDKVGGKGPATTFDF
TTKGILNVAVEGELWRLRGTDGKAPGMIGWWPAKAVTFVDNHDTG
STQHMWPFPSDRVMQGYAYILTHPGTPCIFYDHFFDWGLKEEIDR
LVSVRTRHGIHNESKLQIIEADADLYLAEIDGKVIVKLGPRYDVG
NLIPGGFKVAAHGNDYAVWEKIHDEL

**Figure 2-34 Amino acid sequence of ERD2 and Ligand**
Methionines and cysteines are underlined and highlighted in yellow in the protein sequence of both ERD2b (panel A) and its ligand Amy-HDEL (panel B). Total number of methionines and cysteines are indicated next to the names of each sequence. Predicted transmembrane domains of ERD2b are highlighted in blue in panel A. Signal peptide of Amy-HDEL is also highlighted in blue in panel B and the methionine within the signal peptide does not count. Possible glycosylation site is highlighted in red letters for Amy-HDEL.

showing that the expected radioactive signal strength for equal number of molecules is a 3:2 ratio for Amy-HDEL: ERD2-HAb. Results obtained from quantitative phosphorimaging can thus be corrected to obtain the relative number of molecules of Amy-HDEL and ERD2-HAb.

Figure 2-35 shows a flow chart of the experiment for stoichiometry measurement. Reproducing the experimental conditions in Figure 2-30, plasmid concentrations for Amy-HDEL and ERD2-HAb were chosen to yield equal GUS activities individually. The cell suspension were generated from pooled transfections, either without DNA (mock), with plasmid encoding Amy-HDEL alone, and finally a mixture of Amy-HDEL + ERD2-HAb. Since protoplasts suspensions contain individual cells that do not form clumps, it is possible to divide a transfected cell suspension into equal portions volumetrically. Each suspension was therefore split into three portions, one for measurement of secreted and cellular Amy activity, one for metabolic labelling during the same incubation period and subsequent immunoprecipitations of medium and cells, and one for verifying the GUS activity. Samples were taken strictly volumetrically in order to calculate the secretion index, either from amylase activities or quantification of $^{35}$S β-radiation. This would permit calculation of the total number of ERD2-HAb molecules relative to the total number
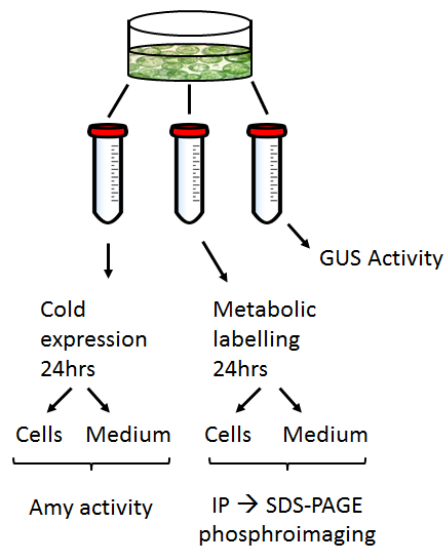


**Figure 2-35 Work flow of radio labelling**
Plasmids encoding Amy-HDEL and ERD2-HA are expressed and co-expressed with each other in tobacco protoplasts via electroporation. Work flow of the experiment is illustrated. Electroporated protoplasts were split to three fractions for GUS activity, Amy activity or IP. Equal amount of protoplasts were used for cold expression and metabolic labelling. Leftover were used for GUS activity. Results of radio labelling is analysed by phosphroimaging after transfer of the samples from SDS-PAGE.

of Amy-HDEL molecules in the system, as well as the number of Amy-HDEL molecules recovered in the cells or removed from the medium via addition of ERD2-HAb. After correction by the 3:2 ratio between ligand and receptor, it would be possible to calculate how many ligands have been successfully retained by how many receptors in relative numbers.

Figure 2-36 shows that the secretion index as calculated from enzymatic activities dropped by a factor 20 as a result of co-transfection with receptor plasmid. Activity lost from the medium was partially recovered in the cells. A slight reduction in total enzyme activity was observed which can explain the discrepancy. This could be due to competition for translocation pores at the level of the rough ER, through which both receptors and ligands must translocate to enter the secretory pathway. Measurement of the GUS activity confirmed that ligand and receptor encoding plasmids were transfected at approximately equal rates because the GUS activity is approximately 2-fold higher in the sample co-transfected with both ligand and
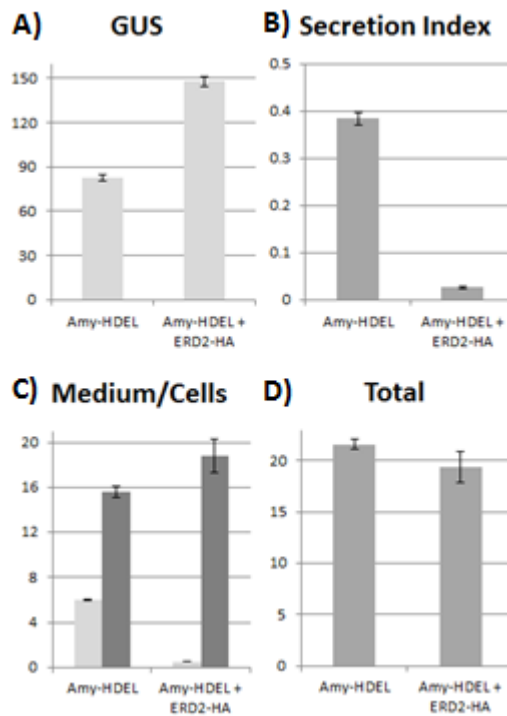


**Figure 2-36 *In vivo* bio-assay confirmation for radio labelling**
HDEL ligand (Amy-HDEL) and ERD2-HA were sub-cloned into GUS vector and co-expressed in tobacco protoplasts. GUS activity is illustrated in panel A. 5μg of DNA was used for both ligand and receptor. Secretion index was calculated and shown in panel B. Amylase activity in the medium (light grey bars) and cells (dark grey bars) are indicated in panel C. Total amylase activity is illustrated in panel D. Error bars represent standard deviation of two independent repeats. Units of α-amylase activity are ΔO.D./ml/min and secretion index units are considered as arbitrary.

receptor plasmid compared to ligand plasmid alone.

Figure 2-37 shows an X-ray autoradiogram of the resulting immunoprecipitation with either anti-Amy antibodies for the quantification of the ligands or anti-HA antibodies for the receptor. At the expected molecular weights, a weak signal for ERD2-HAb was obtained only in the extract from cells co-transfected with both Amy-HDEL and ERD2-HAb encoding plasmids, as expected. Signals for Amy-HDEL were much stronger and well beyond the expected 3:2 ratio caused by a 3:2 ratio for either the number of methionine residues or cysteine residues in Amy-HDEL versus ERD2-HAb. This shows that the total number of
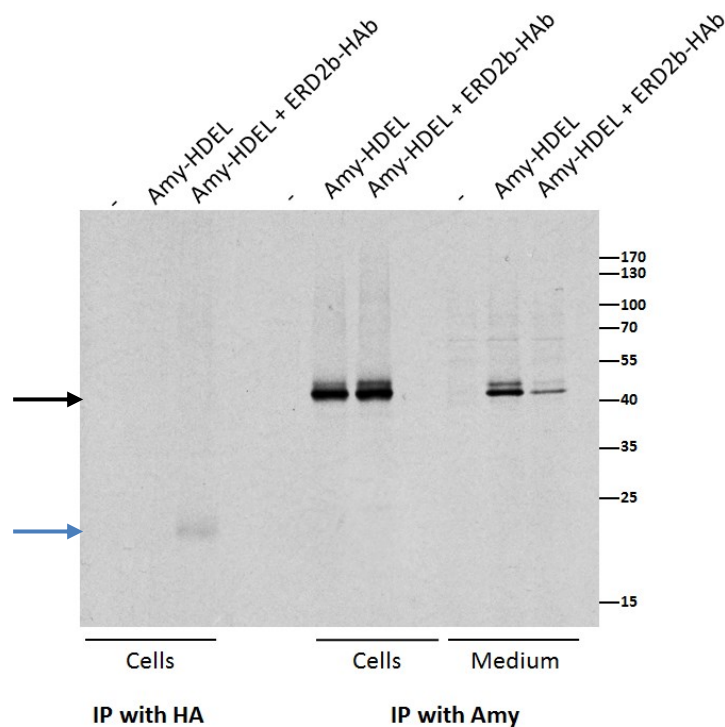


**Figure 2-37 Radio labelling of ligand and ERD2**

Ligand Amy-HDEL was expressed and co-expressed with ERD2-HAb in tobacco protoplasts. After electroporation, radio label $^{35}$S was added and incubated for 24 hours. Cells and medium fractions were harvested and IP with either HA or amylase antibody (Amy). Samples were equalised volumetrically and same amount was loaded. Autoradiograph was obtained after 20 hours exposure. Size marker is indicated on the right. ERD2 has a size around 23kDa (as indicated by a blue arrow) and amylase has a size around 45kDa (as shown by a black arrow).

introduced ligands is much higher than the number of receptors. To quantify the difference, the samples were analysed by phosphorimaging, which has a much greater dynamic range and approximately 10-fold higher sensitivity than X-ray film (Johnström *et al*., 2012), comparable to liquid scintillation, but yet offering the selection of regions of appropriate molecular weight from the protein blot. Figure

2-38 shows a summary of all results obtained from the quantifications. Quantification of introduced HA-tagged receptors as well as Amy-HDEL in cells and medium in the presence or absence of co-expressed receptors permitted calculation of the secretion index (Figure 2-38A), the total signal of receptor and cargo (Figure 2-38B), the individual cargo levels in cells and medium (Figure 2-38C) and the amounts gained in the cells or recovered from the medium as a result of introduced receptors (Figure 2-38D).
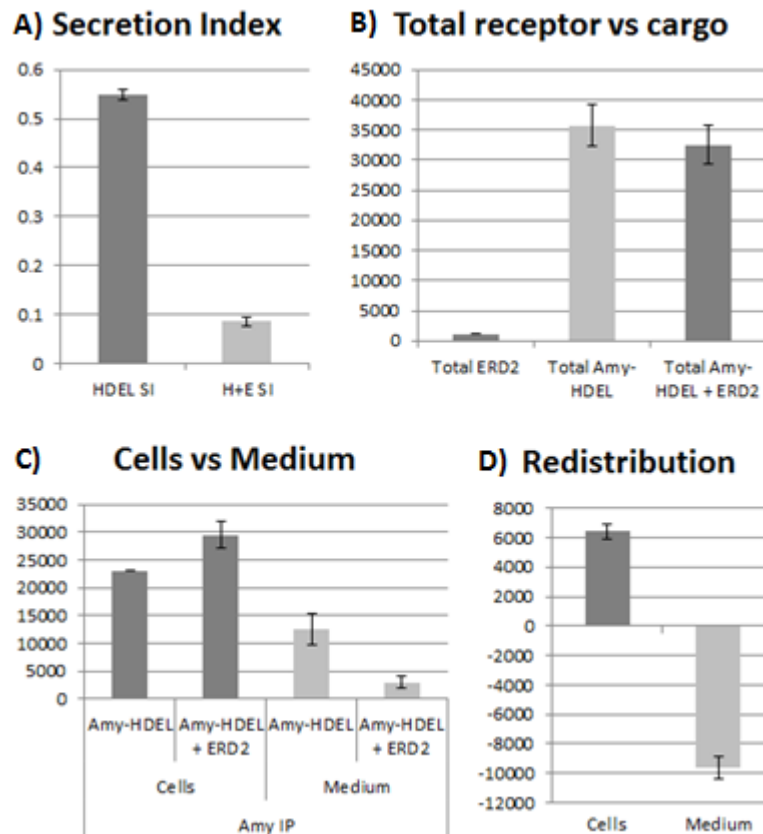


**Figure 2-38 Radio labelled ligand and receptor data analysis**
Phosphorimage intensity of each sample peak is manually pick according to their molecular size and calculated as intensity per sample and this is then converted to secretion index (SI) (panel A, HDEL represents sample containing Amy-HDEL alone and H+E represents sample containing Amy-HDEL and ERD2-HA). Total intensity amount of ERD2, its ligand Amy-HDEL and co-expression of the two is illustrated in panel B. Cells and medium fractions are indicated in panel C. Cargo redistribution as the differences between cargo Amy-HDEL alone and with addition of the receptor ERD2 in both cells and medium are shown in panel D. Sample peak selection and detection were achieved by Aida version 4.14 and detector Fuji FLA-5000 respectively. Error bars are standard errors of two independent repeats. Units are pixel intensity.

After correcting the value of total ERD2 in Figure 2-38B by multiplying with 1.5 to correct for the number of methionine and cysteine residues in ERD2, the average

taken from the amount of Amy-HDEL recovered in the cells and the amount retrieved from the medium (Figure 2-38D) is approximately 4.5 times higher compared to the number of receptors introduced. This suggests that at the highest receptor concentration used in the dilution experiment (Figure 2-30), each receptor has mediated the retention of multiple ligands. However, since the receptor can be 100-fold diluted and yet retains 50% of the retention capacity (Figure 2-30); the actual receptor-ligand ratio is in excess of 1 to 200. It should also be noted that co-transfections are not 100% efficient, in particular at low plasmid concentrations and therefore this ratio is an under-estimation of the true capabilities of the receptor.

### 2.3.3  Discussion

### 2.3.3.1 The use of quantitative expression systems that permit dose-response assays

Results in this chapter illustrate the importance of expression systems that yield reproducible results and permit experimental conditions under which a single variable can be studied. In this work the sole variable was either the amount of receptor or a specification made to the receptor. The protoplast system is ideally suited to generate identical portions of cell suspensions because protoplasts don't form cell aggregates and permit pipetting of equal aliquots. Variables can be introduced by changing the concentration of a plasmid, or by introducing changes to a gene on a plasmid. In the latter case, differences in the quality of plasmid preps can be corrected by introducing an internal marker, and the dual expression vector harbouring the cytosolic reporter enzyme GUS (Gershlick *et al*., 2014) has proven useful in this project. The sensitivity of the dose-response assay was of such quality that it could be used to equalise the transfection efficiency between receptor and cargo plasmids and carry out serial dilutions of the receptor plasmid (Figure 2-30). The system was also instrumental in demonstrating how epitope tagging can change the biological activity of ERD2 (Figure 2-31, Figure 2-32).

### 2.3.3.2 Context-dependence of epitope tags and suitability of antibodies for immunoprecipitation

Although epitope tags have been ubiquitously used in cell biology, including the analysis of ERD2 (Lewis and Pelham, 1990), it is not widely recognised that different epitope tagged proteins may not be detected with the same affinity by the antibodies. Results obtained in this chapter were totally unexpected, as they

illustrated a strong reduction in the HA-tag affinity to its antibody after fusion of a small tetrapeptide HDEL to its C-terminus (Figure 2-31). Epitope tags are often fused to either the N-terminus or the C-terminus of a protein, but often also internally. From experiments in this chapter it must be concluded that care must be taken when quantification of the number of molecules is required.

A second lesson to be learned from work carried out in this chapter is that antibodies may be suitable for the detection of denatured proteins, native proteins or either of them. Anti-HA antibodies were shown to work for both western blotting as well as immunoprecipitations of HA-tagged ERD2 fusions whilst antibodies generated against the first cytosolic loop of ERD2 were only suitable for western blotting (Figure 2-32) but not for immunoprecipitation (Figure 2-33). It is possible that the first cytosolic loop of ERD2 is masked by another associated protein, but Figure 2-36 revealed no additional co-precipitating radioactive bands when ERD2-HAb was immunoprecipitated with anti-HA antibodies. Alternatively, it is possible that the synthesised peptide displayed a structure more similar to the denatured ERD2 protein and folds up differently in native ERD2. It is unfortunate the C-terminal HA tagging of ERD2 led to a 50% reduction in the biological activity. Perhaps insertion of a glycine linker between the C-terminus of ERD2 and the HA tag may lead to an increase in biological activity, and this may be worthwhile attempting in the future.

## 2.3.3.3 ERD2 can redistribute extra-stoichiometric levels of ligands

The most exciting result of this chapter is the clear demonstration that many ligands can be re-distributed by few receptors. This was first recognised when it became clear how much the ERD2 plasmid can be diluted without affecting the additional ER retention capacity (Figure 2-28). This was exacerbated when it became clear that with the same plasmid transfection rate as estimated by the internal marker GUS and the use of the same promoter, Amy-HDEL was produced at much higher rate as ERD2 (Figure 2-37). The combined data in Figure 2-30 and Figure 2-38 suggest that one ERD2 molecule can mediate the retention of at least 200 HDEL proteins and probably more if data could be corrected for the lower plasmid co-transfection rates when dilutions of the plasmids were transfected. The co-transfection efficiency is unknown under these conditions, and therefore the exact ratio between receptors and redistributed ligands remains unknown. But it is

nevertheless certain that few ERD2 molecules can mediate re-distribution of many ligands. Since the ligands can continue to escape to the Golgi after each recycling step, the recycling mechanism either depends on fast receptor recycling, binding to multiple ligands simultaneously, or a combination of both.

If COPII coated membrane carriers are the sole transport shuttles that carry cargo from the ER to the Golgi apparatus, then receptors and escaping cargo would leave the ER via the same pathway. The only way in which receptors could be returned to the Golgi more efficiently than bulk flow it is when they contain active sorting signals for integration into the COPII coated membrane and that they occupy a significant amount of the carrier surface. If COPII-mediated transport is vesicle mediated, the internal volume for aqueous solutes may be small, but yet it is clear that secretion of soluble proteins such as Amy occurs at high rates. It has yet to be shown that ERD2 is transported in a COPII-dependent manner to the Golgi. If ERD2 returns to the Golgi via a different pathway that excludes lumenal contents, perhaps via a specific tubular transport carrier which is composed mainly of ERD2 and reticulons to restrict the lumen to a minimum, then faster recycling can be envisaged, but this requires experimental proof.

The compact nature of ERD2 makes it hard to imagine how it could bind to several ligands simultaneously. However, the so-far published evidence surrounding ERD2-ligand interactions has never produced firm evidence of a direct interaction, because peptide binding studies were not carried out with purified components (Townsley *et al*., 1993). Furthermore, ligand-binding specificity assays distinguishing different receptors for different tetrapeptides (Lewis *et al*., 1990; Semenza and Pelham, 1992) could not be reproduced in plants (Chapter I). One way in which receptor-ligand interactions could be enhanced is by postulating a soluble adapter that can bind many HDEL-proteins simultaneously but has only one binding site for ERD2. This cannot be ruled out by the *in vitro* peptide binding studies with microsomes isolated from ERD2 overexpressing cells (Townsley *et al*., 1993), because the postulated  adaptor molecule may have been present in the microsomal preparations. Future work will reveal which of the potential models can explain how few receptors recycle many ligands.

## 2.4  Chapter IV Functional analysis of ERD2 and ERP1

### 2.4.1  Introduction

Results in chapter I, II and III show that receptor saturation and suppression of ligand secretion by ectopic expression of further receptors is a very powerful tool to measure ERD2 activity *in vivo*, without the need to select knock-down mutants and risk lethal or developmental phenotypes. This rapid and technically robust *in vivo* ERD2 activity assay can now be used to ask new questions about the biology of ERD2.

In principle, four different steps in the ERD2 transport cycle can be distinguished, although this is most likely a simplification. First of all, the receptor is thought to bind to its ligands in the Golgi, as it has been shown that addition of the KDEL peptide for ER retention to cathepsin D resulted in a molecule that was retained in the ER but continued to receive Golgi specific modifications of the mannose 6 phosphate route (Pelham, 1988). Upon ligand-binding, the receptor may initiate the recruitment of COPI machinery, in order to mediate retrograde transport to the ER. There is no direct evidence for this, but indirect evidence arose from the fact that ERD2 was found in COPI vesicles (Orci *et al*., 1997) and shown to recruit ARF1-GAP to Golgi membranes (Aoe *et al*., 1997). GTP-hydrolysis by ARF1 may be used to drive the uncoating of the COPI vesicles to facilitate fusion with the ER. However, specific targeting signals for Golgi-retention or retrograde transport back to the ER have never been identified (Pfeffer, 2007), and the typical di-lysine motifs found in COPI cargo are not conserved in ERD2, nor have the lysine residues present in the ERD2 carboxy terminus been implicated in retrograde transport (Townsley *et al*., 1993). The third step in the receptor cycle is expected to be the release of its ligand upon arrival in the ER, but it has not been shown which physico-chemical conditions would stimulate this process. Finally, the free receptor should return to the Golgi in a most efficient manner and certainly faster than bulk flow in order to mediate retention of the far more abundant ligands.

The results from the bio-assay illustrated in Figure 2-28 and Figure 2-30 show that the method detects subtle differences in the performance of ERD2 derivatives. The sensitivity range of the dose-response assay is ideally suited for the evaluation of functional mutants of ERD2. Since all 4 steps described above will contribute to the ability of ERD2 to suppress Amy-HDEL secretion, it should be possible to collect mutants in all four transport steps, notably 1) ligand binding, 2) retrograde

Golgi to ER transport, 3) ligand-release, and 4) anterograde ER to Golgi transport. There may be other processes that mediate Golgi retention as well. Earlier studies focused mainly on ligand-binding and ligand-induced redistribution to the Golgi apparatus (Townsley *et al*., 1993; Scheel and Pelham, 1998). The bioassay developed in this thesis may yield new classes of mutants, or help to re-evaluate earlier characterised mutants in different ways. In this respect it is also noteworthy that almost all the fluorescent fusions generated in this study are biologically inactive, except for ERD2-RFP which retains some 10% of the activity of the untagged receptor. Previous localisation studies with fluorescent ERD2 fusions may thus be obsolete as they do not build on a functionally active molecule. Since fusion proteins are intrinsically unstable, it is possible that presumed successful genetic complementation studies arose from biologically active cleavage products of ERD2 which had lost the fluorescent tag and were present together with fusion protein that was inactive.

In addition to the above mentioned fundamental question about the ER retention system, the host laboratory has identified a family of ERD2-related membrane proteins, the so-called ERP gene family (Hadlington and Denecke, 2000). These genes code for proteins with an additional N-terminal transmembrane domain compared to ERD2. The ERP gene family is highly conserved among higher plants and other photosynthetic organisms including *Physcomitrella*, *Selaginella*, *Ostreococcus*, *Volvox*, *Chlamydomonas*, and diatoms. ERPs are also found in the oomycete *Phytophora infestans* and some protists such as *Tetrahymena* and *Plasmodium*, but are absent from all animals, yeasts and most fungi. It is unclear how organisms with both ERD2 and ERPs differ from organisms that just contain ERD2, and what the biological role of ERP proteins is. ERP proteins also remain to be localised in plants.

In this chapter the quantitative *in vivo* bio-assay for ERD2 in mediating ER retention of soluble proteins is explored to verify if ERP proteins play a role in ER retention like ERD2, to study the C-terminus of ERD2 and its role in the biological function of ERD2, and finally several earlier reported mutations that were classified as ligand-binding mutants (Townsley *et al*., 1993; Scheel and Pelham, 1998).

## 2.4.2  Results

## 2.4.2.1 A member of the ERP gene family does not play a role in ER retention of soluble proteins

Although the ERD2-related protein family has been identified 15 years ago soon after the completion of the *Arabidopsis thaliana* gene sequencing project (Hadlington and Denecke, 2000), no functional studies have been reported on this class of proteins. Figure 2-39 shows an alignment of ERP1, one representative of this family, with ERD2, illustrating that it contains an extension of just under 50 amino acids at the N-terminus of a backbone that resembles the ERD2 sequence. The N-terminal extension may contain an additional transmembrane domain, but the topology is unknown.

```
              10        20        30        40        50        60        70        80
     ....|....|....|....|....|....|....|....|....|....|....|....|....|....|....|....|
ERP1 MKATTKTPIHVVWSWVRRQPPKVKAFLAVVTGMAALVLLRFIVHDHD-NLF-VAAEAVHSIGICVLIYKLMKEKTCAGLS
ERD2 ----------------------------------------------MNIFRLAGDMTHLASVLVLLLKIHTIKSCAGVS

              90       100       110       120       130       140       150       160
     ....|....|....|....|....|....|....|....|....|....|....|....|....|....|....|....|
ERP1 LKSQELTAIFLAVR---LYCSIVMEYDIHTILDLATLGTTLWVIFMIRF--KLRASYMEDKDNFPLYYVLAPCVALAVFI
ERD2 LKTQELYAIVFATRYLDIFTSFVSLY--NTSMKLVFLGSSFSIVWYMKYHKAVHRTYDREQDTFRHWFLVLPCFLLALLI

             170       180       190       200       210       220       230       240
     ....|....|....|....|....|....|....|....|....|....|....|....|....|....|....|....|
ERP1 HPSTSHNIINRISWALCVYLEAVSVLPQLRVMQNTKIVEPFTAHYVFALGVARFLSCAHWVLQVVDTRGRLLVALGYGLW
ERD2 H--EKFT-FLEVLWTSSLYLEAVAILPQLVLLQRTRNIDNLTGQYIFLLGGYRGLYILNW---IY----RYFTEPHFVHW

             250       260       270       280
     ....|....|....|....|....|....|....|....|....
ERP1 PSMVLISEIVQTFILADFCYYYVKSVFGGQLVLRLPSGVV
ERD2 --ITWIAGFVQTLLYADFFYYYFLS-WKNNKKLQLPA---
```

**Figure 2-39 ERP1 and ERD2 amino acid sequence alignment**
Protein sequence of ERP1 is aligned with that of ERD2. Conserved amino acids are highlighted in dark grey and similar ones are highlighted in light grey. Missing parts are indicated by dashed line.

To test the localisation of this construct, an N-terminal YFP fusion and a C-terminal RFP fusion were constructed. Figure 2-40A shows a hypothetical topology that remains to be tested. Both fusion proteins were readily detected in tobacco leaves but failed to co-localise with each other (Figure 2-40B). Whilst YFP-ERP1 labels the ER, ERP1-RFP seems to label more punctate structures that were difficult to identify. Since it is not clear which of the two fusion proteins is representative of the native ERP1 localisation, it was decided to first test the potential function of ERP1.
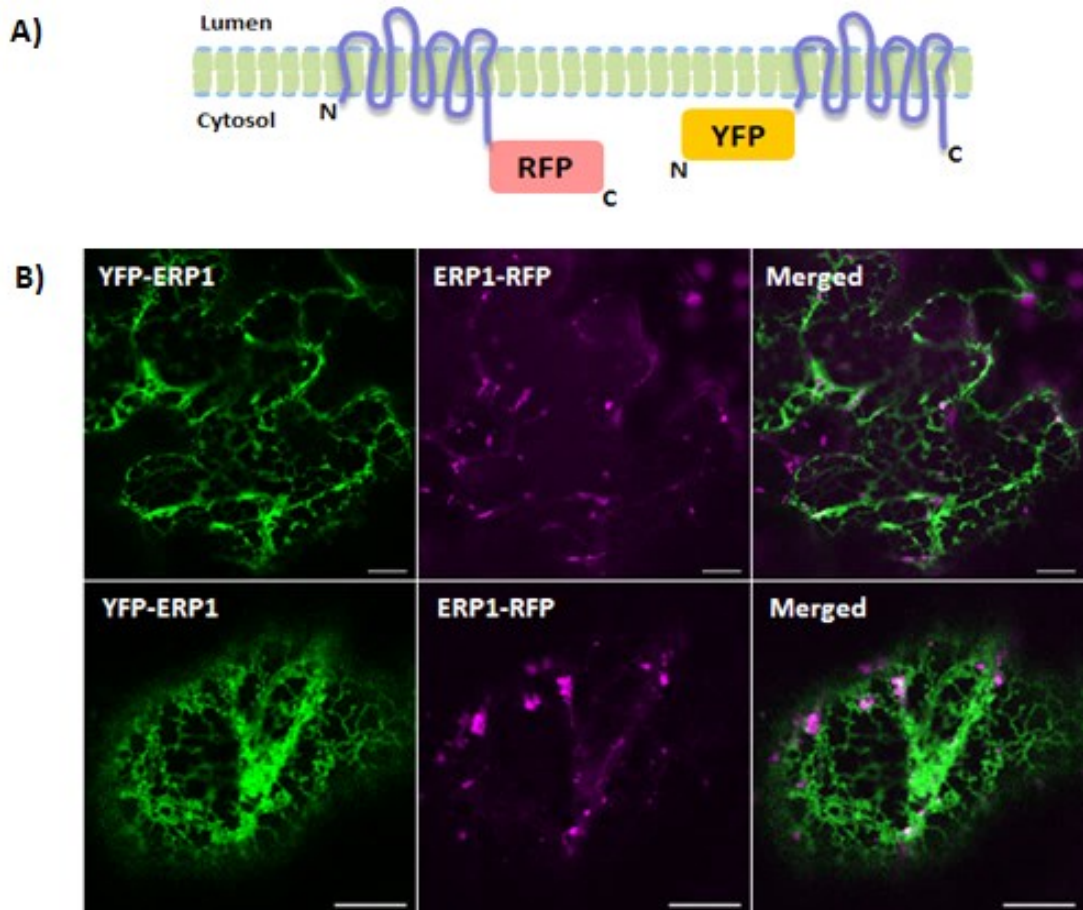
**Figure 2-40 ERP1 N-terminal and C-terminal fusions topology and *in vivo* co-localisation**
ERP1 was predicted to have eight transmembrane domains with both N- and C-terminus in the cytosol. Predicted topology of florescent fusions of ERP1 either at its C- (ERP1-RFP, on the left) or N-terminus (YFP-ERP1, on the right) are overviewed (panel A). These fusions are driven by 35S promoter and were co-expressed with each other in tobacco leaf epidermis cells via *Agrobacterium* mediated leaf infiltration (panel B). Images were obtained after two and a half day of the infiltration. All scale bars are 10μm.

The similarity between ERD2 and ERPs suggests that ERPs may play a function in ER retention too. To test if ERP1 overexpression influences Amy-HDEL secretion, its coding region was inserted into a dual expression vector carrying the internal marker GUS and compared with a similar ERD2 expression plasmid. After adjusting the plasmid preparation to yield equal levels of GUS as the positive control harbouring ERD2, co-expression experiments were carried out with the model cargo Amy-HDEL. Figure 2-41 shows that in contrast to ERD2, ERP1 has no ability to suppress the secretion of Amy-HDEL caused by ERD2 overload. In contrast, ERP1 overexpression seemed to slightly increase Amy-HDEL secretion, although Figure 2-40 is only a pilot experiment that was not pursued further due to

time constraints, the uncertainty regarding the biological relevance of the two fluorescent fusions, and outstanding work on ERD2 that took precedence.

However, the preliminary results obtained on this class of proteins suggest that ERPs carry out a different function and probably do not assist in ERD2-mediated retention of soluble ER residents. The gene family is highly conserved in plants and *Arabidopsis thaliana* contains 5 different ERPs, whilst only two true ERD2 proteins have been identified in this species. Further work on this class of proteins was beyond the scope of this thesis but may form the basis for future research.
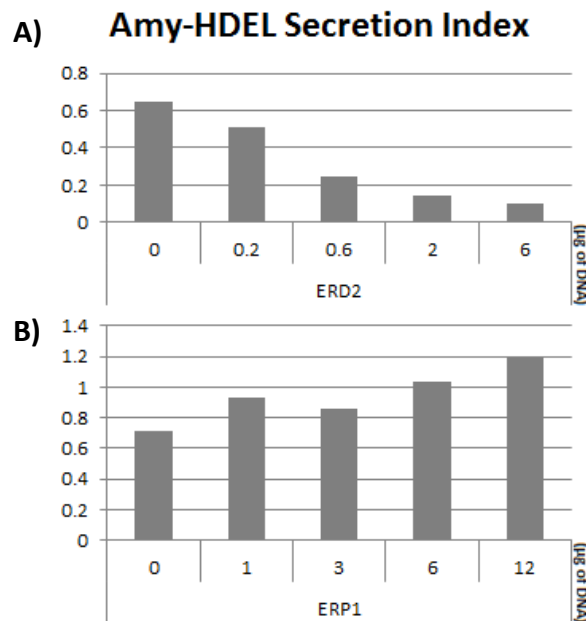


**Figure 2-41 ERP1 functionality in transient expression with HDEL ligand**
Dose response of ERP1 (panel B) with ligand Amy-HDEL is compared with that of wild type ERD2 (panel A) in tobacco protoplast transient expression. Constant amount of Amy-HDEL was used and the amount of ERD2 and ERP1 is indicated below each lane. GUS expression is similar (data not shown). No error bars were obtained due to the nature of the pilot experiment. Units of α-amylase activity are ΔO.D./ml/min and secretion index units are considered as arbitrary.

## 2.4.2.2 Importance of the ERD2 C-terminus in receptor function *in vivo*

Results obtained in chapters II and III suggest a crucial role of the ERD2 C-terminus that was previously overlooked (Townsley *et al.*, 1993). It is possible that the C-terminus is involved in signalling to cytosolic components to initiate retrograde transport, and that important residues are partially masked when a

fluorescent protein is fused to the C-terminus. Even the addition of the small HA epitope tag to the C-terminus compromised the performance of ERD2 in suppressing Amy-HDEL secretion although this was only clear at low plasmid concentrations (Figure 2-29 & Figure 2-30). Replacement of the last 9 amino acids of ERD2 by the HA tag completely abolished biological activity of the resulting fusion protein (ERD2-HAa, Figure 2-29). For this reason it was justified to investigate the C-terminal 9 amino acids of ERD2 in more detail.

Figure 2-42A shows a schematic model of the topology of ERD2 which has been supported by results in chapter II and the sequence of amino acids comprising the predicted cytosolic tail of ERD2. Since positively charged amino acids have been implicated in mediating interaction with COPI coats for retrograde transport back to the ER (Cosson and Letourneur, 1994), all lysine residues were mutated to alanine. In addition, two leucines and a proline were mutated to alanine as they were conserved amongst ERD2 sequences. The point mutations were verified by sequencing, followed by sub-cloning the mutant coding region into the dual expression GUS vector used before. Figure 2-42B shows that the various plasmids encoding mutant ERD2 were at least as well transfected as the wild type ERD2 control because all GUS activities were at least identical or above the GUS levels obtained for the control. Figure 2-42C shows that mutation of the three lysine residues had no effect on ERD2 functionality. In contrast, mutation of either of the two leucine residues diminished the ability of ERD2 to suppress Amy-HDEL secretion. Mutation of the proline residue had only a minor influence of ERD2 function.

Dose-response analysis of all the point-mutations (Figure 2-43) confirmed that the lysines could be replaced by alanine without compromising biological activity. In contrast, the two hydrophobic leucine residues appeared to be crucial for ERD2 function, and mutation of the proline residue revealed a weaker but yet reproducible effect on ERD2 functions. Since the effect of a single mutation of leucine to alanine only exhibited a partial effect on ERD2 function, a double mutant was generated in which both leucine residues were replaced by glycine. Dose-response analysis revealed that the double mutant (LLGG) had lost all biological activity (Figure 2-44C).
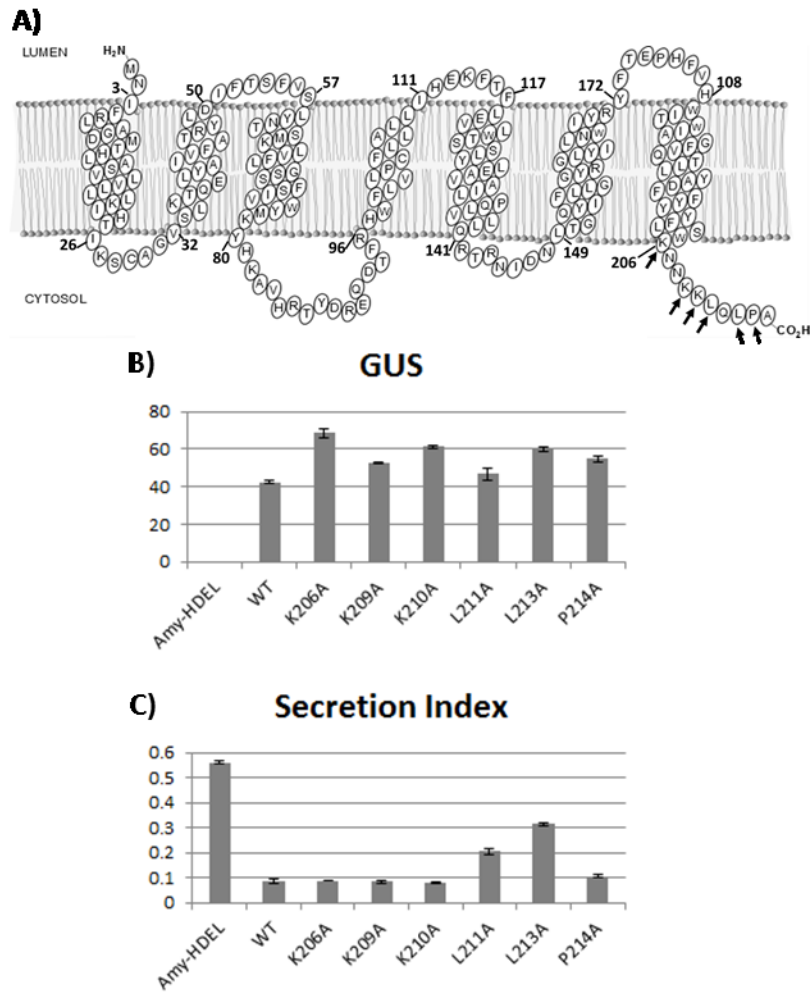
**Figure 2-42 C-terminal point mutations of ERD2**
Six C-terminal point mutations (K206A, K209A, K210A, L211A, L213A and P214A) of ERD2 were generated and sub-cloned to the GUS vector. The position of each mutation is indicated by black arrows in the predicted structure of ERD2 (panel A). These point mutations were co-expressed with Amy-HDEL in tobacco protoplasts and their results are compared with wild type ERD2 (WT). GUS expressions of all constructs are illustrated in panel B and cargo molecule (Amy-HDEL) without GUS is used as a negative control. Constant amount of Amy-HDEL was used for both WT and point mutations co-expression. Secretion index of cargo alone and in combination with WT and point mutations are shown in panel C. Error bars are standard deviations of three independent repeats. Units of α-amylase activity are ΔO.D./ml/min and secretion index units are considered as arbitrary.
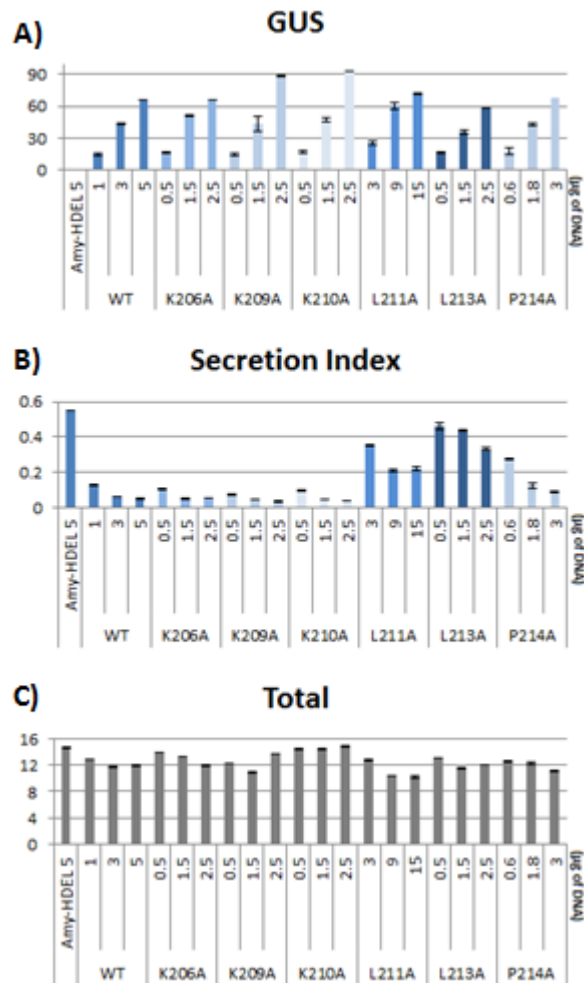
**Figure 2-43 Dose response of C-terminal point mutations in tobacco protoplast**
Co-expression of C-terminal point mutations (K206A, K209A, K210A, L211A, L213A and P214A) with ligand Amy-HDEL with three different dosages of mutants is compared with that of wild type ERD2 (WT). Ligand alone (Amy-HDEL) is used as a negative control. Similar GUS expressions of ERD2 and its mutants are illustrated in panel A. Corresponding secretion index is shown underneath (panel B). Comparable total activity of α-amylase-HDEL (Amy-HDEL) is indicated in panel C either with or without effectors. The amount of DNA used is indicated below each lane. Error bars represent standard deviation of three independent repeats. Units of α-amylase activity are ΔO.D./ml/min and secretion index units are considered as arbitrary.

## 2.4.2.3 Re-evaluation of earlier published ligand-binding mutants reveals a novel phenotype

In two consecutive studies, Pelham and co-workers generated a very thorough analysis of the primary structure of human ERD2 and identified several mutations that were classified as ligand-binding mutants. Here the equivalent mutations were generated on *Arabidopsis thaliana* ERD2 (Figure 2-44A) and analysed in the same manner as the C-terminal mutants (Figure 2-42). Figure
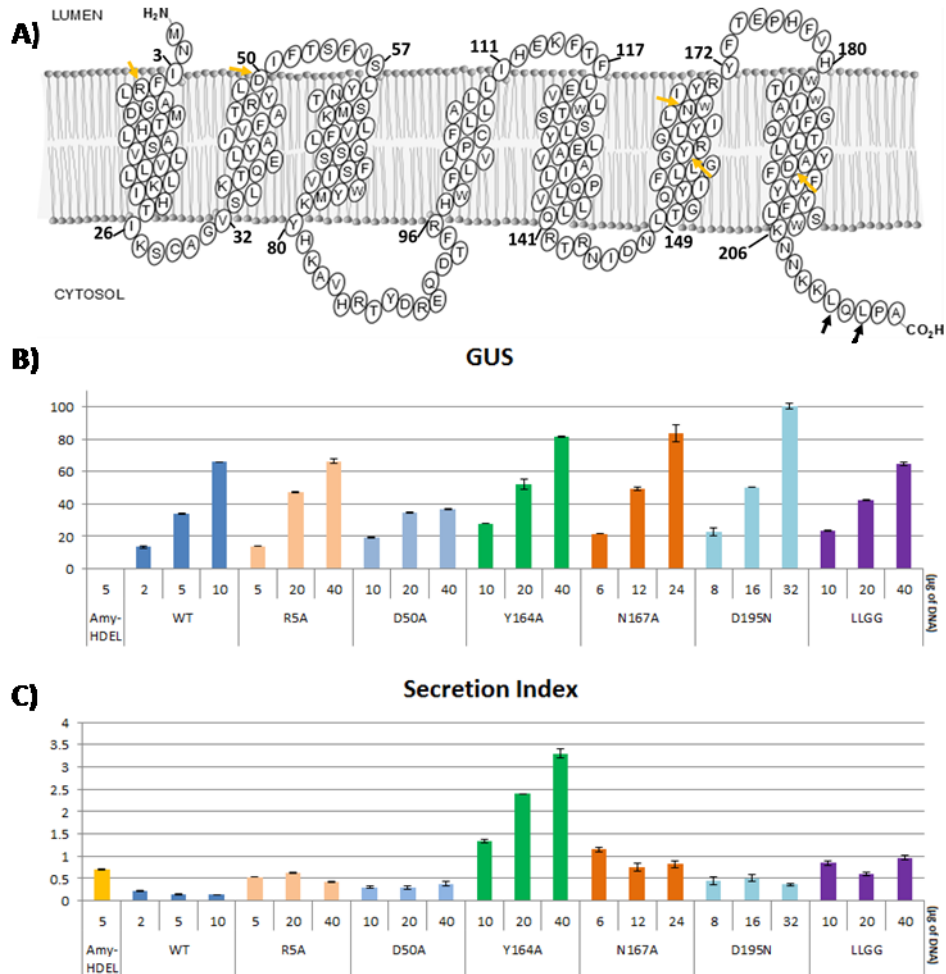


**Figure 2-44 Comparison of published ERD2 mutants in tobacco protoplasts**
Several previous published mutations of ERD2 by H. Pelham were selected (R5A, D50A, Y164A, N167A and D195N) and co-expressed with ligand Amy-HDEL. In addition, double leucine mutation (LLGG) was generated. Positions of all mutations are indicated by arrows (yellow for point mutations and black for LLGG) in panel A. GUS expressions of both wild type ERD2 (WT) and its mutants are illustrated in panel B and non-GUS ligand Amy-HDEL is used as a negative control. Constant amount of Amy-HDEL is applied for all samples and the amount of DNA used is indicated below each lane. Corresponding secretion index is shown underneath (panel C). Error bars represent standard deviation of three independent repeats. Units of α-amylase activity are ΔO.D./ml/min and secretion index units are considered as arbitrary.

2-44B&C shows that all mutants were compromised in their ability to reduce Amy-HDEL secretion. However, one mutation stood out as it exhibited an unexpected dominant effect by strongly stimulating Amy-HDEL secretion.

To test the induced secretion induced by ERD2 (Y164A) further, a detailed dose-response analysis was carried out to compare its effect on Amy-HDEL with the control cargo Amy. This was important in order to test if the mutant causes a general increase in the exocytic pathway. Figure 2-45 shows that with equal transfection rates, ERD2 (Y164A) mediates induced secretion of Amy-HDEL beyond the level caused by normal ERD2 saturation, without having an effect on constitutive Amy secretion. The effect is therefore ligand-specific and the result suggests that the Y164A mutation causes ERD2 to interfere with endogenous wild type ERD2 in a dominant manner. Conditions that cause induced secretion of ER
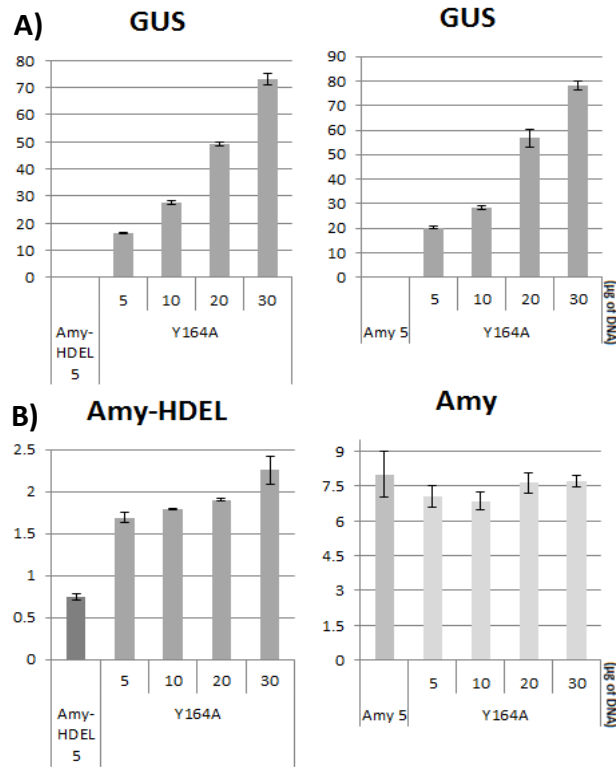


**Figure 2-45 Mutation analysis reveal an induced ligand secretion phenotype**
Dose response of mutant Y164A with ligand Amy-HDEL is compared with non-ligand Amy in tobacco protoplast transient expression. Constant amount of Amy-HDEL and Amy was used and the amount of mutant Y164A which was used is indicated below each lane. GUS expression is presented in panel A corresponding to their α-amylase-HDEL (Amy-HDEL) and α-amylase (Amy) secretion index in panel B. Error bars represent standard deviation of three independent repeats. Units of α-amylase activity are ΔO.D./ml/min and secretion index units are considered as arbitrary.

residents are rare and the mutant constitutes a useful tool in this respect that may shed light on new transport principles.

In order to understand why ERD2 (Y164A) causes induced secretion of Amy-HDEL, a new double vector was constructed that contains either wild type ERD2 or the Y164A mutant of ERD2 on the same T-DNA as the Golgi marker ST-YFP. The resulting *Agrobacterium* strain was co-infiltrated with another strain harbouring a plasmid encoding for the soluble fluorescent ER marker RFP-HDEL. When ERD2 (Y164A) was co-expressed with ST-YFP and RFP-HDEL, the latter was clearly detectable in the Golgi bodies and co-localised with ST-YFP (Figure 2-46). This is unprecedented when RFP-HDEL is expressed alone with the Golgi marker ST-YFP. In the presence of wild type ERD2, RFP-HDEL showed a normal ER pattern, with no evidence for leakage of RFP-HDEL to structures distal of the ER. The results suggest that the Y164A mutant somehow interferes with the recycling of RFP-HDEL but at the same time causes its accumulation in the Golgi.
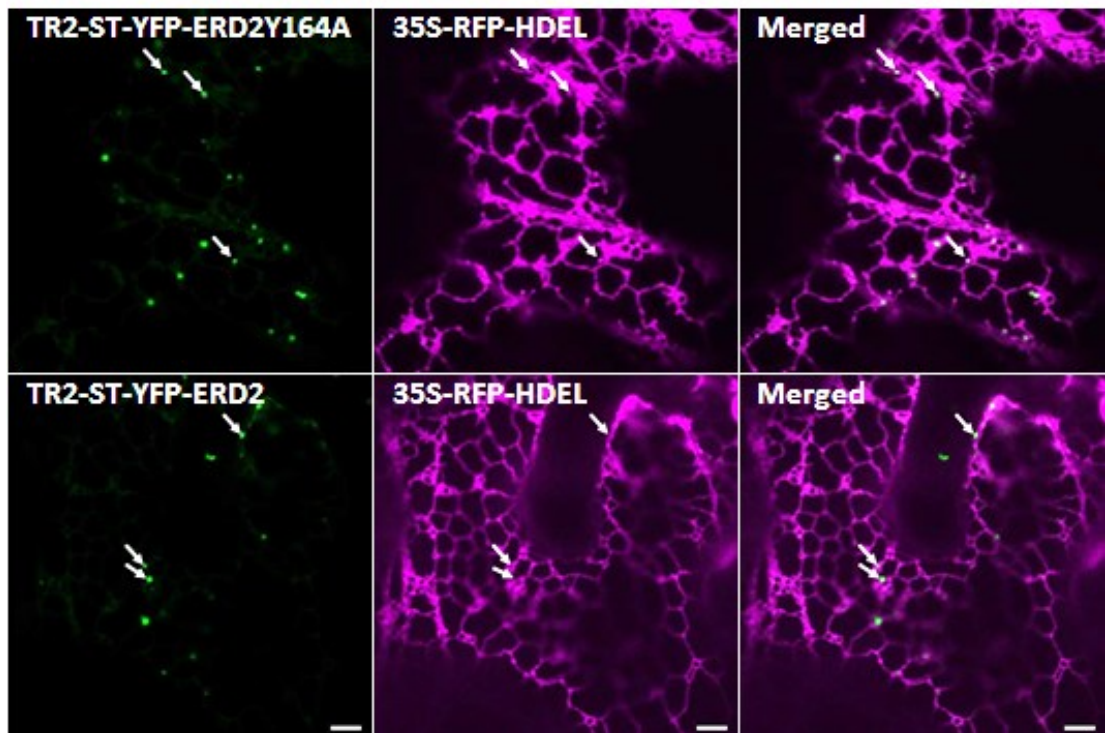


**Figure 2-46 ERD2 secretion mutant induces mis-localisation of HDEL ligand *in vivo***
Wild type ERD2 (bottom left) and its mutant ERD2Y164A (top left) were sub-cloned into a double expression vector containing Golgi marker ST-YFP with TR2 promoter and co-expressed with ER marker RFP-HDEL (middle panel) under the 35S promoter in tobacco leaf epidermis cells via *Agrobacterium* mediated infiltration. Both ERD2 and its mutant are driven under 35S promoter. Images were obtained after two and a half days of infiltration. Merged images are on the right panel. Examples of punctate structures for co-localisation and non-co-localisation are indicated by white arrows. All scale bars are 10μm.

## 2.4.3 Discussion

### 2.4.3.1 What is the role of ERPs?

In this chapter the receptor bio-assay was harnessed to test the potential role of a new ERD2-related (ERP) protein family in ER retention. Although no function similar to that of ERD2 could be assigned, the data obtained still suggest that it is an important gene family in plants. The pilot experiment testing the influence of ERP1 overexpression on Amy-HDEL transport did reveal the opposite effect of ERD2, as illustrated by a weak stimulation of Amy-HDEL secretion. Whilst this result requires further verification, it would also be interesting to test the influence of ERP1 on constitutive secretion, vacuolar sorting or the targeting of membrane spanning proteins of the tonoplast and the plasma membrane. This approach may yield faster results than attempting a gene knockout strategy, which would be hard in *Arabidopsis thaliana* with five ERP family members. The use of unicellular algae such as *Ostreococcus* or *Chlamydomonas* which have just single genes for ERD2 and ERP may have to be considered. Subcellular localisation of ERP would certainly require generation of antibodies to test the localisation of the native protein and compare the results with those obtained with either YFP-ERP1 or ERP1-RFP. In conclusion, research into ERP gene function is just in its infancy but thanks to the bio-assay on Amy-HDEL transport it could quickly be ruled out that ERPs are simply isoforms of ERD2, which they are clearly not.

### 2.4.3.2 Different classes of ligand-binding mutants

Results in Figure 2-42, Figure 2-43 and Figure 2-44 illustrate a critical role of two leucine residues in the C-terminus of ERD2. The second of these leucine residues is extremely conserved amongst ERD2 proteins throughout the eukaryotic kingdoms and it has a proline residue in the penultimate position of the coding region. The role of the C-terminus would have remained undiscovered as earlier studies suggested that the C-terminus is dispensable for ERD2 function (Townsley *et al.*, 1993).

However, the most exciting of the characterised mutants is the Y164A substitution which is not a loss of function phenotype but instead a dominant induction of secretion. The induced secretion phenotype distinguishes the Y164A mutant from the other 4 mutations that behave like loss of function mutants only. It is possible that the dominant effect by ERD2(Y164A) is caused by compromised

ligand-binding and competition for recycling machinery as demonstrated for a truncated mutant of the plant vacuolar sorting receptor (VSR) in which the ligand-binding domain was replaced by a fluorescent protein (Luis *et al*., 2005; daSilva *et al*., 2006). Alternatively, the mutant could be mis-targeted to the cell surface or a compartment from which soluble proteins can easily reach the cell surface. Results in Figure 2-45 are also interesting because secreted cargo is usually not detected in transit through the Golgi. Therefore, the mutant must exhibit another disruptive effect on export of soluble proteins from the Golgi, both in anterograde and retrograde orientation, in order to mediate accumulation of RFP-HDEL in the Golgi bodies.

To distinguish between these various possibilities, it will be important to generate fluorescent fusions with ERD2 that do not lose their biological activity. In this study the best current candidate is ERD2-RFP as it retains 10% biological activity and may be targeted in a biologically relevant manner. Further research will have to focus on testing the various mutants on the ERD2-RFP fusion in order to determine aberrant targeting of the receptor.

# 3    General discussion and considerations for the future

## 3.1    New tools and new questions

Although the plant homologue of yeast ERD2 was identified more than two decades ago (Lee *et al*., 1993), functional studies in plants are very scarce. Reports of its expression and regulation (Bar-Peled *et al*., 1995) as well as its subcellular localisation in the Golgi and the ER (Boevink *et al*., 1998) were merely descriptive. The report that its overexpression can induce ER export sites (daSilva *et al*., 2004) was perhaps the first functional indication for a role in ER-Golgi trafficking and that it may contain an active ER export signal for its fast return to the Golgi, once retrograde transport is completed and ligands have been released. The first genetic knock-out was published 5 years later (Li *et al*., 2009) but yielded contradictory information about its biological function. The authors observed that one HDEL containing protein, the calreticulin isoform CRT3, was specifically influenced by ERD2b in *Arabidopsis thaliana*, the lack of which caused CRT3 to be more rapidly degraded. However, ERD2b knockout did not influence other HDEL proteins like CRT1 and 2, or the ER chaperone BiP.

Functional transport studies demonstrating a role in reducing secretion were reported using the cargo molecule GFP-HDEL which is very slowly secreted. Overexpression of ERD2a-YFP yielded a 50% reduction of the amount of GFP-HDEL present in the medium, but the much higher intracellular GFP-HDEL levels were also reduced (Montesinos *et al*., 2014). The effect was not quantitative enough to provide a reliable activity assay for the functional analysis of ERD2 in plants. In Chapter I, two fundamentally different artificial cargo molecules were introduced that can be used to study ERD2 activity. As soluble cargo, the reporter barley α-amylase (Amy) is an ideal cargo molecule because it is readily secreted, but ER retained when the tetrapeptide HDEL was fused to its C-terminus. The Golgi marker ST-YFP also re-distributed to the ER upon fusion to the HDEL peptide and Amy-HDEL could compete with ST-YFP-HDEL for endogenous receptors. Under saturating conditions, both molecules leak out to post ER compartments, and this can be suppressed in a dose-responsive manner by overexpressed ERD2. These two assays are the first quantitative and dose-responsive ERD2 activity assays that are sensitive enough to carry out functional studies of ERD2. With the help of the Amy-HDEL cargo system, it was possible to show that one ERD2 molecule can mediate the ER retention of over 200 HDEL ligands. The bio-assay was also

instrumental in identifying and comparing the effect of specific mutations in ERD2 that altered its biological activity, and to show that the ERD2-related ERP gene family (Hadlington and Denecke, 2000) plays no role in ER retention. These and other findings are explored below in the light of future work that can be carried out to further our understanding of the biological function and mode of action of ERD2.

The main limiting factor in our current understanding is caused by the fact that fluorescent fusions generated to localise ERD2 are either completely inactive in the bio-assay or show only a fraction of its original activity. For instance, ERD2-YFP proved to be inactive in suppressing Amy-HDEL secretion, a result that leaves reasonable doubt about the results obtained with GFP-HDEL (Montesinos *et al.*, 2014). Subcellular localisation studies with ERD2-GFP or ERD2-YFP may not reflect the true distribution between ER and Golgi as ligand-binding may influence the distribution of ERD2 steady state levels between Golgi and ER (Lewis and Pelham, 1992a). As discussed in Chapter II, further research into the actual topology of ERD2 also remains to be carried out using protease protection assays, but the same concern regarding the biological activity of fluorescent ERD2 fusions remain. Only two tagged versions of ERD2 remained partially biologically active, a C-terminal HA tagged ERD2 retained 50% of its activity whilst a C-terminal RFP tagged ERD2 retained only 10 % of the original activity (Chapter II). All other fluorescent fusions were inactive.

Further research into more active fusion proteins may explore the use of a linker between the C-terminus and the tag. Alternative positions of the tags, such as one of the cytosolic loops, may be explored as well although they may interfere with transport if not ligand binding. Generation of a more active fluorescent ERD2 fusion that permits in vivo imaging may be instrumental in characterising point mutations that affect the biological activity of ERD2 as described in Chapter IV, as they could be used to distinguish between transport mutants and ligand binding mutants. Although work in this thesis has opened up new doors for the analysis of ERD2 in plants, new questions and challenges will have to be overcome as well. One of these includes the characterisation of the ERP gene family, which was beyond the scope of this thesis.

## 3.2  Towards a complete transport cycle of ERD2

One of the biggest limitations in our understanding of many biological processes is the lack of a complete picture of all the steps to close the circle of events in the process. Loss of function genetics merely helps to establish a role for a gene product, either directly or indirectly in a process of interest. To make further progress it is necessary to modify gene products and identify mechanisms. The bio-assay that has been used in this thesis to study ERD2 function can be used to identify mutants in all aspects of the transport cycle. Earlier *in vitro* studies focused on ligand-binding or subcellular localization of ERD2 (Townsley *et al*., 1993; Scheel and Pelham, 1998). However, the ability of ERD2 to suppress Amy-HDEL secretion *in vivo* will also be compromised by ligand-release mutants or transport mutants. As illustrated by Figure 2-44 the assay has even revealed a dominant mutation that causes further induced secretion of Amy-HDEL. Given the high sensitivity of the assay and the potential of identifying new classes of mutants, one of the first steps as a continuation of this project would be to carry out further mutagenesis and create a catalogue of mutants with different phenotypes. However, individual point mutations are time-consuming, even for a small protein such as ERD2, and combinations of point mutations would be beyond the reach of individual laboratories. However, nature itself may provide a pool of natural ERD2 variants. Protein-protein interactions within the anterograde or retrograde transport machinery between the ER and the Golgi may not be totally conserved between eukaryotic kingdoms. Despite the high degree of sequence conservation in the ERD2 family, it is possible that searching through the kingdoms and including ERD2 variants from organisms as diverse as *Saccharomyces cerevisiae* (yeast), *Phytophthora infestans* (oomycete), *Thalassiosira pseudonana* (marine diatom), *Plasmodium falciparum* (protist), *Dictyostelium discoideum* (slime mold), or *Puccinia graminis* (fungus) may reveal differences that lead to a different phenotype in the bioassay. Once differences are established, hybrids can be engineered between different ERD2 variants to narrow down regions of interest that are responsible for the difference between functional and non-functional ERD2 molecules in the bio-assay. This strategy has been successfully applied to study the ligand-binding specificity of yeast ERD2 (Semenza and Pelham, 1992), but may also be successful for the identification of anterograde and retrograde transport signals. Identified regions can then be subject to more detailed mutational analysis.

Finally, results obtained in the last chapter have already yielded ERD2 mutants with different phenotypes that can be classified into two categories. Most of the mutants show a loss-of-function phenotype in the bio-assay, the inability to suppress Amy-HDEL secretion. One mutant however showed a dominant effect and induced Amy-HDEL secretion even further. It is likely that the two classes of mutants affect different transport steps. A combination of the mutants would reveal if they are synergistic or antagonistic and may shed light on the nature of the defect by combinatorial analysis. For instance, loss of ligand-binding may cause competition with endogenous ERD2 if recycling still occurs, but not if recycling has been compromised as well.

## 3.3 Explaining the high efficiency of the ERD2-mediated ER retention mechanism

Two models have been proposed in Chapter III to explain the extra-stoichiometric retention of ERD2-ligands. ERD2 may either be transported much faster to the Golgi apparatus than bulk flow, perhaps via a different transport carrier. Alternatively, ERD2 could bind to several ligands simultaneously, perhaps with the help of an adaptor protein.

The first model may be tested using standard COPII transport inhibitors such as Sec12 overproduction or GTP-trapped Sar1 co-expression (Phillipson *et al*., 2001). If ERD2 export to the Golgi is less sensitive than a typical Golgi marker such as ST-YFP, it is conceivable that ERD2 either uses a different carrier, or it contains a stronger signal for incorporation into the same carrier. It is possible that the Brefeldin A like effect observed in mammalian cells (Hsu *et al*., 1992) is explained by a scenario in which ERD2 uses the same carrier as bulk flow but progressively excludes bulk flow by changing the shape of the transport carrier, may be by constricting the diameter of the vesicle or tubular carrier to avoid bulk flow. This would lead to a reduction of constitutive secretion whilst ER retention is up-regulated.

Ligand-binding studies have never been carried out with purified ERD2 in the absence of other secretory pathway proteins. For this reason, a lumenal adaptor between ERD2 and its ligands may be found that boosts receptor performance. There is multiple precedence in nature for protein adaptors, such as adaptors linking membrane cargo to clathrin coats to initiate vesicle budding or adaptors to link the cytoskeleton to membrane spanning proteins in cell adhesion. Likewise, the

signal recognition particle is a soluble adaptor that recruits ribosomes synthesizing signal peptide containing polypeptides to the translocation pore on the rough ER. In these examples, the adaptor does not provide an enhancement role, but this does not rule out that adaptors can be used for such a function. Even though ERD2 appears to be the limiting factor in the plant ER retention capacity (as demonstrated multiple times by the ability of ERD2 to suppress Amy-HDEL secretion), it is possible that an adaptor exists and is present in excess. To identify new players of the ER retention machinery besides ERD2, transgenic plants with an inducible gene encoding Amy-HDEL can be engineered. Next generation sequencing of mRNA extracted from cells at different times after inducing Amy-HDEL expression may reveal new key-players that were below the resolution of genetic screens.

## 3.4 Impact on food security and sustainable bio-manufacturing

One of the most promising outcomes of this project is that introduction of small numbers of ERD2 molecules can have a big impact on the ER retention capacity of plant cells and that this might be exploited to specifically engineer food crops that produce higher levels of edible proteins or non-food crops for the renewable manufacturing of high value proteins for medicine and industry. One of the first follow up experiments that I would envisage is the generation of stable transgenic plants with a constitutively up-regulated ER retention capacity. Although experiments presented in this thesis have not provided evidence for a Brefeldin A effect of overexpressed ERD2 (Hsu *et al*., 1992), it is possible that ectopically expressed ERD2 did not reach the levels required for ERD2 toxicity. Transient expression experiments in tobacco leaf protoplasts are carried out with non-replicating plasmids, whilst transient expression in mammalian cells usually involves replicating plasmids, thus leading to much higher copy numbers and extreme overexpression of the plasmid-borne genes. Pilot experiments with stable transgenic plants should be carried out with a range of promoters to test if stable ERD2 overproduction can be achieved. Reagents generated in this thesis can be used include the antibodies to the second cytosolic loop of ERD2 which could be used to test ERD2 protein levels in transgenic plant lines. Those lines with higher ERD2 protein levels can then be used to test for Amy-HDEL retention efficiency in protoplasts assays. Using the GUS internal marker on the Amy-HDEL plasmid used in Figure 2-28, protoplast preparations from different plant lines can be compared

for transfection efficiency and protein synthesis rates, and the Amy-HDEL retention efficiency can be compared.

In addition to the model plant tobacco, food crops can also be envisaged. Carbohydrate crops (sugar and starch crops) are by far the most productive carbon capturing crops that store solar energy in the form of edible calories. Regretfully, the most productive of these, for instance potato, sweet potato and cassava, exhibit notoriously low protein content. In order to enhance food production for a growing population on Earth, a significant contribution could be made if it is possible to engineer these starch crops to contain more edible protein. In contrast to cereal seed, starch tubers contain lytic vacuoles and it may be difficult to manipulate protein content in this organelle. Engineering starch crops with a higher ER retention capacity could thus be envisaged and ER retained derivatives of storage proteins such as bean phaseolin, pea vicilin, wheat glutelin or maize zein (Mainieri *et al*., 2014) may help feed the world in the future.

# 4 Materials and Methods

## 4.1 Molecular biology techniques

All DNA manipulations were performed according to established procedures and most of the media and buffers were prepared according to (Sambrook *et al*., 1989) unless stated otherwise. Agarose gels were made up in 0.5x TBE (Tris, boric acid and EDTA) buffer and restriction digestion were carried out in TE buffer supplemented with restriction buffers and restriction enzymes from New England Biolabs (NEB). *E.coli* strain MC1060 was used for all construct amplifications (Casadaban and Cohen, 1980).

PCR amplifications were set up by the KOD DNA polymerase protocol from Novagen, Darmstadt, Germany (Novagen, 2011). Oligonucleotides were purchased either from Sigma (UK) or Eurogentec (Liege, Belgium). DNA was amplified using a thermocycler (GeneCycler BioRad, Hercules, CA, USA) and conditions were adjusted according to the reaction.

Point mutagenesis of all ERD2 mutants were performed by using primer pairs which are list in the Table 1. Other primers which are used in this thesis are also listed in the same table. A typical PCR cycling condition for amplification is as following:

1. Initial denaturing 95°C, 2.5mins

2. Denaturing 95°C, 30sec

3. Annealing 55°C, 10sec

4. Extension 72°C, 25sec

5. Final extension 72°C, 5mins

Step 2-4 is then repeated for 15-25 cycles depending on the amplification product.

| Name and direction | Primer sequence |
|---|---|
| Cool 35S sense | CACTATCCTTCGCAAGACC |
| YFP-HDEL anti | GGTTACACTCTAGACTAGAGTTCATCATGGTCCTCCTTGTACAGCT CGTCCATGCCGAG |
| ERD2b-HAa anti | ATTGAAACTCTAGAAATTAAGCGTAATCTGGAACATCGTATGGGTAC TTCCAGCTTAGGAAATAATAATAG |

| | |
|---|---|
| ERD2b-HAb anti | ATTGAAACTCTAGAAATTAAGCGTAATCTGGAACATCGTATGGGTAAGCTGGTAATTGGAGCTTTTTGTTG |
| Amy-HA anti | AATGTTTGAACGATCTGCTTCGGATCCTCTAAGCGTAATCTGGAACATCGTATGGGTAGATCTTCTCCCATACGGCATAGTCATTGC |
| Amy-HA-HDEL anti | ACGATCTGCTTCGGATCCTCTAGAGCTCGTCGTGAGCGTAATCTGGAACATCGTATGGGTAGATCTTCTCCCATACGGCATAGTCATTGCCG |
| ERD2b-K206A sense | TTATTTCCTAAGCTGGGCGAACAACAAAAGCTCC |
| ERD2b-K206A anti | GGAGCTTTTTGTTGTTCGCCCAGCTTAGGAAATAA |
| ERD2b-K209A sense | TAAGCTGGAAGAACAACGCAAAGCTCCAATTACCA |
| ERD2b-K209A anti | TGGTAATTGGAGCTTTGCGTTGTTCTTCCAGCTTA |
| ERD2b-K210A sense | CTGGAAGAACAACAAAGCGCTCCAATTACCAGCTTA |
| ERD2b-K210A anti | TAAGCTGGTAATTGGAGCGCTTTGTTGTTCTTCCAG |
| ERD2b-L211A sense | GAAGAACAACAAAAAGGCCCAATTACCAGCTTAAT |
| ERD2b-L211A anti | ATTAAGCTGGTAATTGGGCCTTTTTGTTGTTCTTC |
| ERD2b-L213A sense | CAACAAAAAGCTCCAAGCACCAGCTTAATTTCTA |
| ERD2b-L213A anti | TAGAAATTAAGCTGGTGCTTGGAGCTTTTTGTTG |
| ERD2b-P214A sense | CAAAAAGCTCCAATTAGCAGCTTAATTTCTAGAGGA |
| ERD2b-P214A anti | TCCTCTAGAAATTAAGCTGCTAATTGGAGCTTTTTG |
| ERD2b-R5A sense | CCAAATCGATGAACATTTTCGCATTAGCTGGTGATATGACT |
| ERD2b-R5A anti | AGTCATATCACCAGCTAATGCGAAAATGTTCATCGATTTGG |
| ERD2b-D50A sense | GCGACGCGTTATTTGGCTATTTTCACGAGTTTTG |
| ERD2b-D50A anti | CAAAACTCGTGAAAATAGCCAAATAACGCGTCGC |
| ERD2b-Y164A sense | TTGGGGGGTACCGTGGATTAGCCATCCTCAACTGGATCTACCG |
| ERD2b-Y164A anti | CGGTAGATCCAGTTGAGGATGGCTAATCCACGGTACCCCCCAA |
| ERD2b-N167A sense | GTGGATTATACATCCTCGCCTGGATCTACCGTTACTTC |
| ERD2b-N167A anti | GAAGTAACGGTAGATCCAGGCGAGGATGTATAATCCAC |
| ERD2b-LLGG sense | GCTGGAAGAACAACAAAAAGGGCCAAGGACCAGCTTAATTTCTAGAGG |
| ERD2b-LLGG anti | CCTCTAGAAATTAAGCTGGTCCTTGGCCCTTTTTGTTGTTCTTCCAGC |

**Table 1 Primers used for constructing DNA plasmids in this thesis**

### 4.1.1 DNA plasmids

All plasmids which include in this thesis are listed in Table 2. Many of them are already available in the host laboratory and others are generated over the course of this thesis work. Majority of vector backbones are pUC18 origin or C58ClRif[R] for *Agrobacterium tumefaciens* mediated infiltration.

GFP fusions of calreticulin (GFP-Cal and GFP-CalΔHDEL) were cloned from pOF12 Cal and pOF8 CalΔHDEL to pOF35 GFP-BP80 Long TM and then sub-cloned to plant vector for *Agrobacterium* mediated transient expression. These fusions were driven under the overexpression 35S cauliflower mosaic virus promoter (35S).

All α-amylase constructs (Amy, Amy-HDEL, Amy-KDEL, Amy-EDDDHDEL, Amy-CRT2 and Amy-CRT2ΔHDEL) are already available in the host lab and as shown in publications which are listed in Table 2. In addition, double vector containing ST-CFP under the TR-DNA derived mas 2' promoter (TR2) with either 35S driven ERD2a or ERD2b are also already available.

ST-YFP-HDEL was generated by PCR amplification on template ST-YFP with YFP-HDEL anti primer together with cool 35S primer (Table 1). This is then sub-cloned to TR2 driven vector and sub-cloned to plant vector for *Agrobacterium* mediated transient expression. HA tagged ERD2b and Amy fusions (ERD2b-HAa/b, Amy-HA and Amy-HA-HDEL) were also generated by PCR amplification and the following primer pairs: cool35S & ERD2b-HAa, cool35S & ERD2b-HAb, cool35S & Amy-HA and cool35S & Amy-HA-HDEL were used respectively.

| Name | Description | Reference/Generated by |
|---|---|---|
| secGFP | 35S::secGFP::3'nos | Denecke *et al.*, 1990 |
| secGFP-HDEL | 35S::secGFP-HDEL::3'nos | Denecke *et al.*, 1990 |
| pOF12 | 35S::GFP-calreticulin::3'nos | O. Foresti |
| pOF8 | 35S::GFP-calreticulinΔHDEL::3'nos | O. Foresti |
| Amy | 35S::α-amylase::3'nos | Crofts *et al.*, 1999 |
| Amy-HDEL | 35S::α-amylase-HDEL::3'nos | Phillipson *et al.*, 2001 |
| Amy-KDEL | 35S::α-amylase-KDEL::3'nos | Phillipson *et al.*, 2001 |
| Amy-EDDDHDEL | 35S::α-amylase-EDDDHDEL::3'nos | Phillipson *et al.*, 2001 |

| Amy-CRT2 | 35S::α-amylase- calreticulin::3'nos | Denecke and Botterman 1992 |
|---|---|---|
| Amy-CRT2ΔHDEL | 35S::α-amylase- calreticulin ΔHDEL::3'nos | Denecke and Botterman 1992 |
| pAG10 | TR2::ST-CFP::3'ocs-35S::ERD2a::3'nos | A. Grippa |
| pAP10 | TR2::ST-CFP::3'ocs-35S::ERD2b::3'nos | A. Pilgram |
| ST-YFP | 35S::ST-YFP::3'nos | Brandizzi *et al*., 2003 |
| TR2-ST-YFP | TR2::ST-YFP::3'nos | F. Bottanelli |
| pJA14 | 35S::ST-YFP-HDEL::3'nos | J. An |
| pJA15 | TR2::ST-YFP-HDEL::3'nos | J. An |
| pJA34 | TR2::ST-YFP-HDEL::3'ocs-35S::Amy::3'nos | J. An |
| pJA35 | TR2::ST-YFP-HDEL::3'ocs-35S::Amy-HDEL::3'nos | J. An |
| pJA36 | TR2::ST-RFP::3'ocs-35S::ERD2b::3'nos | J. An |
| pJA37 | TR2::ST-RFP::3'ocs-35S::PAT::3'nos | J. An |
| pIKA9 | TR2::GUS::3'ocs-35S::Amy::3'nos | I. K. Adam |
| pIKA21 | TR2::GUS::3'ocs-35S::Amy-HDEL::3'nos | I. K. Adam |
| pCL2 | TR2::GUS::3'ocs-35S::Amy-KDEL::3'nos | C. Lachaux |
| pOF122 | 35S::YFP-ERD2b::3'nos | O. Foresti |
| pJA10 | 35S::ERD2b-YFP::3'nos | J. An |
| pOF53 | 35S::ST-RFP::3'nos | O. Foresti |
| pOF127 | 35S::RFP-HDEL::3'nos | O. Foresti |
| pAG8 | 35S::ERD2b-RFP::3'nos | A. Grippa |
| pAP5 | TR2::ERD2b-YFP::3'nos | A. Pilgram |
| pAP2 | TR2::ERD2b-RFP::3'nos | A. Pilgram |
| pJA11 | 35S::YFP-ERD2b-RFP::3'nos | J. An |
| pJCA24 | 35S::secYFP-ERD2b::3'nos | J. Alvim |
| pCSJ1 | 35S::secYFP-ERD2b-RFP::3'nos | J. Corbacho |
| pJA31 | TR2::GUS::3'ocs-35S::ERD2b::3'nos | J. An |
| pJA47 | TR2::GUS::3'ocs-35S::ERD2b-YFP::3'nos | J. An |
| pJA48 | TR2::GUS::3'ocs-35S::ERD2b-RFP::3'nos | J. An |
| pJA50 | TR2::GUS::3'ocs-35S::YFP-ERD2b-RFP::3'nos | J. An |

| pJA51 | TR2::GUS::3'ocs-35S::YFP-ERD2b::3'nos | J. An |
|---|---|---|
| pJA71 | TR2::GUS::3'ocs-35S::secRFP-ERD2b::3'nos | J. An |
| pJA32 | TR2::GUS::3'ocs-35S::ERD2b-HAa::3'nos | J. An |
| pJA33 | TR2::GUS::3'ocs-35S::ERD2b-HAb::3'nos | J. An |
| pJA27 | TR2::GUS::3'ocs-35S::Amy-HA::3'nos | J. An |
| pJA28 | TR2::GUS::3'ocs-35S::Amy-HA-HDEL::3'nos | J. An |
| pOF120 | 35S::YFP-ERP1::3'nos | O. Foresti |
| pAG9 | 35S::ERP1-RFP::3'nos | A. Grippa |
| pJA49 | TR2::GUS::3'ocs-35S::ERP1::3'nos | J. An |
| pJA41 | TR2::GUS::3'ocs-35S::ERD2bK206A::3'nos | J. An |
| pJA42 | TR2::GUS::3'ocs-35S::ERD2bK209A::3'nos | J. An |
| pJA43 | TR2::GUS::3'ocs-35S::ERD2bK210A::3'nos | J. An |
| pJA44 | TR2::GUS::3'ocs-35S::ERD2bL211A::3'nos | J. An |
| pJA45 | TR2::GUS::3'ocs-35S::ERD2bL213A::3'nos | J. An |
| pJA46 | TR2::GUS::3'ocs-35S::ERD2bP214A::3'nos | J. An |
| pJA62 | TR2::GUS::3'ocs-35S::ERD2bR5A::3'nos | J. An |
| pJA63 | TR2::GUS::3'ocs-35S::ERD2bD50A::3'nos | J. An |
| pJA64 | TR2::GUS::3'ocs-35S::ERD2bY164A::3'nos | J. An |
| pJA65 | TR2::GUS::3'ocs-35S::ERD2bN167A::3'nos | J. An |
| pJA66 | TR2::GUS::3'ocs-35S::ERD2bD195N::3'nos | J. An |
| pJA67 | TR2::GUS::3'ocs-35S::ERD2bLLGG::3'nos | J. An |
| pCM141 | TR2::ST-YFP::3'ocs-35S::ERD2b::3'nos | C. D. Marcos |
| pCM142 | TR2::ST-YFP::3'ocs-35S::ERD2bY164A::3'nos | C. D. Marcos |

**Table 2 List of all used constructs**
List of constructs which used in this project either generated within the course of this study or already exist in the lab. Abbreviation: 35S: cauliflower mosaic virus promoter; 3'nos: 3' untranslated end of nopaline synthase gene; TR2: TR-DNA derived mas 2' promoter; ERD2: ER retention defective 2; ERP: ERD2-related protein; PAT: phosphinothricin acetyl transferase.

## 4.1.2 DNA minipreps

Fresh overnight liquid cultures with a single colony that was inoculated in 3 ml of LB medium the night before were used to fill approximately 1.5 ml of each culture

in a labelled Eppendorf tube. The tubes were then centrifuged 1 minute at 14,000 rpm and the supernatant was removed. Hence the pellets were re-suspended in 150 µl of TES and 20 µl of lysozyme solution was quickly added to incubated 5 minutes at room temperature. Then 300 µl of distilled water was added to the suspensions and tubes were incubated at 73°C for 15 minutes. Subsequently, the tubes were centrifuged at 14,000 rpm for 15 minutes and the supernatants were recovered in new labelled tubes. Then 30 µl of 5 M NaClO$_4$ was added to the supernatants and the tubes were shaken. 400 µl of isopropanol was then added and mixed following 15 minutes centrifugation at 14,000 rpm. Supernatants were removed as previously and tubes were centrifuged for further 2 minutes to remove the leftover liquid in the tube. Finally, tubes were dried at 37°C with open cap for 15 minutes and pellets were then re-suspended in 50 µl of TE by shaking for 5 minutes on a vibrator.

### 4.1.3  DNA sequencing

All recombinant plasmid constructs were verified by sequencing using automated Big Dye ABI sequencing. Plasmid preparations suitable for sequencing were carried out using Wizard® plus DNA purification system (Promega, Madison USA), following the manufacture's instruction. All reaction and gel runs were performed by the sequencing services of the DNA sequencing facility of Oxford University.

### 4.1.4  *E.Coli* competent cells preparation

An aliquot of cells of the MC1061 *E.coli* strain from a glycerol stock was streaked out on a LB-agar plate and let to grow overnight at 37°C.  One isolated colony was then used to inoculate 3 ml 2xYT culture medium and incubated at 37°C with vigorous shaking (200 rpm). When the culture was slightly turbid, it was poured into 200 ml of pre-warmed 2xYT medium and incubated as before at 37°C. When the culture reached an O.D$_{550}$ of approximately 0.400-0.450 was transferred into four sterile 50 ml conical tubes. These were placed on ice for 5 minutes to arrest cell division. All the following passages were carried out in a cold room at 4°C keeping the tubes on ice. The culture aliquots were centrifuged at 3000g in a swing-out rotor, at 4°C for 20 minutes, after which the supernatant was discarded. The cell pellet were re-suspended in a total of 80 ml of ice-cold TFBI solution and placed on ice for 5 minutes. The cell suspension was centrifuged as before and the

supernatant discarded again. The cell pellet were re-suspended in a total of 8 ml of TFBII, pooled and left on ice for 15 minutes. Using pre-chilled pipettes tips, 100 μl aliquots of homogenous cell suspension were transferred to pre-chilled microfuge tubes (placed on ice). Aliquots were then frozen in dry ice and stored at -80°C.

LB (Luria Bertani) medium: 10 g/L Bacto-tryptone; 5 g/L Bacto-yeast extract; 10 g/L NaCl. The medium was sterilised by autoclaving. For solid medium 15 g/l Bacto Agar was added prior autoclaving.

2xYT medium: 16 g/L bacto tryptone; 10 g/L bacto yeast extract; 5 g/L NaCl. The pH was adjusted to 7 with NaOH and the solution autoclaved to sterilize.

TFBI solution: 30 mM $KC_2H_3O_2$; 100 mM RbCl; 10 mM $CaCl_2 \cdot 2H_2O$; 50 mM $MnCl_2 \cdot 4H_2O$; 15 % v/v glycerol. The pH was adjusted to 5.8 using 0.2 M $CH_3COOH$. The solution was filter sterilised and stored at +4°C.

TFBII solution: 10 mM MOPS; 10 mM RbCl; 75 mM $CaCl_2 \cdot 2H_2O$;15 % v/v glycerol. The pH was adjusted to 6.6 using 5 M KOH. The solution was filter sterilised and stored at +4°C.

## 4.2 Plant material and transient expression experiment

The soil-grown tobacco plant (*Nicotiana tabacum*) used during *Agrobacterium tumefaciens* mediated leaf infiltration experiment and α-amylase assay are described in published protocol. Tobacco protoplasts experiment were performed as published protocol as well (Denecke and Vitale 1995). GFP fusions (GFP-HDEL, GFP-Cal and GFP-CalΔHDEL) were analysed by CLSM. Detail descriptions of the procedures are as following.

### 4.2.1 Preparation of protoplasts

Tobacco leaf protoplasts were prepared with supplement of 1× digestion mix which was prepared from TEX buffer (B5 salts, 500 mg/l MES, 750 mg/l $CaCl_2$ [2 $H_2O$] 250 mg/l $NH_4NO_3$, and 0.4 M sucrose [13.7%], brought to pH 5.7 with KOH) supplemented with 0.2% Macerozyme R10 and 0.4% Cellulase R10 (Yakult). Stocks with 10-fold concentrated digestion enzymes were prepared by dissolving the lyophilized powders in TEX buffer for 2 h, followed by centrifugation at 5000 *g* for 15 minutes and filter sterilization (0.2 μm) of the clear supernatant. The filtered supernatant was aliquot in 5 ml and kept at −80°C for routine use. The 1× digestion mix was always prepared freshly by addition of 45 ml of TEX buffer to these stocks.

Overnight digestions of floating leaves were prepared by using a needle bed. These digestions were then filtered through a 100-µm nylon mesh and brief washed with electroporation buffer (0.4 M sucrose [13.7%], 2.4 g/l HEPES, 6 g/l KCl, and 600 mg/l CaCl$_2$, brought to pH 7.2 with KOH) to release further protoplasts from the tissue remnants. The protoplast suspensions were then centrifuged in Falcon tubes (50 ml) for 15 minutes at 100 g at room temperature in a swing-out rotor. Centrifugation was stopped without brake to prevent re-suspension of the floating protoplast band. The pellet and the underlying medium were removed and discarded using a peristaltic pump and a sterile Pasteur pipette until the band of floating living protoplasts reached the bottom. Then the cells were re-suspended in 25 ml of electroporation buffer and a further centrifugation at 100g for 10 minutes was initiated. The pellet and the underlying medium were removed again and this procedure was repeated twice.

### 4.2.2  Electroporation of protoplast

After the final wash, protoplasts were re-suspended in electroporation buffer at a concentration of 5 × 10$^6$ protoplasts/ml. 500 µl of the obtained protoplasts mix was then pipetted into a disposable 1-ml plastic cuvette and was mixed with 15 µl of Wizard prep plasmid DNA or 1-2 µl of the maxi prep plasmid DNA depending on availability. The protoplast suspensions were then incubated for 5 minutes and electroprated for 5 seconds with stainless steel electrodes at a distance of 3.5 mm. A complete exponential discharge of a 1000-µF capacitor charged at 160 V was connected to the electrodes. Electroporated protoplasts were rested for 15 minutes and were then removed from the cuvettes by washing in 1 ml of TEX buffer twice and transferred to 5 cm Petri dishes. All incubations were performed for 24 h.

### 4.2.3  Harvesting of electroporated protoplast

After incubation, 2.5 ml of the cell suspension was harvested in a small clear Falcon tube (15 ml) and centrifuged at 80g for 5 minutes. Approximately 1 ml of the underlying medium was manually removed with a refined Pasteur pipette. This obtained medium was further cleared by centrifugation in a refrigerated microfuge (4°C, 18,000g, and 10 minutes) and was kept on ice for further analysis (see α-amylase assay). The cells were diluted 10-fold with 250 mM NaCl in 15 ml Falcon tubes to recover the total cell population of the remaining suspension. Hence the suspension was centrifuged for 3 minutes at 200g. The supernatant was then

removed with a peristaltic pump and the compact cell pellet was kept on ice for subsequent extraction and analysis (see α-amylase assay).

### 4.2.4 *In vivo* labelling

The label is taken from –80°c, thawed (37°c heating block) and zip spin to ensure all liquid is at the bottom of the tube. 6 repeats of electroporated 2.5ml protoplasts of the same DNA for each sample were pool together. After 1hour rest, majority of the underlying solution as well as dead cells were removed and samples were equalised by weight to reduce the volume to 5ml protoplast. 2ml of protoplasts was subject to cold amylase assay as an expression control and 2ml of protoplasts was then labelled with $S^{35}$ for 24hours at room temperature in the dark. After this incubation, labelled samples were harvested and cell and medium fractions were isolated. Both were then subject to immunoprecipitation with 1µl of antibody and protein A-sepharose as standard protocol. Resulting samples were mixed 1:1 with sample buffer and loaded on SDS-PADE and then transferred onto nitrocellulose for analysis.

### 4.2.5 Tobacco leaf infiltration

Fresh overnight *Agrobacterium tumefaciens* pre-cultures in MGL were infiltrated into tobacco leaves with appropriated concentration as fixed optical density (O.D.) 0.1 and infiltrated leaf areas were analysed after 2 days of further growth. 1 ml of the culture was first centrifuged at 5000 rpm (2200 g) for 5 minutes at room temperature to remove the majority of the culture medium and the pellet was re-suspended in 1 ml of the infiltration buffer. This suspension was centrifuged again and the pellet was re-suspended as previously. The final suspension was diluted to appropriate concentration to obtain an absorbance $OD_{600}$ of approximately 0.1. Small holes were created in the tobacco leaves with a yellow tip and diluted culture samples were injected to the leaves with 1 ml syringe (no needle). The tobacco leaf was firmly held between the nozzle of the syringe that was pressed against the lower (abaxial) epidermis which was covering the small hole and a gloved finger on the other side of the leaf. The injection was performed slowly to allow a good absorption of the leaf and the infiltrated areas were marked with a black marker pen and analysed by appropriate procedure depending on specific experiments.

## 4.3  Bio-rad assay

5 µl of undiluted extracts from transgenic potato leaves were diluted with 155 µl of autoclaved water and were then assayed at room temperature with 40 µl of Bio-rad reagent (contained phosphoric acid and methanol). The absorbance was then measured at 605 nm and readings were recorded.

## 4.4  Alpha-amylase assay

Alpha-amylase assay reagents were purchased from Megazyme (http://secure.megazyme.com). The protoplast samples of centrifuged medium suspensions from the harvesting procedure were extracted and diluted with α-amylase extraction buffer (50 mM malic acid, 50 mM NaCl, 2 mM $CaCl_2$ and 0.02% sodium azide, 0.02% BSA) to obtain suitable dilutions for the assay.  In contrast, the cell pellet samples was re-suspended with the same α-amylase extraction buffer and subsequently sonicated for 5 seconds (amplitude 10 microns). The sonicated cell pellets were then centrifuged for 10 minutes at 18 000 g at 4°C and the supernatants were recovered.

Sample extracts were on ice all the time between assays. The assays were carried out at 45°C using 30 µl of the extract either from the infiltrated leaf samples or protoplast samples. The reaction was hence initiated by addition of 30 µl of the substrate ((R-CAAR4) consisting of blocked *p*-nitrophenyl maltoheptaoside (BPNPG7, 54.5 mg) and thermostable α-glucosidase (125 units at pH 6.0)) which was dissolved according to the manufacturer's instructions in 10 ml of autoclaved distilled water and stored at −80°C as 1 ml aliquots. The reaction was stopped by the addition of 150 µl of reaction stop buffer (1% (w/v) Tris pH 8). Finally the absorbance was measured at 405 nm and readings were recorded. Negative controls for correction of absorbance were obtained from mock-transformed protoplasts or non-infiltrated leaf areas depending on the extracts.

The α-amylase activity was calculated in terms of change in optical density (ΔOD) which was divided per ml of extract used (taking into account the dilutions or concentrations of both protoplast and infiltrated leaf extracts) and was then divided by the time period of the assay in minutes. Only readings within the linear range between ΔOD 0.1 and 1.0 were used for calculations to avoid inaccuracy and substrate limitations. The assay was repeated at least three times for each extract including controls, and the average activity was calculated once appropriate dilutions and incubation times were established.

## 4.5  Beta-Glucuronidase (GUS) assay

From 2.5ml overnight incubation of the electroporated protoplasts 500µl were taken and mixed directly with 500µl of GUS extraction buffer. The remaining 2ml protoplasts were centrifuged for alpha-amylase assay. 1ml diluted protoplasts were then sonicated (60% amplitude for 5s) and vortex before centrifugation at 4°C for 20mins. 10µl of supernatant was diluted 10x with GUS extraction buffer and mixed with 100µl of GUS reaction buffer and incubated at 37°C for 16hours. Reaction is then stopped by adding 80µl of GUS stop buffer and the optical absorbance is read at $\lambda405$. Due to the endogenous absorbance of chlorophyll at $\lambda405$ each sample 'zero stop' was used to subtract background reading by adding the stop buffer first. GUS Solutions:

Extraction buffer: 50mM (P) Sodium buffer pH7.0, 10mM Na2EDTA, 0.1% sodium lauryl sarcosine, 0.1% Triton X-100 and 10mM beta-MeEtOH (add prior to use)

Reaction buffer (2x):50mM (P) Sodium buffer pH 7.0, 0.1% Triton, 2mM PNPG and 10mM beta-MeEtOH (add prior to use)

Stop Solution: 2.5M 2-amino-2methyl propanediol

## 4.6  Confocal laser scanning microscopy (CLSM)

Infiltrated tobacco leaf squares (0.5 × 0.5 cm) were immersed in tap water with the lower epidermis facing the cover glass (22 × 50 mm; No. 0). Slides were imaged via an inverted Zeiss LSM700 and LSM800 laser scanning microscope (Zeiss) with a Plan-Neofluar ×40/1.3 oil DIC objective. The confocal images of different fluorophore fusions were obtained after two and a half days of infiltration with the following settings:

- For GFP or GFP and CFP: the excitation lines of an argon ion laser set at 458 nm and the fluorescence was detected using a 545-nm dichroic beam splitter and a 475- to 525-nm band-pass filter.

- For GFP/YFP and RFP combination: excitation of GFP set at 488nm and RFP set at 545nm and the fluorescence was detected between 500-530nm and 565-615nm respectively.

ZEN 2012 (blue edition) (Carl Zeiss) was applied for post-acquisition image processing.

## 4.7 Protein analysis

### 4.7.1 SDS-page and Western blotting

Separation of proteins from leaf/tuber extracts were performed in SDS-polyacrylamide gels comprising of an approximately 2.5 cm stacking gel followed by a 6 cm separation gel. The pre-stained protein ladder ranging from 10 to 160 kDa (Fermentas Life Science) was used as a molecular weight marker. The gels were assembled in-between glass plates of a homemade system and electrophoresis was performed in a homemade apparatus. These devices allowed analysis of up to 30 samples per gel. The different extracts were prepared as described in chapter 3.2.3 and 5.2.3 were loaded in equal volumes after two fold dilution with 2X SDS loading buffer and brief boiling (5 minutes, 95°C). Electrophoresis was performed in running buffer and at a limiting current of 40 mA, and a voltage of 200 V. The gels usually run for 2-3 hours depending on the degree of separation required. Proteins were transferred onto nitrocellulose membranes via electroblotting, which was performed for 2 hours at a current of 500 mA.

Sample buffer

| | |
|---|---|
| 0.1% | Bromophenol blue |
| 5 mM | EDTA |
| 200 mM | Tris pH 8.8 |
| 1 M | Sucrose |
| store at 4°C | |

SDS loading buffer

| | |
|---|---|
| 900 µL | Sample buffer |
| 300 µL | 10 % SDS |
| 18 µL | 1 M DTT |

Stacking gel

5% protogel (30% acrylamide, 0.8% bisacrylamide)

15% sucrose

66 mM Tris-HCl (pH 6.8)

0.1% SDS

0.2% v/v N,N,N',N'-tetramethylethylenediamine

0.033 % w/v ammonium sulphate

Separation gel

12 % protogel (30% acrylamide, 0.8% bisacrylamide)

420 mM Tris-HCl (pH 8.8)

0.1 % SDS

0.055 % v/v N,N,N',N'-tetramethylethylenediamine

0.033 % w/v ammonium sulphate

5X running buffer

30 g/L Tris-HCl

144 g/L Glycine

5 g/L SDS

Electroblotting buffer

3 g/L Tris-HCl

14.4 g/l Glycine

10 % v/v Methanol

87g/L NaCl

22.5g/L $Na_2HPO_4.2H_2O$

2g/L $KH_2PO_4$

The pH was adjusted 7.4

Ponceau solution

0.1 % w/v Ponceau S in 5% v/v acetic acid

Blocking solution in PBS

0.5% tween 20

5% milk powder

10X Phosphate buffered saline (PBS)

## 4.7.2 Immunodetection

After gel blotting, transference of the proteins to the membrane was checked through Ponceau staining. The membrane was washed several times in PBS+0.5 % tween 20 and was then incubated in the blocking solution at room temperature for 1 hour with slow agitation. The blocking solution was washed away with PBS+0.5 % tween 20 and PBS and the primary antibody which has been previously diluted in a 1 % BSA solution with 0.02 % sodium azide in 1x PBS was then added. Rabbit polyclonal antiserum rose against either HA, YFP and ERD2 protein (1:5000 dilutions, Molecular Probes Inc.) were used. After at least two hours incubation, the antibody solution was recovered and the membrane was washed with PBS+0.5 % tween 20. Then the secondary antibody (Goat anti-rabbit IgG horseradish peroxidase labeled, Amersham bioscience) was added (1/15000 dilution in the blocking solution). Immunodetection was performed using enhanced chemiluminescence with freshly prepared ECL solutions 1 and 2. The solutions were mixed over the membranes followed by 5 minutes incubation and exposure to x-ray films.

ECL Solution 1

1 ml 1 M TRIS/HCl (pH 8.5)

100 µL 250 mM Luminol

44 µL 90 mM p-coumaric acid

8.85 mL $dH_2O$

ECL Solution 2

6 µl 30 % $H_2O_2$

1 mL 1 M TRIS/HCl pH 8.5

9 mL $dH_2O$

# 5 References:

Aoe, T., Cukierman, E., Lee, A., Cassel, D., Peters, P.J. and Hsu, V.W. 1997. The KDEL receptor, ERD2, regulates intracellular traffic by recruiting a GTPase-activating protein for ARF1. *The EMBO journal* [online]. **16**(24),pp.7305–7316.

Barlowe, C., D'Enfert, C. and Schekman, R. 1993. Purification and characterization of SAR1p, a small GTP-binding protein required for transport vesicle formation from the endoplasmic reticulum. *The Journal of biological chemistry* [online]. **268**(2),pp.873–879.

Barlowe, C. and Schekman, R. 1993. SEC12 encodes a guanine-nucleotide-exchange factor essential for transport vesicle budding from the ER. *Nature* [online]. **365**(6444),pp.347–349.

Barlowe, C.K., Orci, L., Yeung, T., Hosobuchi, M., Hamamoto, S., Salama, N., Rexach, M.F., Ravazzola, M., Amherdt, M. and Schekman, R. 1994. COPII: a membrane coat formed by Sec proteins that drive vesicle budding from the endoplasmic reticulum. *Cell* [online]. **77**(6),pp.895–907.

Bar-Peled, M., Conceicao, A., Frigerio, L. and Raikhel, N. V. 1995. Expression and Regulation of aERD2, a Gene Encoding the KDEL Receptor Homolog in Plants, and Other Genes Encoding Proteins Involved in ER-Golgi Vesicular Trafficking. *The Plant cell* [online]. **7**(6),pp.667–676.

Batoko, H., Zheng, H.Q., Hawes, C. and Moore, I. 2000. A rab1 GTPase is required for transport between the endoplasmic reticulum and golgi apparatus and for normal golgi movement in plants. *The Plant cell*. **12**(11),pp.2201–2218.

Beckers, C.J., Keller, D.S. and Balch, W.E. 1987. Semi-intact cells permeable to macromolecules: use in reconstitution of protein transport from the endoplasmic reticulum to the Golgi complex. *Cell* [online]. **50**(4),pp.523–34.

Blobel, G. and Dobberstein, B. 1975a. membranes. I. Presence of proteolytically processed and unprocessed nascent immunoglobulin light chains on membrane-bound ribosomes of murine myeloma. *The Journal of cell biology* [online]. **67**,pp.835–851.

Blobel, G. and Dobberstein, B. 1975b. Transfer of proteins across membranes. II. Reconstitution of functional rough microsomes from heterologous components. *The Journal of cell biology* [online]. **67**(3),pp.852–62.

Boevink, P., Oparka, K., Santa Cruz, S., Martin, B., Betteridge, a and Hawes, C. 1998. Stacks on tracks: the plant Golgi apparatus traffics on an actin/ER network. *The Plant journal : for cell and molecular biology* [online]. **15**(3),pp.441–7.

Bonifacino, J.S. and Glick, B.S. 2004. The mechanisms of vesicle budding and fusion. *Cell* [online]. **116**(2),pp.153–66.

Bottanelli, F., Gershlick, D.C. and Denecke, J. 2012. Evidence for sequential action of Rab5 and Rab7 GTPases in prevacuolar organelle partitioning. *Traffic* [online]. **13**(2),pp.338–54.

Brach, T., Soyk, S., Müller, C., Hinz, G., Hell, R., Brandizzi, F. and Meyer, A.J. 2009. Non-invasive topology analysis of membrane proteins in the secretory pathway. *The Plant journal : for cell and molecular biology* [online]. **57**(3),pp.534–41.

Brandizzi, F., Hanton, S., DaSilva, L.L.P., Boevink, P., Evans, D., Oparka, K., Denecke, J. and Hawes, C. 2003. ER quality control can lead to retrograde transport from the ER lumen to the cytosol and the nucleoplasm in plants. *The Plant journal : for cell and molecular biology* [online]. **34**(3),pp.269–281.

Brizzard, B. 2008. Epitope tagging. *BioTechniques* [online]. **44**(5),pp.693–5.

Casadaban, M.J. and Cohen, S.N. 1980. Analysis of gene control signals by DNA fusion and cloning in Escherichia coli. *Journal of Molecular Biology* [online]. **138**(2),pp.179–207.

Ceriotti, a and Colman, a 1988. Binding to membrane proteins within the endoplasmic reticulum cannot explain the retention of the glucose-regulated protein GRP78 in Xenopus oocytes. *The EMBO journal* [online]. **7**(3),pp.633–8.

Chrispeels, M.J. and Herman, E.M. 2000. Endoplasmic reticulum-derived compartments function in storage and as mediators of vacuolar remodeling via a new type of organelle, precursor protease vesicles. *Plant physiology* [online]. **123**,pp.1227–1234.

Cosson, P. and Letourneur, F. 1994. Coatomer interaction with di-lysine endoplasmic reticulum retention motifs. *Science (New York, N.Y.)* [online]. **263**(5153),pp.1629–31.

Craddock, C.P., Hunter, P.R., Szakacs, E., Hinz, G., Robinson, D.G. and Frigerio, L. 2008. Lack of a vacuolar sorting receptor leads to non-specific missorting of soluble vacuolar proteins in Arabidopsis seeds. *Traffic* [online]. **9**(3),pp.408–16.

Crofts, A., Leborgne-Castel, N., Pesca, M., Vitale, A. and Denecke, J. 1998. BiP and calreticulin form an abundant complex that is independent of endoplasmic reticulum stress. *The Plant cell* [online]. **10**(5),pp.813–24.

Crofts, A.J.A., Leborgne-castel, N., Hillmer, S., Robinson, D.G.D., Phillipson, B., Carlsson, L.E., Ashford, D.A. and Denecke, J. 1999. Saturation of the endoplasmic reticulum retention machinery reveals anterograde bulk flow. *The Plant cell* [online]. **11**(11),pp.2233–48.

daSilva, L.L.P., Foresti, O., Denecke, J. and Luis, L.P. 2006. Targeting of the plant vacuolar sorting receptor BP80 is dependent on multiple sorting signals in the cytosolic tail. *The Plant cell* [online]. **18**(6),pp.1477–97.

daSilva, L.L.P., Snapp, E.L., Denecke, J., Lippincott-Schwartz, J., Hawes, C. and Brandizzi, F. 2004. Endoplasmic reticulum export sites and Golgi bodies behave as single mobile secretory units in plant cells. *The Plant cell* [online]. **16**,pp.1753–1771.

Dean, N. and Pelham, H.R. 1990. Recycling of proteins from the Golgi compartment to the ER in yeast. *The Journal of cell biology* [online]. **111**(2),pp.369–77.

Denecke, J., Botterman, J. and Deblaere, R. 1990. Protein secretion in plant cells can occur via a default pathway. *The Plant Cell Online* [online]. **2**,pp.51–59.

Denecke, J., Carlsson, L.E., Vidal, S., Höglund, a S., Ek, B., van Zeijl, M.J., Sinjorgo, K.M. and Palva, E.T. 1995. The tobacco homolog of mammalian calreticulin is present in protein complexes in vivo. *The Plant cell* [online]. **7**(4),pp.391–406.

Denecke, J. and Goldman, M. 1991. The tobacco luminal binding protein is encoded by a multigene family. *The Plant Cell* [online]. **3**,pp.1025–1035.

Denecke, J., Rycke, R. De and Botterman, J. 1992. Plant and mammalian sorting signals for protein retention in the endoplasmic reticulum contain a conserved epitope. *The EMBO journal* [online]. **11**,pp.2345–2355.

Deutscher, S. and Creek, K. 1983. Subfractionation of rat liver Golgi apparatus: separation of enzyme activities involved in the biosynthesis of the phosphomannosyl recognition marker in lysosomal. *Proceedings of the National Academy of Sciences of the United States of America* [online]. **80**,pp.3938–3942.

Dobberstein, B. and Blobel, G. 1977. Functional interaction of plant ribosomes with animal microsomal membranes. *Biochemical and biophysical research communications* [online]. **74**(4).

Emr, S.D., Schekman, R., Flessel, M.C. and Thorner, J. 1983. An MF alpha 1-SUC2 (alpha-factor-invertase) gene fusion for study of protein localization and gene expression in yeast. *Proceedings of the National Academy of Sciences of the United States of America* [online]. **80**(23),pp.7080–4.

Field, J., Nikawa, J., Broek, D., MacDonald, B., Rodgers, L., Wilson, I.A., Lerner, R.A. and Wigler, M. 1988. Purification of a RAS-responsive adenylyl cyclase complex from Saccharomyces cerevisiae by use of an epitope addition method. *Molecular and cellular biology* [online]. **8**(5),pp.2159–65.

Von Figura, K. and Hasilik, a 1986. Lysosomal enzymes and their receptors. *Annual review of biochemistry* [online]. **55**,pp.167–93.

Fischer, R., Twyman, R.M. and Schillberg, S. 2003. Production of antibodies in plants and their use for global health. *Vaccine* [online]. **21**(7-8),pp.820–5.

Fontes, E.B., Shank, B.B., Wrobel, R.L., Moose, S.P., OBrian, G.R., Wurtzel, E.T. and Boston, R.S. 1991. Characterization of an immunoglobulin binding protein

homolog in the maize floury-2 endosperm mutant. *The Plant cell* [online]. **3**(5),pp.483–96.

Foresti, O. and Denecke, J. 2008. Intermediate organelles of the plant secretory pathway: identity and function. *Traffic* [online]. **9**(10),pp.1599–612.

Foresti, O., Gershlick, D.C., Bottanelli, F., Hummel, E., Hawes, C. and Denecke, J. 2010. A recycling-defective vacuolar sorting receptor reveals an intermediate compartment situated between prevacuoles and vacuoles in tobacco. *The Plant Cell* [online]. **22**(12),pp.3992–4008.

French, A.P., Mills, S., Swarup, R., Bennett, M.J. and Pridmore, T.P. 2008. Colocalization of fluorescent markers in confocal microscope images of plant cells. *Nature protocols* [online]. **3**(4),pp.619–628.

Gershlick, D.C., Lousa, C.D.M., Foresti, O., Lee, A.J., Pereira, E.A., Luis, L.P., Bottanelli, F., Denecke, J. and daSilva, L.L.P. 2014. Golgi-dependent transport of vacuolar sorting receptors is regulated by COPII, AP1, and AP4 protein complexes in tobacco. *The Plant cell* [online]. **26**(3),pp.1308–29.

Goldberg, D.E. and Kornfeld, S. 1983. Evidence for extensive subcellular organization of asparagine-linked oligosaccharide processing and lysosomal enzyme phosphorylation. *The Journal of biological chemistry* [online]. **258**(5),pp.3159–65.

Haas, I.G. and Wabl, M. 1983. Immunoglobulin heavy chain binding protein. *Nature* [online]. **306**(5941),pp.387–9.

Hadlington, J.L. and Denecke, J. 2000. Sorting of soluble proteins in the secretory pathway of plants. *Current Opinion in Plant Biology* [online]. **3**(6),pp.461–468.

Hardwick, K.G., Boothroyd, J.C., Rudner, A.D. and Pelham, H.R. 1992. Genes that allow yeast cells to grow in the absence of the HDEL receptor. *The EMBO journal* [online]. **11**(11),pp.4187–95.

Hardwick, K.G., Lewis, M.J., Semenza, J., Dean, N. and Pelham, H.R. 1990. ERD1, a yeast gene required for the retention of luminal endoplasmic reticulum proteins, affects glycoprotein processing in the Golgi apparatus. *The EMBO journal* [online]. **9**(3),pp.623–30.

Hardwick, K.G. and Pelham, H.R. 1992. SED5 encodes a 39-kD integral membrane protein required for vesicular transport between the ER and the Golgi complex. *The Journal of cell biology* [online]. **119**(3),pp.513–21.

Hartmann, E., Rapoport, T. a and Lodish, H.F. 1989. Predicting the orientation of eukaryotic membrane-spanning proteins. *Proceedings of the National Academy of Sciences of the United States of America* [online]. **86**(15),pp.5786–5790.

Haselbeck, A. and Schekman, R. 1986. Interorganelle transfer and glycosylation of yeast invertase in vitro. *Proceedings of the National Academy of Sciences of the United States of America* [online]. **83**,pp.2017–2021.

Hawes, C., Osterrieder, A., Hummel, E. and Sparkes, I. 2008. The plant ER-Golgi interface. *Traffic* [online]. **9**(10),pp.1571–80.

Herman, E., Tague, B., Hoffman, L., Kjemtrup, S. and Chrispeels, M. 1990. Retention of phytohemagglutinin with carboxyterminal tetrapeptide KDEL in the nuclear envelope and the endoplasmic reticulum. *Planta* [online]. **182**(2),pp.305–312.

Hesse, T., Feldwisch, J., Balshüsemann, D., Bauw, G., Puype, M., Vandekerckhove, J., Löbler, M., Klämbt, D., Schell, J. and Palme, K. 1989. Molecular cloning and structural analysis of a gene from Zea mays (L.) coding for a putative receptor for the plant hormone auxin. *The EMBO journal* [online]. **8**(9),pp.2453–61.

Hohl, I., Robinson, D.G., Chrispeels, M.J. and Hinz, G. 1996. Transport of storage proteins to the vacuole is mediated by vesicles without a clathrin coat. *Journal of cell science* [online]. **109 ( Pt 1)**,pp.2539–50.

Hsu, V.W., Shah, N. and Klausner, R.D. 1992. A brefeldin A-like phenotype is induced by the overexpression of a human ERD-2-like protein, ELP-1. *Cell* [online]. **69**(4),pp.625–35.

Hunter, P.R., Craddock, C.P., Di Benedetto, S., Roberts, L.M. and Frigerio, L. 2007. Fluorescent reporter proteins for the tonoplast and the vacuolar lumen identify a single vacuolar compartment in Arabidopsis cells. *Plant physiology* [online]. **145**(4),pp.1371–1382.

Inohara, N., Shimomura, S., Fukui, T. and Futai, M. 1989. Auxin-binding protein located in the endoplasmic reticulum of maize shoots: molecular cloning and complete primary structure. *Proceedings of the National Academy of Sciences of the United States of America* [online]. **86**(10),pp.3564–8.

Janson, I.M., Toomik, R., O'Farrell, F. and Ek, P. 1998. KDEL motif interacts with a specific sequence in mammalian erd2 receptor. *Biochemical and biophysical research communications* [online]. **247**(2),pp.447–51.

Johnström, P., Bird, J.L. and Davenport, A.P. 2012. Quantitative phosphor imaging autoradiography of radioligands for positron emission tomography. *Methods in molecular biology (Clifton, N.J.)* [online]. **897**,pp.205–20.

Kalies, K.U., Görlich, D. and Rapoport, T. a 1994. Binding of ribosomes to the rough endoplasmic reticulum mediated by the Sec61p-complex. *The Journal of cell biology* [online]. **126**(4),pp.925–34.

Kanaseki, T. and Kadota, K. 1969. The 'vesicle in a basket'. A morphological study of the coated vesicle isolated from the nerve endings of the guinea pig brain, with special reference to the mechanism of membrane movements. *Journal of Cell Biology* [online]. **42**(1),pp.202–220.

Klumperman, J. 2000. Transport between ER and Golgi. *Current opinion in cell biology* [online]. **12**(4),pp.445–9.

Koch, G.L. 1987. Reticuloplasmins: a novel group of proteins in the endoplasmic reticulum. *Journal of cell science* [online]. **87 ( Pt 4)**(10),pp.491–492.

Kornfeld, R. and Kornfeld, S. 1985. Assembly of Asparagine-Linked Oligosaccharides. *Annual Review of Biochemistry* [online]. **54**(1),pp.631–664.

Leborgne-Castel, N., Jelitto-Van Dooren, E.P., Crofts, a J. and Denecke, J. 1999. Overexpression of BiP in tobacco alleviates endoplasmic reticulum stress. *The Plant cell* [online]. **11**(3),pp.459–470.

Lee, H.I., Gal, S., Newman, T.C. and Raikhel, N. V 1993. The Arabidopsis endoplasmic reticulum retention receptor functions in yeast. *Proceedings of the National Academy of Sciences of the United States of America* [online]. **90**(23),pp.11433–7.

Lewis, M.J. and Pelham, H.R. 1990. A human homologue of the yeast HDEL receptor. *Nature* [online]. **348**(6297),pp.162–3.

Lewis, M.J. and Pelham, H.R. 1992a. Ligand-induced redistribution of a human KDEL receptor from the Golgi complex to the endoplasmic reticulum. *Cell* [online]. **68**(2),pp.353–64.

Lewis, M.J. and Pelham, H.R. 1992b. Sequence of a second human KDEL receptor. *Journal of molecular biology* [online]. **226**(4),pp.913–6.

Lewis, M.J., Sweet, D.J. and Pelham, H.R. 1990. The ERD2 gene determines the specificity of the luminal ER protein retention system. *Cell* [online]. **61**(7),pp.1359–63.

Li, J., Zhao-Hui, C., Batoux, M., Nekrasov, V., Roux, M., Chinchilla, D., Zipfel, C. and Jones, J.D.G. 2009. Specific ER quality control components required for biogenesis of the plant innate immune receptor EFR. *Proceedings of the National Academy of Sciences of the United States of America* [online]. **106**(37),pp.15973–8.

Lippincott-Schwartz, J., Donaldson, J.G., Schweizer, a, Berger, E.G., Hauri, H.P., Yuan, L.C. and Klausner, R.D. 1990. Microtubule-dependent retrograde transport of proteins into the ER in the presence of brefeldin A suggests an ER recycling pathway. *Cell* [online]. **60**(5),pp.821–36.

Luis, L.P., Taylor, J.P., Hadlington, J.L.J., Sally, L., Snowden, C.J., Fox, S.J., Foresti, O., Hanton, S.L., Snowden, C.J., Fox, S.J., daSilva, L.L.P., Foresti, O., Brandizzi, F. and Denecke, J. 2005. Receptor salvage from the prevacuolar compartment is essential for efficient vacuolar protein targeting. *The Plant cell* [online]. **17**(1),pp.132–48.

Macer, D.R. and Koch, G.L. 1988. Identification of a set of calcium-binding proteins in reticuloplasm, the luminal content of the endoplasmic reticulum. *Journal of cell science* [online]. **91 ( Pt 1)**(9),pp.61–70.

Mainieri, D., Morandini, F., Maitrejean, M., Saccani, A., Pedrazzini, E. and Alessandro, V. 2014. Protein body formation in the endoplasmic reticulum as

an evolution of storage protein sorting to vacuoles: insights from maize γ -zein. *Frontiers in Plant Science* [online]. **5**,p.331.

Malhotra, V., Serafini, T., Orci, L., Shepherd, J.C. and Rothman, J.E. 1989. Purification of a novel class of coated vesicles mediating biosynthetic protein transport through the Golgi stack. *Cell* [online]. **58**(2),pp.329–36.

De Marcos Lousa, C., Gershlick, D.C. and Denecke, J. 2012. Mechanisms and concepts paving the way towards a complete transport cycle of plant vacuolar sorting receptors. *The Plant Cell* [online]. **24**(5),pp.1714–32.

Matsuoka, K. and Nakamura, K. 1991. Propeptide of a precursor to a plant vacuolar protein required for vacuolar targeting. *Proceedings of the National Academy of Sciences of the United States of America* [online]. **88**(3),pp.834–8.

Matsuoka, K. and Neuhaus, J. 1999. Cis-elements of protein transport to the plant vacuoles. *Journal of Experimental botany* [online]. **50**(331),pp.165–174.

Melançon, P., Glick, B.S., Malhotra, V., Weidman, P.J., Serafini, T., Gleason, M.L., Orci, L. and Rothman, J.E. 1987. Involvement of GTP-binding 'G' proteins in transport through the Golgi stack. *Cell* [online]. **51**(6),pp.1053–62.

Montesinos, J.C., Pastor-Cantizano, N., Robinson, D.G., Marcote, M.J. and Aniento, F. 2014. Arabidopsis p24δ5 and p24δ9 facilitate Coat Protein I-dependent transport of the K/HDEL receptor ERD2 from the Golgi to the endoplasmic reticulum. *The Plant journal : for cell and molecular biology* [online]. **80**(6),pp.1014–30.

Moran, L. a, Chauvin, M., Kennedy, M.E., Korri, M., Lowe, D.G., Nicholson, R.C. and Perry, M.D. 1983. The major heat-shock protein (hsp70) gene family: related sequences in mouse, Drosophila, and yeast. *Canadian journal of biochemistry and cell biology = Revue canadienne de biochimie et biologie cellulaire* [online]. **61**(6),pp.488–99.

Munro, S. and Pelham, H.R. 1987. A C-terminal signal prevents secretion of luminal ER proteins. *Cell* [online]. **48**(5),pp.899–907.

Munro, S. and Pelham, H.R. 1986. An Hsp70-like protein in the ER: identity with the 78 kd glucose-regulated protein and immunoglobulin heavy chain binding protein. *Cell* [online]. **46**(2),pp.291–300.

Napier, R.M., Fowke, L.C., Hawes, C., Lewis, M. and Pelham, H.R. 1992. Immunological evidence that plants use both HDEL and KDEL for targeting proteins to the endoplasmic reticulum. *Journal of cell science* [online]. **102 ( Pt 2)**,pp.261–71.

Nash, P.D., Opas, M. and Michalak, M. 1994. Calreticulin: not just another calcium-binding protein. *Molecular and cellular biochemistry* [online]. **135**(1),pp.71–8.

Novagen 2011. KOD Hot Start DNA Polymerase. ,pp.1–9.

Novick, P. and Schekman, R. 1979. Secretion and cell-surface growth are blocked in a temperature-sensitive mutant of Saccharomyces cerevisiae. *Proceedings of the National Academy of Sciences of the United States of America* [online]. **76**(4),pp.1858–62.

Orci, L., Glick, B.S. and Rothman, J.E. 1986. A new type of coated vesicular carrier that appears not to contain clathrin: its possible role in protein transport within the Golgi stack. *Cell* [online]. **46**(2),pp.171–84.

Orci, L., Malhotra, V., Amherdt, M., Serafini, T. and Rothman, J.E. 1989. Dissection of a single round of vesicular transport: sequential intermediates for intercisternal movement in the Golgi stack. *Cell* [online]. **56**(3),pp.357–68.

Orci, L., Stamnes, M. and Ravazzola, M. 1997. Bidirectional transport by distinct populations of COPI-coated vesicles. *Cell* [online]. **90**,pp.335–349.

Orlean, P., Albright, C. and Robbins, P.W. 1988. Cloning and sequencing of the yeast gene for dolichol phosphate mannose synthase, an essential protein. *The Journal of biological chemistry* [online]. **263**(33),pp.17499–507.

Pagny, S., Cabanes-Macheteau, M., Gillikin, J.W., Leborgne-Castel, N., Lerouge, P., Boston, R.S., Faye, L. and Gomord, V. 2000. Protein recycling from the Golgi apparatus to the endoplasmic reticulum in plants and its minor contribution to calreticulin retention. *The Plant cell* [online]. **12**(5),pp.739–56.

Palade, G. 1975. Intracellular aspects of the process of protein secretion. *Science (New York, N.Y.)* [online]. **189**(4200),p.867.

Payne, G. and Schekman, R. 1985. A test of clathrin function in protein secretion and cell growth. *Science* [online]. **230**(4729),pp.1009–1014.

Pelham, H.R. 1988. Evidence that luminal ER proteins are sorted from secreted proteins in a post-ER compartment. *The EMBO journal* [online]. **7**(4),pp.913–8.

Pelham, H.R., Hardwick, K.G. and Lewis, M.J. 1988. Sorting of soluble ER proteins in yeast. *The EMBO journal* [online]. **7**(6),pp.1757–62.

Pfeffer, S.R. 2007. Unsolved mysteries in membrane traffic. *Annual review of biochemistry* [online]. **76**,pp.629–45.

Phillipson, B. a, Pimpl, P., daSilva, L.L., Crofts, a J., Taylor, J.P., Movafeghi, a, Robinson, D.G. and Denecke, J. 2001. Secretory bulk flow of soluble proteins is efficient and COPII dependent. *The Plant cell* [online]. **13**(9),pp.2005–20.

Pimpl, P. and Denecke, J. 2000. ER retention of soluble proteins: retrieval, retention, or both? *The Plant cell* [online]. **12**(9),pp.1517–21.

Pimpl, P., Taylor, J.P., Snowden, C., Hillmer, S., Robinson, D.G. and Denecke, J. 2006. Golgi-mediated vacuolar sorting of the endoplasmic reticulum chaperone BiP may play an active role in quality control within the secretory pathway. *The Plant cell* [online]. **18**(1),pp.198–211.

Pohlmann, R., Waheed, a, Hasilik, a and von Figura, K. 1982. Synthesis of phosphorylated recognition marker in lysosomal enzymes is located in the cis part of Golgi apparatus. *The Journal of biological chemistry* [online]. **257**(10),pp.5323–5.

Robert, S., Kleine-Vehn, J., Barbez, E., Sauer, M., Paciorek, T., Baster, P., Vanneste, S., Zhang, J., Simon, S., Čovanová, M., Hayashi, K., Dhonukshe, P., Yang, Z., Bednarek, S.Y., Jones, A.M., Luschnig, C., Aniento, F., Zažímalová, E. and Friml, J. 2010. ABP1 mediates auxin inhibition of clathrin-dependent endocytosis in Arabidopsis. *Cell* [online]. **143**(1),pp.111–21.

Robinson, D.G., Brandizzi, F., Hawes, C. and Nakano, A. 2015. Vesicles versus Tubes: Is Endoplasmic Reticulum-Golgi Transport in Plants Fundamentally Different from Other Eukaryotes? *Plant Physiology* [online]. **168**(2),pp.393–406.

Rose, J.K. and Doms, R.W. 1988. Regulation of protein export from the endoplasmic reticulum. *Annual Review of Cell Biology* [online]. **4**,pp.257–288.

Roth, T. and Porter, K. 1964. Yolk protein uptake in the oocyte of the mosquito Aedes aegypti. *The Journal of Cell Biology* [online]. **20**(2),pp.313–332.

Sambrook, J., Fritsch, E.F. and Maniatis, T. 1989. *Molecular Cloning: A Laboratory Manual.*

Di Sansebastiano, G.P., Paris, N., Marc-Martin, S. and Neuhaus, J.M. 2001. Regeneration of a lytic central vacuole and of neutral peripheral vacuoles can be visualized by green fluorescent proteins targeted to either type of vacuoles. *Plant physiology* [online]. **126**(1),pp.78–86.

Scheel, a a and Pelham, H.R. 1998. Identification of amino acids in the binding pocket of the human KDEL receptor. *The Journal of biological chemistry* [online]. **273**(4),pp.2467–72.

Schekman, R. 1985. Protein localization and membrane traffic in yeast. *Annual review of cell biology* [online]. **1**(1),pp.115–43.

Semenza, J.C., Hardwick, K.G., Dean, N. and Pelham, H.R. 1990. ERD2, a yeast gene required for the receptor-mediated retrieval of luminal ER proteins from the secretory pathway. *Cell* [online]. **61**(7),pp.1349–57.

Semenza, J.C. and Pelham, H.R. 1992. Changing the specificity of the sorting receptor for luminal endoplasmic reticulum proteins. *Journal of molecular biology* [online]. **224**(1),pp.1–5.

Singh, P., Tang, B.L., Wong, S.H. and Hong, W. 1993. Transmembrane topology of the mammalian KDEL receptor. *Molecular and cellular biology* [online]. **13**(10),pp.6435–41.

Sorger, P.K. and Pelham, H.R. 1987. Purification and characterization of a heat-shock element binding protein from yeast. *The EMBO journal* [online]. **6**(10),pp.3035–41.

Stevens, T.H., Rothman, J.H., Payne, G.S. and Schekman, R. 1986. Gene dosage-dependent secretion of yeast vacuolar carboxypeptidase Y. *The Journal of cell biology* [online]. **102**(5),pp.1551–7.

Takaiwa, F., Takagi, H., Hirose, S. and Wakasa, Y. 2007. Endosperm tissue is good production platform for artificial recombinant proteins in transgenic rice. *Plant biotechnology journal* [online]. **5**(1),pp.84–92.

Tatu, U. and Helenius, A. 1997. Interactions between newly synthesized glycoproteins, calnexin and a network of resident chaperones in the endoplasmic reticulum. *Journal of Cell Biology* [online]. **136**(3),pp.555–565.

Tillmann, U., Viola, G., Kayser, B., Siemeister, G., Hesse, T., Palme, K., Löbler, M. and Klämbt, D. 1989. cDNA clones of the auxin-binding protein from corn coleoptiles (Zea mays L.): isolation and characterization by immunological methods. *The EMBO journal* [online]. **8**(9),pp.2463–7.

Townsley, F.M., Frigerio, G. and Pelham, H.R. 1994. Retrieval of HDEL proteins is required for growth of yeast cells. *The Journal of cell biology* [online]. **127**(1),pp.21–8.

Townsley, F.M., Wilson, D.W. and Pelham, H.R. 1993. Mutational analysis of the human KDEL receptor: distinct structural requirements for Golgi retention, ligand binding and retrograde transport. *The EMBO journal* [online]. **12**(7),pp.2821–9.

Valls, L. a, Hunter, C.P., Rothman, J.H. and Stevens, T.H. 1987. Protein sorting in yeast: the localization determinant of yeast vacuolar carboxypeptidase Y resides in the propeptide. *Cell* [online]. **48**(5),pp.887–97.

Vitale, a and Raikhel, N. 1999. What do proteins need to reach different vacuoles? *Trends in plant science* [online]. **4**(4),pp.149–155.

Vitale, A. and Denecke, J. 1999. The endoplasmic reticulum-gateway of the secretory pathway. *The Plant cell* [online]. **11**(4),pp.615–28.

Waheed, a, Pohlmann, R., Hasilik, a and von Figura, K. 1981. Subcellular location of two enzymes involved in the synthesis of phosphorylated recognition markers in lysosomal enzymes. *The Journal of biological chemistry* [online]. **256**(9),pp.4150–2.

Walter, P. and Blobel, G. 1981a. Translocation of proteins across the endoplasmic reticulum III. Signal recognition protein (SRP) causes signal sequence-dependent and site-specific arrest of chain elongation that is released by microsomal membranes. *The Journal of cell biology* [online]. **91**(2 Pt 1),pp.557–61.

Walter, P. and Blobel, G. 1981b. Translocation of proteins across the endoplasmic reticulum. II. Signal recognition protein (SRP) mediates the selective binding to microsomal membranes of in-vitro-assembled polysomes synthesizing secretory protein. *The Journal of cell biology* [online]. **91**(2 Pt 1),pp.551–6.

Walter, P., Ibrahimi, I. and Blobel, G. 1981. Translocation of proteins across the endoplasmic reticulum. I. Signal recognition protein (SRP) binds to in-vitro-assembled polysomes synthesizing secretory protein. *The Journal of cell biology* [online]. **91**(2 Pt 1),pp.545–50.

Wieland, F.T., Gleason, M.L., Serafini, T. a and Rothman, J.E. 1987. The rate of bulk flow from the endoplasmic reticulum to the cell surface. *Cell* [online]. **50**(2),pp.289–300.

Wilson, D.W., Lewis, M.J. and Pelham, H.R. 1993. pH-dependent binding of KDEL to its receptor in vitro. *The Journal of biological chemistry* [online]. **268**(10),pp.7465–8.

Xu, G., Li, S., Xie, K., Zhang, Q., Wang, Y., Tang, Y., Liu, D., Hong, Y., He, C. and Liu, Y. 2012. Plant ERD2-like proteins function as endoplasmic reticulum luminal protein receptors and participate in programmed cell death during innate immunity. *The Plant journal : for cell and molecular biology* [online]. **72**(1),pp.57–69.

Yang, J., Barr, L. a., Fahnestock, S.R. and Liu, Z.-B. 2005. High yield recombinant silk-like protein production in transgenic plants through protein targeting. *Transgenic Research* [online]. **14**(3),pp.313–324.